# Comparative geochemical study on Furongian–earliest Ordovician (Toledanian) and Ordovician (Sardic) felsic magmatic events in south-western Europe: underplating of hot mafic magmas linked to the opening of the Rheic Ocean

J. Javier Álvaro[a]*, Teresa Sánchez-García[b], Claudia Puddu[c], Josep Maria Casas[d], Alejandro Díez-Montes[e], Montserrat Liesa[f] & Giacomo Oggiano[g]

[a] *Instituto de Geociencias (CSIC-UCM), Dr. Severo Ochoa 7, 28040 Madrid, Spain, jj.alvaro@csic.es*

[b] *Instituto Geológico y Minero de España, Ríos Rosas 23, 28003 Madrid, Spain, t.sanchez@igme.es*

[c] *Dpto. Ciencias de la Tierra, Universidad de Zaragoza, 50009 Zaragoza, Spain, claudiapuddugeo@gmail.com*

[d] *Dpt. de Dinàmica de la Terra i de l'Oceà, Universitat de Barcelona, Martí Franquès s/n, 08028 Barcelona, Spain, casas@ub.edu*

[e] *Instituto Geológico y Minero de España, Plaza de la Constitución 1, 37001 Salamanca, Spain, al.diez@igme.es*

[f] *Dept. de Mineralogia, Petrologia i Geologia aplicada, Universitat de Barcelona, Martí Franquès s/n, 08028 Barcelona, Spain, mliesa@ub.edu*

[g] *Dipartimento di Scienze della Natura e del Territorio, 07100 Sassari, Italy, giacoggi@uniss.it*

* Corresponding author

## ABSTRACT

A geochemical comparison of Early Palaeozoic felsic magmatic episodes throughout the south-western European margin of Gondwana is made, and includes (i) Furongian–Early Ordovician (Toledanian) activies recorded in the Central Iberian and Galicia-Trás-os-Montes Zones of the Iberian Massif, and (ii) Early–Late Ordovician (Sardic) activities in the eastern Pyrenees, Occitan Domain (Albigeois, Montagne Noire and Mouthoumet massifs) and Sardinia. Both phases are related to uplift and denudation of an inherited palaeorelief, and stratigraphically preserved as distinct angular discordances and paraconformities involving gaps of up to 22 m.y. The geochemical features of the Toledanian and Sardic, felsic-dominant activies point to a predominance of magmatic byproducts derived from the melting of metasedimentary rocks, rich in $SiO_2$ and $K_2O$ and with peraluminous character. $Zr/TiO_2$, Zr/Nb, Nb/Y and Zr vs. Ga/Al ratios, and REE and $\varepsilon Nd_{(t)}$ values suggest the contemporaneity, for both phases, of two geochemical scenarios characterized by arc and extensional features evolving to distinct extensional and rifting conditions associated with the final outpouring of mafic tholeiitic-dominant lava flows. The Toledanian and Sardic magmatic phases are linked to neither metamorphism nor penetrative deformation; on the contrary, their unconformities are associated with foliation-free open folds subsequently affected by the Variscan deformation. The geochemical and structural framework precludes subduction generated melts reaching the crust in a magmatic arc to back-arc setting, but favours partial melting of sediments and/or granitoids in a continental lower crust triggered by the underplating of hot mafic magmas related to the opening of the Rheic Ocean.


**Keywords**: granite, orthogneiss, geochemistry, Cambrian, Ordovician, Gondwana.

## 1. Introduction

A succession of Early–Palaeozoic magmatic episodes, ranging in age from Furongian (former “late Cambrian”) to Late Ordovician, is widespread along the south-western European margin of Gondwana. Magmatic pulses are characterized by preferential development in different palaeogeographic areas and linked to the development of stratigraphic unconformities, but they are related to neither metamorphism nor penetrative deformation (Gutiérrez Marco et al., 2002; Montero et al., 2007). In the Central Iberian Zone of the Iberian Massif (representing the western branch of the Ibero-Armorican Arc; Fig. 1A–B), this magmatism is mainly represented by the Ollo de Sapo Formation, which has long been recognized as a Furongian–Early Ordovician (495–470 Ma) assemblage of felsic-dominant volcanic, subvolcanic and plutonic igneous rocks. This magmatic activity is contemporaneous with the development of the Toledanian Phase, which places Lower Ordovician (upper Tremadocian–Floian) rocks onlapping an inherited palaeorelief formed by Ediacaran–Cambrian rocks and involving a sedimentary gap of ca. 22 m.y. This unconformity can be correlated with the “Furongian gap” identified in the Ossa-Morena Zone of the Iberian Massif and the Anti-Atlas Ranges of Morocco (Álvaro et al., 2007, 2018; Álvaro and Vizcaïno, 2018; Sánchez-García et al., 2019), and with the “lacaune normande” in the central and North-Armorican Domains (Le Corre et al., 1991).

Another felsic-dominant magmatic event, although younger (Early–Late Ordovician) in age, has been recognized in some massifs situated along the eastern branch of the Variscan Ibero-Armorican Arc, such as the Pyrenees, the Occitan Domain and Sardinia (Fig. 1A, C–E). This magmatism is related to the Sardic unconformity, where Furongian–Lower Ordovician rocks are unconformably overlain by those attributed to the Sandbian–lower Katian (former Caradoc). The Sardic Phase is related to both: (i) a sedimentary gap of ca. 16–20 m.y., and an unconformity that geometrically ranges from 90° (angular discordance) to 0° (paraconformity) (Barca and Cherchi, 2004;

Funneda and Oggiano, 2009; Álvaro et al., 2016, 2018; Casas et al., 2019); and (ii) a Mid Ordovician development of cleavage-free folds lacking any contemporaneous metamorphism (for an updated revision, see Casas et al., 2019). The gap is 16-20 m.y. and the magmatic activity took place during a time span of about 25-30 m.y. (from 475 to 445 Ma) so, both ranges can be considered as broadly contemporaneous.

Although a general consensus exists to associate this Furongian–Ordovician magmatism with the opening of the Rheic Ocean and the drift of Avalonia from northwestern Gondwana (Díez Montes et al., 2010; Nance et al., 2010; Thomson et al., 2010; Álvaro et al., 2014a), the origin of this magmatism has received different interpretations. In the Central Iberian Zone, for instance, several geodynamic models have been proposed, such as: (i) subduction-related melts reaching the crust in a magmatic arc to back-arc setting (Valverde-Vaquero and Dunning, 2000; Castro et al., 2009); (ii) partial melting of sediments or granitoids in a continental lower crust affected by the underplating of hot mafic magmas during an extensional regime (Bea et al., 2007; Montero et al., 2009; Díez Montes et al., 2010); and (iii) post-collisional decompression melting of an earlier thickened continental crust, and without significant mantle involvement (Villaseca et al., 2016). In the Occitan Domain (southern French Massif Central and Mouthoumet massifs) and the Pyrenees, Marini (1988), Pouclet et al. (2017) and Puddu et al. (2019) have suggested a link to mantle thermal anomalies. Navidad et al. (2018) proposed that the Pyrenean magmatism was induced by progressive crustal thinning and uplift of lithospheric mantle isoterms. In Sardinia, Oggiano et al. (2010), Carmignani et al. (2001), Gaggero et al. (2012) and Cruciani et al. (2018) have suggested that a subduction scenario, mirroring an Andean-type active margin, caused the main Mid–Ordovician magmatic activity. In the Alps, the Sardic counterpart is also interpreted as a result of the collision of the so-called Qaidam Arc with the Gondwanan margin, subsequently followed by the accretion of the Qilian Block (Von Raumer and Stampfli, 2008; Von Raumer et al., 2013, 2015). This geodynamic interpretation is mainly suggested for the Alpine Briançonnais-Austroalpine basement,

where the volcanosedimentary complexes postdating the Sardic tectonic inversion and folding stage portray a younger arc-arc oblique collision (450 Ma) of the eastern tail of the internal Alpine margin with the Hun terrane, succeeded by conspicuous exhumation in a transform margin setting (430 Ma) (Zurbriggen et al., 1997; Schaltegger et al., 2003; Franz and Romer, 2007; Von Raumer and Stampfli, 2008; Von Raumer et al., 2013; Zurbriggen, 2015, 2017).

Until now the Toledanian and Sardic magmatic events had been studied on different areas and interpreted separately, without taking into account their similarities and differences. In this work, the geochemical affinities of the Furongian–Early Ordovician (Toledanian) and Early–Late Ordovician (Sardic) felsic magmatic activities recorded in the Central Iberian and Galicia-Trás-os-Montes Zones, Pyrenees, Occitan Domain and Sardinia are compared. The re-appraisal is based on 17 new samples from the Pyrenees, Montagne Noire and Sardinia, completing the absence of analysis in these areas and wide-ranging a dataset of 93 previously published geochemical analyses throughout the study region in south-western Europe. This comparison may contribute to a better understanding of the meaning and origin of this felsic magmatism, and thus, to discuss the geodynamic scenario of this Gondwana margin (Fig. 1A) during Cambrian–Ordovician times, bracketed between the Cadomian and Variscan orogenies.

## 2. Emplacement and age of magmatic events

This section documents the emplacement (summarized in Fig. 2) and age (Fig. 3) of the Toledanian and Sardic magmatic events throughout the south-western basement European Variscan Belt, in the northwestern margin of Gondwana during Cambro–Ordovician times.

### 2.1. Iberian Massif

In the Ossa Morena and southern Central Iberian Zones of the Iberian Massif (Fig. 1A–B), the so-called Toledanian Phase is recognized as an angular discordance that separates variably tilted Ediacaran–Cambrian Series 2 rifting volcanosedimentary packages from overlying passive-margin successions. The Toledanian gap comprises, at least, most of the Furongian and basal Ordovician, but the involved erosion can incise into the entire Cambrian and the upper Ediacaran Cadomian basement (Gutiérrez-Marco et al., 2019; Álvaro et al., 2019; Sánchez-García et al., 2019). Recently, Sánchez-García et al. (2019) have interpreted the Toledanian Phase as a break-up (or rift/drift) unconformity with the Armorican Quartzite (including the Purple Series and Los Montes Beds; McDougall et al., 1987; Gutiérrez-Alonso et al., 2007; Shaw et al., 2012, 2014) sealing an inherited Toledanian palaeorelief (Fig. 2).

The phase of uplift and denudation of an inherited palaeorelief composed of upper Ediacaran–Cambrian rocks is associated with the massive outpouring of felsic-dominant calc-alkaline magmatic episodes related to neither metamorphic nor cleavage features. This magmatic activity is widely distributed throughout several areas of the Iberian Massif, such as the Cantabrian Zone and the easternmost flank of the West Asturian-Leonese Zone, where sills and rhyolitic lava flows and volcaniclastics mark the base of the Armorican Quartzite (dated at ca. 477.5 Ma; Gutiérrez-Alonso et al., 2007, 2016), and the lower Tremadocian Borrachón Formation of the Iberian Chains (Álvaro et al., 2008). Similar ages have been reported from igneous rocks of the Basal Allochthonous Units and the Schistose Domain in the Galicia-Trás-os-Montes Zone (500–462 Ma; Valverde-Vaquero et al., 2005, 2007; Montero et al., 2009; Talavera et al., 2008, 2013; Dias da Silva et al., 2012, 2014; Díez Fernández et al., 2012; Farias et al., 2014) and different areas of the Central Iberian Zone, including the contact between the Central Iberian and Ossa-Morena Zones, where the Carrascal and Portalegre batoliths are intruded and the felsic volcanosedimentary Urra Formation marks the unconformity that separates Cambrian and Ordovician strata (494–470 Ma,

Solá et al., 2008; Antunes et al., 2009; Neiva et al., 2009; Romaõ et al., 2010; Rubio-Ordóñez et al., 2012; Villaseca et al., 2013) (Fig. 1B).

The most voluminous Toledanian-related volcanic episode is represented by the Ollo de Sapo Formation, which crops out throughout the northeastern Central Iberian Zone. It mainly consists of felsic volcanosedimentary and volcanic rocks, interbedded at the base of the Lower Ordovician strata and plutonic bodies. The Ollo de Sapo volcanosedimentary Formation has long been recognized as an enigmatic Furongian–Early Ordovician (495–470 Ma) magmatic event exposed along the core of a 600 km-long antiform (labelled as *77* in Fig. 1B) (Valverde-Vaquero and Dunning, 2000; Bea et al., 2006; Montero et al., 2007, 2009; Zeck et al., 2007; Castiñeiras et al., 2008a; Díez Montes et al., 2010; Navidad and Castiñeiras, 2011; Talavera et al., 2013; López-Sánchez et al., 2015; Díaz-Alvarado el al., 2016; Villaseca et al., 2016; García-Arias et al., 2018). The peak of magmatic activity was reached at ca. 490–485 Ma and its most recognizable characteristic is the presence of abundant megacrysts of K-feldspar, plagioclase and blue quartz. There is no evident space-time relationship in its distribution (for a discussion, see López-Sánchez et al., 2015) and, collectively, the Ollo de Sapo Formation rocks record a major tectonothermal event whose expression can be found in most of the Variscan massifs of continental Europe including the Armorican and Bohemian massifs (e.g., von Quadt, 1997; Kröner and Willmer, 1998; Linnemann et al., 2000; Tichomirowa et al., 2001; Friedl et al., 2004; Mingram et al., 2004; Teipel et al., 2004; Ballèvre et al., 2012; El Korh et al., 2012; Tichomirowa et al., 2012; for a summary, see Casas and Murphy, 2018). The large volume of magmatic rocks located in the European Variscan Belt led some authors to propose the existence of a siliceous Large Igneous Province (LIP) (Díez Montes et al., 2010; Gutiérrez-Alonso et al., 2016), named Ibero-Armorican LIP by García-Arias et al. (2018).

The Sardic Phase has been proposed marking a stratigraphic discontinuity close to the Middle–Upper Ordovician boundary interval in some areas of the Central Iberian (e.g., Buçaco and the Truchas Syncline; Martínez Catalán et al., 1992; Días da Silva et

192 al., 2016) and the Morais Allochthonous Complex of the Galicia-Trás-os-Montes Zones
193 (Días da Silva, 2014; Días da Silva et al., 2014, 2016). In the Truchas Syncline, the
194 significance of the discontinuity (or discontinuities) was questioned by a biostratigraphic
195 study of conodonts and the re-interpretation of some of these scouring surfaces as the
196 result of Hirnantian glaciogenic incisions (Sarmiento et al., 1999). The pre–Hirnantian
197 discontinuities have been interpreted as linked to the development of “horsts and half-
198 grabens of local extent” , as a result of which “tilting and gentle folding of the Lower–
199 Middle Ordovician strata, due to the rotation of individual half-grabens and horsts,
200 create the Sardic unconformity in Iberia” (Da Silva et al., 2016: pp. 1131 and 1143).
201 However, the presence of synsedimentary listric faults associated with local outpouring
202 of a basic volcanism, related to extensional pulses in the Ordovician passive-margin
203 platform fringing Northwest Gondwana, cannot be associated with the Sardic Phase.
204 As summarized in this work, the Sardic Phase is characterized by generalized cortical
205 uplift, denudation of exposed uplifted areas under subaerial exposure, stratigraphic
206 gaps of about 25–30 m.y., broad intrusion of felsic granitic plutons (now orthogneisses
207 after Variscan deformation and metamorphism) with calc-alkaline affinity, and record of
208 alluvial-to-fluvial deposits onlapping the unconformity. These are the features that
209 characterize the Ordovician Sardic Phase, not the record of Ordovician volcanism and
210 of local listric faults (e.g., Casas et al., 2010, 2019; Álvaro et al., 2016).

211 In contrast, the Sardic aftermath is represented by a basic-dominant volcanic
212 activity, mainly of tholeiitic affinity, and lining rifting branches highlighting the onset of
213 listric-fault networks; this event could be geodynamically compared with some
214 processes recorded in the Central Iberian and the Galician-Trás-os-Montes Zones, but
215 not with the Sardic Phase. Therefore, the presence of the Sardic Phase in Iberia was
216 already ruled out by the information published during the last two decades, and should
217 not be maintained except if the above-reported tectonothermal events are really found
218 in Iberia. The presence of an Ordovician volcanism associated with listric faults is not
219 an argument to support the record of the Sardic Phase.

220

221 **2.2. Central and Eastern Pyrenees**

222

223 In the central and eastern Pyrenees (Fig. 1D), earliest Ordovician volcanic-free
224 passive-margin conditions, represented by the Jujols Group (Padel et al., 2018), were
225 succeeded by a late Early–Mid Ordovician phase of uplift and erosion that led to the
226 onset of the Sardic unconformity (Fig. 2). Uplift was associated with magmatic activity,
227 which continued until Late Ordovician times. An extensional interval took place then
228 developing normal faults that controlled the sedimentation of post–Sardic siliciclastic
229 deposits infilling palaeorelief depressions. Acritarchs recovered in the uppermost part
230 of the Jujols Group suggest a broad Furongian–earliest Ordovician age (Casas and
231 Palacios, 2012), conterminous with a maximum depositional age of ca. 475 Ma, based
232 on the age of the youngest detrital zircon populations (Margalef et al*.,* 2016). On the
233 other hand, a ca. 459 Ma U–Pb age for the Upper Ordovician volcanic rocks overlying
234 the Sardic Unconformity has been proposed in the eastern Pyrenees (Martí et al.,
235 2019), and ca. 452–455 Ma in the neighbouring Catalan Coastal Ranges, which
236 represent the southern prolongation of the Pyrenees (Navidad et al., 2010; Martínez et
237 al., 2011). Thus, a time gap of about 16–23 m.y. can be related to the Sardic Phase in
238 the eastern Pyrenees and the neighbouring Catalan Coastal Ranges.

239 Coeval with the late Early–Mid Ordovician phase of generalized uplift and
240 denudation, a key magmatic activity led to the intrusion of voluminous granitoids, about
241 500 to 3000 m thick and encased in strata of the Ediacaran–Lower Cambrian
242 Canaveilles Group (Fig. 2). These granitoids constitute the protoliths of the large
243 orthogneissic laccoliths that punctuate the backbone of the central and eastern
244 Pyrenees. These are, from west to east (Fig. 1D), the Aston (467–470 Ma ; Denèle et
245 al., 2009; Mezger and Gerdes, 2016), Hospitalet (about 472 Ma, Denèle et al., 2009),
246 Canigó (472–462 Ma, Cocherie et al., 2005; Navidad et al., 2018), Roc de Frausa
247 (477–476 Ma; Cocherie et al., 2005; Castiñeiras et al., 2008b) and Albera (about 470

248 Ma; Liesa et al., 2011) massifs, which comprise a dominant Floian–Dapingian age. It is
249 noticeable the fact that only a minor representation of coeval basic magmatic rocks are
250 outcropped. The acidic volcanic equivalents have been documented in the Albera
251 massif, where subvolcanic rhyolitic porphyroid rocks have yielded similar ages to those
252 of the main gneissic bodies at about 474–465 Ma (Liesa et al., 2011). Similar acidic
253 byproducts are represented by the rhyolitic sills of Pierrefite (Calvet et al., 1988).

254 The late Early–Mid Ordovician ("Sardic") phase of uplift was succeeded by a Late
255 Ordovician extensional interval responsible for the opening of (half-)grabens infilled
256 with the basal Upper Ordovician alluvial-to-fluvial conglomerates (La Rabassa
257 Conglomerate Formation). At map scale, a set of NE-SW trending normal faults
258 abruptly controlling the thickness of the basal Upper Ordovician formations can be
259 recognized in the La Cerdanya area (Casas and Fernández, 2007; Casas, 2010).
260 Sharp variations in the thickness of the Upper Ordovician strata have been
261 documented by Hartevelt (1970) and Casas and Fernández (2007). Drastic variations
262 in grain size and thickness can be attributed to the development of palaeotopographies
263 controlled by faults and subsequent erosion of uplifted palaeoreliefs, with subsequent
264 infill of depressed areas by alluvial fan and fluvial deposits, finally sealed by Silurian
265 sediments (Puddu et al., 2019). A Late Ordovician magmatic pulse contemporaneously
266 yielded a varied set of magmatic rocks. Small granitic bodies are encased in the
267 Canaveilles strata of the Canigó massif. They constitute the protoliths of the Cadí
268 (about 456 Ma; Casas et al., 2010), Casemí (446 to 452 Ma; Casas et al., 2010), Núria
269 (ca. 457 Ma; Martínez et al., 2011) and Canigó G-1 type (ca. 457 Ma; Navidad et al.,
270 2018) gneisses.

271 The lowermost part of the Canaveilles Group (the so-called Balaig Series) host
272 metre-scale thick bodies of metadiorite sills related to an Upper Ordovician protolith,
273 (ca. 453 Ma, SHRIMP U–Pb in zircon; Casas et al., 2010). Coeval calc-alkaline
274 ignimbrites, andesites and volcaniclastic rocks are interbedded in the Upper Ordovician
275 succession of the Bruguera and Ribes de Freser areas (Robert and Thiebaut, 1976;

Ayora, 1980; Robert, 1980; Martí et al., 1986, 2019). In the Ribes area, a granitic body with granophyric texture, dated at ca. 458 Ma by Martínez et al. (2011), intruded at the base of the Upper Ordovician succession. In the La Pallaresa dome, some metre-scale rhyodacitic to dacitic subvolcanic sills, Late Ordovician in age (ca. 453 Ma, Clariana et al., 2018), occur interbedded within the pre-unconformity strata and close to the base of the Upper Ordovician.

### 2.3. Occitan Domain: Albigeois, Montagne Noire and Mouthoumet massifs

The parautochthonous framework of the southern French Massif Central, named Occitan Domain by Pouclet et al. (2017), includes among others, from south to north, the Mouthoumet, Montagne Noire and Albigeois massifs. The domain represents the southeastern prolongation of the Variscan South Armorican Zone (including southwestern Bretagne and Vendée). Since Gèze (1949) and Arthaud (1970), the southern edge of the French Massif Central has been traditionally subdivided, from north to south, into the northern, axial and southern Montagne Noire (Fig. 1C). The Palaeozoic succession of the northern and southern sides includes sediments ranging from late Ediacaran to Silurian and from Terreneuvian (Cambrian) to Visean in age, respectively. These successions are affected by large scale, south-verging recumbent folds that display a low to moderate metamorphic grade. Their emplacement took place in Late Visean to Namurian times (Engel et al., 1980; Feist and Galtier, 1985; Echtler and Malavieille, 1990). The Axial Zone consists of plutonic, migmatitic and metamorphic rocks forming a regional ENE-WSW oriented dome (Fig. 1C), where four principal lithological units can be recognized (i) schists and micaschists, (ii) migmatitic orthogneisses, (iii) metapelitic metatexites, and (iv) diatexites and granites (Cocherie, 2003; Faure et al., 2004; Roger et al., 2004, 2015; Bé Mézème, 2005; Charles et al., 2009; Rabin et al., 2015). The Rosis micaschist synform subdivides the eastern Axial

303 Zone into the Espinouse and Caroux sub-domes, whereas the southwestern edge of
304 the Axial Zone comprises the Nore massif.

305 In the Occitan Domain, two main Cambro–Ordovician felsic events can be identified
306 giving rise to the protoliths of (i) the Larroque metarhyolites in the northern Montagne
307 Noire and Albigeois, thrusted southward from Rouergue; and (ii) the migmatitic
308 ortogneisses that form the Axial Zone of the Montagne Noire (Fig. 2).

309 (i) The Larroque volcanosedimentary Complex is a thick (500–1000 m) package of
310 porphyroclastic metarhyolites located on the northern Montagne Noire (Lacaune
311 Mountains), Albigeois (St-Salvi-de-Carcavès and St-Sernin-sur-Rance nappes) and
312 Rouergue; the Variscan setting of the formation is allochthonous in the Albigeois and
313 parautochthonous in the rest. This volcanism is encased in the so-called “Série schisto-
314 gréseuse verte” (see Guérangé-Lozes et al., 1996; Guérangé-Lozes and Alabouvette,
315 1999) (Pouclet et al., 2017) (Fig. 2). The Larroque volcanic rocks consist of deformed
316 porphyroclastic rhyolites rich in largely fragmented, lacunous (rhyolitic) quartz and
317 alkali feldspar phenocrysts. The metarhyolites occur as porphyritic lava flows, sills and
318 other associated facies, such as aphyric lava flows, porphyritic and aphyric pyroclastic
319 flows of welded or unwelded ignimbritic types, fine to coarse tephra deposits, and
320 epiclastic and volcaniclastic deposits. These rocks are named “augen gneiss” or
321 augengneiss and do not display a high-grade gneiss paragenesis but a general lower
322 grade metamorphic mineralogy. The Occitan augengneisses mimic the Ollo de Sapo
323 facies from the Central Iberian Zone because of their large bluish quartz phenocrysts.
324 Based on geochemical similarities and contemporaneous emplacement, Pouclet et al.
325 (2017) suggested that this event also supplied the Davejean acidic volcanic rocks in
326 the Mouthoumet Massif, which represent the southern prolongation of the Montagne
327 Noire (Fig. 2), and the Génis rhyolitic unit of the western Limousin sector.

328 (ii) Some migmatitic orthogneisses make up the southern Axial Zone, from the
329 western Cabardès to the eastern Caroux domes. The orthogneisses, derived from
330 Ordovician metagranites bearing large K-feldspar phenocrysts, were emplaced at

about 471 Ma (Somail Orthogneiss, Cocherie et al., 2005), 456 to 450 Ma (Pont de Larn and Gorges d'Héric gneisses, Roger et al., 2004) and ca. 455 Ma (Sain Eutrope gneiss, Pitra et al., 2012). They intruded a metasedimentary pile, traditionally known as "Schistes X" and formally named St. Pons-Cabardès Group (Fig. 2). The latter consists of schists, greywackes, quartzites and subsidiary volcanic tuffs and marbles (Demange et al., 1996; Demange, 1999; Alabouvette et al., 2003; Roger et al., 2004; Cocherie et al., 2005). The group is topped by the Sériès Tuff, dated at about 545 Ma (Lescuyer and Cocherie, 1992), which represents a contemporaneous equivalent of the Cadomian Rivernous rhyolitic tuff (542.5 to 537.1 Ma) from the Lodève inlier of the northern Montagne Noire (Álvaro et al., 2014b, 2018; Padel et al., 2017). Age of migmatization has been inferred from U–Pb dates on monacite from migmatites and anatectic granites at 333 to 327 Ma (Bé Mézème, 2005; Charles et al., 2008); as a result, the 330–325 Ma time interval can represent a Variscan crustal melting event in the Axial Zone.

As in the Pyrenees, the Middle Ordovician is absent in the Occitan Domain. Its gap allows distinction between a Lower Ordovician pre-unconformity sedimentary package para- to unconformably overlain by an Upper Ordovician–Silurian succession (Álvaro et al., 2016; Pouclet et al., 2017).

### 2.4. Sardinia

In Sardinia the Cambro–Ordovician magmatism is well represented in the external (southern) and internal (northern) nappe zones of the exposed Variscan Belt (Fig. 1E), and ranges in age from late Furongian to Late Ordovician. A Furongian–Tremadocian (ca. 491–480 Ma) magmatic activity, predating the Sardic phase, is mostly represented by felsic volcanic and subvolcanic rocks encased in the San Vito sandstone Formation. The Sardic-related volcanic products differ from one nappe to another: intermediate and basic (mostly metandesites and andesitic basalts) are common in the nappe

359 stacking of the central part of the island (Barbagia and Goceano), whereas felsic
360 metavolcanites prevail in the southeastern units. Their age is bracketed between 465
361 and 455 Ma (Giacomini et al., 2006; Oggiano et al., 2010; Pavanetto et al., 2012;
362 Cruciani et al., 2018) and matches the Sardic gap based on biostratigraphy (Barca et
363 al., 1988).

364 Teichmüller (1931) and Stille (1939) were the first to recognize in southwestern
365 Sardinia an intra–Ordovician stratigraphic hiatus. Its linked erosive unconformity is
366 supported by a correlatable strong angular discordance in the Palaeozoic basement of
367 the Iglesiente-Sulcis area, External Zone (Carmignani et al., 2001). This major
368 discontinuity separates the Cambrian–Lower Ordovician Nebida, Gonnesa and Iglesias
369 groups (Pillola et al., 1998) from the overlying coarse-grained ("Puddinga") Monte
370 Argentu metasediments (Leone et al., 1991, 2002; Laske et al., 1994). The gap
371 comprises a chronostratigraphically constrained minimum gap of about 18 m.y. that
372 includes the Floian and Dapingian (Barca et al., 1987, 1988; Pillola et al., 1998; Barca
373 and Cherchi, 2004) (Fig. 2). The hiatus is related to neither metamorphism nor
374 cleavage, though some E–W folds have been documented in the Gonnesa Anticline
375 and the Iglesias Syncline (Cocco et al., 2018), which are overstepped by the
376 "Puddinga" metaconglomerates. Both the E–W folds and the overlying
377 metaconglomerates were subsequently affected by Variscan N–S folds (Cocco and
378 Funneda, 2011, 2017). Sardic-related volcanic rocks are not involved in this area, but
379 Sardic-inherited palaeoreliefs are lined with breccia slides that include metre- to
380 decametre-scale carbonate boulders ("Olistoliti"), some of them hosting
381 synsedimentary faults contemporaneously mineralized with ore bodies (Boni and
382 Koeppel, 1985; Boni, 1986; Barca, 1991; Caron et al., 1997). The lower part of the
383 unconformably overlying Monte Argentu Formation deposited in alluvial to fluvial
384 environments (Martini et al., 1991; Loi et al., 1992; Loi and Dabard, 1997).

385 A similar gap was reported by Calvino (1972) in the Sarrabus-Gerrei units of the
386 External Nappe Zone. The so-called "Sarrabese Phase" is related to the onset of thick,

387 up to 500 m thick, volcanosedimentary complexes and volcanites (Barca et al., 1986;
388 Di Pisa et al., 1992) with a Darriwilian age for the protoliths of the metavolcanic rocks
389 (465.4 to 464 Ma; Giacomini et al., 2006; Oggiano et al., 2010). In the Iglesiente-Sulcis
390 region (Fig. 1E), Carmignani et al. (1986, 1992, 1994, 2001) suggested that the
391 "Sardic-Sarrabese phase" should be associated with the compression of a Cambro–
392 Ordovician back-arc basin that originated the migration of the Ordovician volcanic arc
393 toward the Gondwanan margin.

394 Some gneissic bodies, interpreted as the plutonic counterpart of metavolcanic rocks,
395 are located in the Bithia unit (e.g., the Monte Filau area, 458 to 457 Ma, surrounded by
396 a Mid–Ordovician andalusite thermal aureole; Pavanetto et al*.,* 2012; Costamagna et
397 al., 2016) and in the internal units (Lodè orthogneiss, ca. 456 Ma; Tanaunella
398 orthogneiss, ca. 458 Ma, Helbing and Tiepolo, 2005; Golfo Aranci orthogneiss, ca. 469
399 Ma, Giacomini et al., 2006).

400 The Sardic palaeorelief is sealed by Upper Ordovician trangressive deposits. The
401 sedimentary facies show high variability, but the –mostly terrigenous– sediments vary
402 from grey fine- to medium-sized sandstones, to muddy sandstones and mudstones.
403 They are referred to the Katian Punta Serpeddì and Orroeledu formations (Pistis et al.,
404 2016). This post–Sardic sedimentary succession is coeval with a new magmatic
405 pulsation represented by alkaline to tholeiitic within-plate basalts (Di Pisa et al., 1992;
406 Gaggero et al., 2012).

407

408 **3. Geochemical data**

409

410 **3.1. Materials and methods**

411

412 The rocks selected for geochemical analysis (231 samples; see tectonostratigraphic
413 location in Fig. 1 and stratigraphic emplacement in Fig. 2) have recorded different
414 degrees of hydrothermalism and metamorphism, as a result of which only the most

immobiles elements have been considered. The geochemical calculations, in which the major elements take part, have been made from values recalculated to 100 in volatile free compositions; Fe is reported as $FeO_t$.

The geochemical dataset of the Central Iberian Zone includes 152 published geochemical data, from which 85 are plutonic and 67 volcanic and volcaniclastic rocks from the Ollo de Sapo Formation (Galicia, Sanabria and Guadarrama areas), and the contact between the Central Iberian and Ossa Morena Zones (Urra Formation and Portalegre and Carrascal granites). Other data were yielded from six volcanic rocks of the Galicia-Trás-os-Montes Zone (Saldanha area) (Fig. 1B; Repository Data).

The dataset of the eastern Pyrenees consists of 38 samples, six of which are upper Lower Ordovician volcanic rocks, and seven upper Lower Ordovician plutonic rocks, together with nine Upper Ordovician volcanic and 14 Upper Ordovician plutonic rocks (Repository Data). New data reported below include two samples of subvolcanic sills intercalated in the pre–Sardic unconformity succession (Clariana et al., 2018; Margalef, unpubl.; Table 1).

The study samples from the Occitan Domain comprise six metavolcanic rocks, four from the Larroque volcanosedimentary Complex in the Albigeois and northern Montagne Noire and two from the Mouthoumet massif (Pouclet et al., 2017) (Repository Data), and four new samples for the Axial Zone gneisses (Table 1).

In the Sardinian dataset, 25 published analyses are selected: five correspond to the Golfo Aranci orthogneiss (Giacomini et al., 2006), six to metavolcanics from the central part of the island (Giacomini et al., 2006; Cruciani et al., 2013), and five to metavolcanics and one to gneisses from the Bithia unit (Cruciani et al., 2018) (Repository Data). Ten new analyses are added from the Monte Filau and Capo Spartivento gneisses of the Bithia unit, and from the Punta Bianca gneisses embedded within the migmatites of the High-grade Metamorphic complex of the Inner Zone (Table 1).

Whole-rock major and trace elements and rare earth element (REE) compositions were determined at ACME Laboratories, Vancouver, Canada. $LiBO_2$ fusion followed by X-ray fluorescence spectroscopy (XRF) analysis was used to determine major elements. Rare earth and refractory elements were measured by ICP–MS following a lithium metaborate/tetraborate fusion and nitric acid digestion on 0.2 g of sample. For base metals, 0.5 g of sample was digested in Aqua Regia at 95 ºC and analyzed by inductively coupled plasma - atomic emission spectrometry (ICP–AES). Analyses of standards and duplicate samples indicate precision to better than 1 % for major oxides, and 3–10 % for minor and trace elements.

Additional Sm–Nd isotopic analyses were performed at Centro de Geocronologia y Geoqulmica Isotopica from the Complutense University, Madrid. They were carried out in whole-rock powders using a $^{150}Nd$–$^{149}Sm$ tracer by isotope dilution-thermal ionization mass spectrometry (ID–TIMS). The samples were first dissolved through oven digestion in sealed Teflon bombs with ultra pure reagents to perform two-stage conventional cation-exchange chromatography for separation of Sm and Nd (Strelow, 1960; Winchester, 1963), and subsequently analysed using a Sector 54 VG-Micromass multicollector spectrometer. The measured $^{143}Nd/^{144}Nd$ isotopic ratios were corrected for possible isobaric interferences from $^{142}Ce$ and $^{144}Sm$ (only for samples with $^{147}Sm/^{144}Sm<0.0001$) and normalized to $^{146}Nd/^{144}Nd=0.7219$ to correct for mass fractionation. The Lajolla Nd international isotopic standard was analysed during sample measurement, and gave an average value of $^{143}Nd/^{144}Nd=0.5114840$ for 9 replicas, with an internal precision of ± 0.000032 (2σ). These values were used to correct the measured ratios for possible sample drift. The estimated error for the $^{147}Sm/^{144}Nd$ ratio is 0.1%.

A general classification of the analyzed samples, following Winchester and Floyd (1977), can be seen in Figure 4A–B, and the geographical coordinates of the new samples in Table 1. For geochemical comparison (summarized in Table 2), two large groups or suites are differentiated in order to check the similarities and differences

between the magmatic rocks, and to infer a possible geochemical trend following a palaeogeographic SW–NE transect. The description reported below follows the same palaeogeographic and chronological order.

### 3.2. Furongian–to–Mid Ordovician Suite

In the Central Iberian and Galicia-Trás-os-Montes Zones, the Furongian–to–Mid Ordovician magmatic activity is pervasive. Their main representative is the Ollo de Sapo Formation, which includes volcanic and subvolcanic rocks (67 samples) as well as plutonic rocks (85 samples) (data from Murphy et al., 2006; Díez-Montes, 2007; Montero et al., 2007, 2009; Solá, 2007; Solá et al., 2008; Talavera, 2009; Villaseca et al., 2016). From the Parautochthon Schistose Domain of the Galicia-Trás-os Montes Zone, six samples of rhyolite tuffs of the Saldanha Formation (Dias da Silva et al., 2014) are selected, which share geochemical features with the Ollo de Sapo Formation. In summary, five facies are differentiated in the Central Iberian and Galicia-Trás-os Montes Zones: the Ollo de Sapo orthogneisses, some leucogneisses, metagranites and volcanic rocks, and the San Sebastián orthogneiss (for a geochemical characterization, see Table 2).

In the central and eastern Pyrenees, an Early−Mid Ordovician magmatic activity gave rise to the intrusion of voluminous (about 500−3000 m in size) aluminous granitic bodies, encased into the Canaveilles beds (Álvaro et al., 2018; Casas et al., 2019). They constitute the protoliths of the large orthogneissic laccoliths that form the core of the domal massifs scattered throughout the backbone of the Pyrenees. Rocks of the Canigó, Roc de Frausa and Albera massifs have been taken into account in this work, in which volcanic rocks of the Pierrefite and Albera massifs, and the so-called *G2* and *G3* orthogneisses by Guitard (1970) are also included. All subgroups vary compositionally from subalkaline andesite to rhyolite, as illustrated in the Pearce's

(1996) diagram of Figure 5 (data compiled from Vilà et al., 2005; Castiñeiras et al., 2008b; Liesa et al., 2011; Navidad et al., 2018).

Although most rocks in this area are acidic, it is remarkable the presence of minor mafic bodies (Cortalet and Marialles metabasites, not studied in this work), which could indicate a mantle connection with parental magmas during the Mid and Late Ordovician. As well, it should be noted that there are no andesitic rocks in the area.

In the Occitan Domain, six samples of the Larroque volcanosedimentary Complex (Early Tremadocian in age) represent basin floors and subaerial explosive and effusive rhyolites (Pouclet et al., 2017). The porphyroclastic rocks of the Larroque metarhyolites were sampled in the Saint-Géraud and Larroque areas from the Saint-Sernin-sur-Rance nappe and the Saint-André klippe above the Saint-Salvi-de-Carcavès nappe (Pouclet et al., 2017).

In the Middle Ordovician rocks of Sardinia, 11 samples are selected, five of which correspond to orthogneisses of the Aranci Gulf, in the Inner Zone of the NE island (Giacomini et al., 2006), completed with six volcanic rocks of the External Zone (Giacomini et al., 2006; Cruciani et al., 2018) (Table 2).

### 3.3 Upper Ordovician Suite

In the central and eastern Pyrenees, four Upper Ordovician subgroups are distinguished based on their field occurrence and geochemical and geochronological features: the *G1*-type orthogneisses *sensu* Guitard (1970); the Cadí and Casemí orthogneisses and the metavolcanic rocks that include the Ribes de Freser rhyolites; the Els Metges volcanic tuffs; and the rhyolites from Andorra and Pallaresa areas (the latter dated at ca. 453 Ma; Clariana et al., 2018) (Table 2). The suite is completed with the Somail orthogneisses of the Axial Montagne Noire (dated at ca. 450 Ma at Gorges d'Héric; Roger et al., 2004) and the orthogneisses from the Sardinian External Zone

524 (dated at ca. 458–457 Ma at Monte Filau; Pavanetto et al., 2012) and the volcanic roks
525 from the Sardinian Nappe Zone (Table 2).
526
527 **4. Geochemical framework**
528
529 A geochemical comparison between the Furongian–Ordovician felsic rocks of all the
530 above-reported groups offers the opportunity to characterize the successive sources of
531 crustal-derived melts along the south-western European margin of Gondwana.
532 The geochemical features point to a predominance of materials derived from the
533 melting of metasedimentary rocks, rich in $SiO_2$ and $K_2O$ (average $K_2O/Na_2O$ = 2.25)
534 and peraluminous ($0.4 < C_{norm} < 4.5$ and $0.94 < A/CNK > 3.12$), with only three samples
535 with A/CNK <1 (samples 100786 of the Casemí subgroup, and T26 and T27 of the San
536 Sebastián subgroup).
537 The result of plotting the REE content vs. average values of continental crust
538 (Rudnick and Gao, 2004; Fig. 6) yields a flat spectra and a base level shared by most
539 of the considered groups. The total content in REE is moderate to high (average REE =
540 176 ppm, ranging between 482.2 and 26.0 ppm; Fig. 7), with a maximum in the
541 subgroup of the Middle Ordovician volcanic rocks from Sardinia (average REE = 335
542 ppm, *VOL-SMO*), and with LREE values more fractionated than HREE ones, and
543 negative anomalies of Eu, which would indicate a characteristic process of magmatic
544 evolution with plagioclase fractionation. These features are common in peraluminous
545 granitoids.
546 All subgroups display similar chondritic normalized REE patterns (Fig. 7), with an
547 enrichment in LREE relative to HREE, which should indicate the involvement of crustal
548 materials in their parental magmas. Nevertheless, some variations can be highlighted,
549 such as the lesser fractionation in REE content of some subgroups. These are the
550 leucogneisses from the Iberian massif (*LG*, $La/Yb_n$ = 2.01), the Upper Ordovician
551 orthogneisses from Sardinia (*OG-SUO*, $La/Yb_n$ = 2.94), the Casemí orthogneisses

552 ($La/Yb_n$ = 4.42) and the Middle Ordovician volcanic rocks from Sardinia (*OG-SUO*,
553 $La/Yb_n$ = 2.94). This may be interpreted as a greater degree of partial fusion in the
554 origin of their parental magmas (Rollinson, 1993).

555 There are three geochemical groups displaying $(Gd/Yb)_n$ values > 2, and $(La/Yb)_n$
556 values ≥ 9. These groups are *OSS* (Central Iberian Zone), *VOL-OD* (Occitan Domain)
557 and *G1* (Pyrenees), and share higher alkalinity features.

558 Some *V1* rocks from the Pyrenees (Pierrefite Formation) show no negative
559 anomalies in Eu. Their parental magmas could have been derived from deeper origins
560 and related to residual materials of the lower continental crust, in areas of production of
561 K-rich granites (Taylor and McLenan, 1989).

562 The spider diagrams (Fig. 8), however, exhibit strong negative anomalies in Nb, Sr
563 and Ti, which indicate a distinct crustal affiliation (Díez-Montes, 2007). Only the San
564 Sebastián orthogneisses (*OSS*) show distinct discrepancies in respect of the remaining
565 samples from the Ollo de Sapo Formation. They display lower negative anomalies in
566 Nb and a more alkaline character by comparison with the rest of the Ollo de Sapo
567 rocks, which point to alkaline affinities and greater negative anomalies in Nb.

568 Despite some small differences in the chemical ranges of some major elements,
569 most felsic Ordovician rocks from the Iberian massif (Central Iberian and Galicia-Trás-
570 os Montes Zones), eastern Pyrenees, Occitan Domain and Sardinia share a common
571 chemical pattern. The Lower–Middle Ordovician rocks of the eastern Pyrenees show
572 less variation in the content of Zr and Nb (Fig. 8B). The volcanic rocks of these groups
573 show a different REE behaviour, which would indicate different sources. Two groups
574 are distinguished in Figure 7, one with greater enrichment in REE and negative
575 anomaly of Eu, and another with lesser content of HREE and without Eu negative
576 anomalies.

577 Figure 9 illustrates how the average of all the considered groups approximates the
578 mean values of the Rudnick and Gao's (2003) upper continental crust (UCC). In this
579 figure, small deviations can be observed, some of them toward lower continental crust

(LCC) values and others toward bulk continental crust (BCC), indicating variations in their parental magmas but with quite similar spectra. Overall chondrite-normalized patterns are close to the values that represent the upper continental crust, with slight enrichments in the Th/Nb, Th/La and Th/Yb ratios.

Finally, in the Occitan volcanic rocks (*VOL-OD*) the rare earth elements are enriched and fractionated (33.2 ppm < La < 45.6 ppm; 11.2 < La/Yb < 14.5). The upper continental crust normalized diagram exhibits negative anomalies of Ti, V, Cr, Mn and Fe associated with oxide fractionation, of Zr and Hf linked to zircon fractionation, and of Eu related to plagioclase fractionation. The profiles are comparable to the Vendean Saint-Gilles rhyolitic ones. The Th vs. Rb/Ba features are also similar to those of the Saint-Gilles rhyolites, and the Iberian Ollo de Sapo and Urra rhyolites (Solá et al., 2008; Díez Montes et al., 2010).

## 4. Discussion

### 4.1 Inferred tectonic settings

In order to clarify the evolution of geotectonic environments, the data have been represented in different discrimination diagrams. The $Zr/TiO_2$ ratio (Lentz, 1996; Syme, 1998) is a key index of compositional evolution for intermediate and felsic rocks. In the Syme diagram (Fig. 10), most rocks from the Central Iberian Zone represent a characteristic arc association, although there are some contemporaneous samples characterized by extensional-related values (Zr/Ti = 0.10, *LG*). The rocks of the Middle–Ordovician San Sebastián orthogneisses (*OSS*) show values of Zr/Ti = 0.08, intermediate between extensional and arc conditions. This could be interpreted as a sharp change in geotectonic conditions toward the Mid Ordovician (Fig. 10A). For a better comparison, the samples of the San Sebastián orthogneisses (*OSS*) and the granites (*GRA*) have been distinguished with a shaded area in all the diagrams, since

608 they have slightly different characteristics to the rest of the samples from the Ollo de
609 Sapo group. The samples *G1* (Pyrenees) and *VOL* (Central Iberian Zone) broadly
610 share similar values, as a result of which, the three latter groups (*OSS*, *G1* and *VOL*)
611 arrange following a good correlation line. The same trend seems to be inferred in the
612 eastern Pyrenees (Fig. 10B), where the Middle Ordovician subgroups display arc
613 features, but half of the Upper Ordovician subgroups show extensional affinities (*G1*
614 and Casemí orthogneisses). In the case of the Occitan orthogneisses (Fig. 10C), they
615 show arc characters, which contrast with the contemporaneous volcanic rocks
616 displaying extensional values with Zr/Ti = 0.10. This disparity between plutonic and
617 volcanic rocks could be interpreted as different conditions for the origin of these
618 magmas. In Sardinia (Fig. 10D), the same evolution from arc to extensional conditions
619 is highlighted for the Upper Ordovician samples, although some Middle Ordovician
620 volcanic rocks already shared extensional patterns (Zr/Ti = 0.09). In summary, there
621 seems to be a geochemical evolution in the Ordovician magmas grading from arc to
622 extensional environments.

623 In the Nb–Y tectonic discriminating diagram of Pearce et al. (1984) (Fig. 11), most
624 samples plot in the volcanic arc-type, though some subgroups project in the whitin-
625 plate and anomalous ORG. The majority of samples display very similar Zr/Nb and
626 Nb/Y ratios, typical of island arc or active continental margin rhyolites (Díez-Montes et
627 al., 2010). Only some samples plot separately: *OSS* samples with highest Nb contents
628 (>20 ppm), and some volcanic rocks of the Occitan Domain (average Nb =16.87 ppm).
629 In the eastern Pyrenees, the Middle Ordovician rocks plot in the volcanic arc field,
630 whereas the Upper Ordovician ones point in the ORG type, except the Casemí
631 samples. This progress of magmatic sources agrees with the evolution seen in Figure
632 10. In the Ocitan Domain, *VOL-OD* samples share values with those of the San
633 Sebastián orthogneiss, while *OG-OD* shares values with those of *OG* from the Central
634 Iberian Zone.

635 The Zr vs. Nb diagram (Leat et al., 1986; modified by Piercey, 2011) (Fig. 12)
636 illustrates how magmas evolved toward richer values in Zr and Nb, which is consistent
637 with what it is observed in the Syme diagram (Fig. 10). Figure 12A documents how
638 most samples show a general positive correlation. These different groups correspond
639 to the *OSS* and Portalegre granites, highlighted in the figure. The two groups indicate a
640 tendency toward alkaline magmas. Some samples, such as the Pyrenean *G1*, some
641 Occitan *VOL-OD* samples and some Sardinian *OG-UOS* samples share the same
642 affinity, clearly distinguished from the general geochemical trend exhibited by the
643 Central Iberian Zone.

644 On a Zr vs. Ga/Al diagram (Whalen et al., 1987) (Fig. 13), the samples depict an
645 intermediate character between anorogenic or alkaline (A-type) and orogenic (I&S-
646 type). In the Central Iberian Zone, samples from the San Sebastián orthogneisses and
647 Portalegre granites show characters of A-type granites, while the remaining samples
648 display affinities of I&S-type granites. For the Central Iberian Zone, a clear magmatic
649 shift toward more extensional geotectonic environments is characterized. For the
650 eastern Pyrenees, we find the same situation as in the Central Iberian Zone, with a
651 magmatic evolution toward A-granite type characteristics, indicating more extensional
652 geotectonic environments. In the Occitan Domain, the samples show a clear I&S
653 character. In the Sardinian case, the same seems to happen as in the Central Iberian
654 Zone: the Upper Ordovician orthogneisses suggest a more extensional character.

655 In summary, all the reported diagrams point to a magmatic evolution through time,
656 grading from arc to extensional geotectonic environments (with increased Zr/Ti ratios)
657 and to granite type-A characters. This geotectonic framework is consistent with that
658 illustrated in Figure 10. The geochemical characters of these rocks show a rhyodacite
659 to dacite composition, peraluminous and calc-alkaline K-rich character, and an arc-
660 volcanic affinity for most of samples, but without intermediate rocks associated with
661 andesitic types. Hence a change in time is documented toward more alkaline magmas.
662

663 **4.2 Interpretation of $\varepsilon$Nd values**

664

665 $\varepsilon Nd_{(t)}$ values are useful to interpret the nature of magmatic sources. Most samples of
666 the above-reported groups show no significant differences in isotopic $\varepsilon Nd_{(t)}$ values, and
667 $Nd_{CHUR}$ model ages (Fig. 14). Some exceptions are related to granites from the
668 southern Central Iberian Zone, which display positive values (from +2.6 to –2.4) and
669 $T_{DM}$ values from 0.90 to 3.46 Ga. These granites, space-related with calcalkaline
670 diorites and gabbros, were interpreted by Solá et al. (2008) as the result of
671 underplating and temporal storage of mantle-derived magmas as a potential source for
672 the intrusive "orogenic melts" during Early Palaeozoic extension.
673 Some samples from (i) the Central Iberian Zone, such as VI-3 (Leucogneiss subgroup)
674 and PORT2 and PORT15 (Granite subgroup); (ii) the eastern Pyrenees, such as 99338
675 (G1 subgroup) and 100786 samples (Casemí subgroup); and (iii) the Sardinian CS5,
676 CS8 and CC5 samples (Upper Ordovician Orthogneiss subgroup) display anomalous
677 $T_{DM}$ values and $^{147}Sm/^{144}Nd$ ratios > 0.17 (Table 2; Fig. 14), a character relatively
678 common in some felsic rocks (DePaolo, 1988; Martínez et al., 2011). According to
679 Stern et al. (2012), these values should not be considered, but a possible explanation
680 for these high ratios may be related to the M-type tetrad effect (e.g., Irber, 1999;
681 Monecke et al., 2007; Ibrahim et al., 2015), which affects REE fractionation in highly
682 evolved felsic rocks due to the interaction with hydrothermal fluids. This process can be
683 reflected as an enrichment of Sm related to Nd. Other authors, however, explain this
684 enrichment as a result of both magmatic evolution (e.g., McLennan, 1994; Pan, 1997)
685 and weathering processes after exhumation (e.g., Masuda and Akagi, 1989; Takahasi
686 et al., 2002).

687 In the granites of the southern Central Iberian Zone and the volcanic rocks of
688 Sardinia, positive values in $\varepsilon Nd_{(t)}$ could be interpreted as a more primitive nature of
689 their parental magmas, even though the samples with highest $T_{DM}$ values are those
690 that display higher $^{147}Sm/^{144}Nd$ ratios (> 0.17; Table 2).

691 The volcanic rocks of the Central Iberian Zone display some differences following a
692 N-S transect, being $\varepsilon Nd_{(t)}$ values less variable in the north ($\varepsilon Nd_{(t)}$: –4.0 to –5.0) than in
693 the south ($\varepsilon Nd_{(t)}$: –1.6 to –5.5). The isotopic signature of the Urra volcaniclastic rocks is
694 compatible with magmas derived from young crustal rocks, with intermediate to felsic
695 igneous compositions (Solá et al., 2008). The volcanic rocks of the northern Central
696 Iberian Zone could be derived from old crustal rocks (Montero et al., 2007). The
697 isotopic composition of the granitoids from the southern Central Iberian Zone has more
698 primitive characters than those of the northern Central Iberian Zone, suggesting
699 different sources for both sides (Talavera et al., 2013). *OSS* shows lower inheritance
700 patterns, more primitive Sr–Nd isotopic composition than other rocks of the Ollo de
701 Sapo suite, and an age some 15 m.y. younger than most meta-igneous rocks of the
702 Sanabria region (Montero et al., 2009), likely reflecting a greater mantle involvement in
703 its genesis (Díez-Montes et al., 2008).
704 According to Talavera et al. (2013), the Cambro–Ordovician rocks of the Galicia-
705 Trás-os-Montes Zone schistose area and the magmatic rocks of the northern Central
706 Iberian Zone are contemporary. Both metavolcanic and metagranitic rocks almost
707 share the same isotopic compositions.
708 The Upper Ordovician orthogneisses from the Occitan Domain show very little
709 variation in $\varepsilon Nd_{(t)}$ values (–3.5 to –4.0), typical of magmas derived from young crustal
710 rocks. The variation in TDM values is also small (1.4 to 1.8 Ga) indicating similar
711 crustal residence times to other rock groups.
712 In Sardinia, $\varepsilon Nd_{(t)}$ values present a greater variation (–1.6 to –3.3), but they are also
713 included in the typical continental crustal range. As noted above, anormal TDM values
714 (between 1.2 to 4.5 Ga) may be due to post-magmatic hydrothermal alteration
715 processes.
716

717 **5. Geodynamic setting**

718

719 In the Iberian Massif, the Ediacaran–Cambrian transition was marked by
720 paraconformities and angular discordances indicating the passage from Cadomian
721 volcanic arc to rifting conditions. The axis of the so-called Ossa-Morena Rift lies along
722 the homonymous Zone (Quesada, 1991; Sánchez-García et al., 2003, 2008, 2010)
723 close to the remains of the Cadomian suture (Murphy et al., 2006). Rifting conditions
724 were accompanied by a voluminous magmatism that changed from peraluminous acid
725 to bimodal (Sánchez-García et al., 2003, 2008, 2016, 2019). Some authors (Álvaro et
726 al., 2014; Sánchez-García et al., 2019) propose that this rift resulted from a SW-to-NE
727 inward migration, toward innermost parts of Gondwana, of rifting axes from the Anti-
728 Atlas in Morocco to the Ossa-Morena Zone in the Iberian Massif. According to this
729 proposal the rifting developed later (in Cambro–Ordovician times) in the Iberian,
730 Armorican and Bohemian massifs.

731 The Furongian–Ordovician transition to drifting conditions is associated, in the
732 Iberian Massif, Occitan Domain, Pyrenees and Sardinia, with a stepwise magmatic
733 activity contemporaneous with the record of the Toledanian and Sardic unconformities.
734 These, related to neither metamorphism nor penetrative deformations, are linked to
735 uplift, erosion and irregularly distributed mesoscale deformation that gave rise to
736 angular unconformities up to 90º. The time span involved in these gaps is similar (22
737 m.y. in the Iberian Massif, 16–23 m.y. in the Pyrenees and 18 m.y. in Sardinia). This
738 contrasts with the greater time span displayed by the magmatic activity (30–45 m.y.),
739 which started before the unconformity formation (early Furongian in the Central Iberian
740 Zone vs. Floian in the Pyrenees, Occitan Domain and Sardinia), continued during the
741 unconformity formation (Furongian and early Tremadocian in the Central Iberian Zone
742 vs. Floian–Darriwilian in the Pyrenees, Occitan Domain and Sardinia), and ended
743 during the sealing of the uplifted and eroded palaeorelief (Tremadocian–Floian
744 volcaniclastic rocks at the base of the Armorican Quartzite in the Central Iberian Zone
745 vs. Sandbian–Katian volcanic rocks at the lowermost part of the Upper Ordovician
746 successions in the Pyrenees, Occitan Domain and Sardinia; Gutiérrez-Alonso et al.,

747 2007, 2016; Navidad et al., 2010; Martínez et al., 2011; Álvaro et al., 2016; Martí et al.,
748 2019). In the Pyrenees, Upper Ordovician magmatism and sedimentation coexist with
749 normal faults controlling marked thickness changes of the basal Upper Ordovician
750 succession and cutting the lower part of this succession, the Sardic unconformity and
751 the underlying Cambro–Ordovician sequence (Puddu et al., 2018, 2019).

752 Although the Toledanian and Sardic Phases reflect similar geodynamic conditions in
753 two distinct palaeogeographic areas, at present forming the western and eastern
754 branches of the Variscan Ibero-Armorican Arc, they display different peaks in magmatic
755 activity with a minor chronological overlapping (Fig. 3). This may reflect a SW-to-NE
756 “zip-like” propagation of the latest Ediacaran–Terreneuvian rifting axes in the so-called
757 Atlas-Ossa Morena Rift.

758

759 *Toledanian Phase*

760

761 The Early Ordovician (Toledanian) magmatism of the Central Iberian Zone evolved to a
762 typical passive-margin setting, with geochemical features dominated by acidic rocks,
763 peraluminous and rich in K, and lacking any association with basic or intermediate
764 rocks. Some of the orthogneisses of the Galicia-Trás-os-Montes Zone basal and
765 allochthonous complex units share these same patterns. This fact has been interpreted
766 by some authors as a basin environment subject to important episodes of crustal
767 extension (Martínez-Catalán et al., 2007; Díez-Montes et al., 2010). In contrast,
768 Villaseca et al. (2016) interpreted this absence as evidence against rifting conditions,
769 though the absence of contemporary basic magmatism may be explained by the partial
770 fusion of a thickened crust, through recycling of Neoproterozoic crustal materials. The
771 thrust of a large metasedimentary sequence could generate dehydration and
772 metasomatism of the rocks above this sequence, triggering partial fusion at different
773 levels, although the increase in peraluminosity with the basicity of the orthogneisses is
774 against any AFC process involving mantle materials. However, this increase in

peraluminosity with the basicity has not been revealed in the samples studied above. Following Villaseca et al.'s (2016) model, a flat subduction of the southern part of the Central Iberian Zone would have taken place under its northern prolongation, whereas the reflection of such a subduction is not evident in the field. The calc-alkaline signature of this magmatism has also been taken into account as proof of its relationship with volcanic-arc environments (Valverde-Vaquero and Dunning, 2000). However, calc-alkaline features may be also interpreted as a result of a variable degree of continental crustal contamination and/or previously enriched mantle source (Sánchez-García et al., 2003, 2008, 2016, 2019; Díez-Montes et al., 2010). Finally, other granites not considered here of Tremadocian age have been reported in the southern Central Iberian Zone, such as the Oledo massif and the Beira Baixa-Central Extremadura, which display a I-type affinity (Antunes et al., 2009; Rubio Ordóñez et al., 2012). These granites could represent different sources for the Ordovician magmatism in the Central Iberian Zone.

Sánchez-García et al. (2019) have proposed that the anomaly that produced the large magmatism throughout the Iberian Massif could have migrated from the rifting axis to inwards zones and the acid, peraluminous, K-rich rocks of Mid Ordovician in age should represent the initial stages of a new rifting pulse, resembling the peraluminous rocks of the Early Rift Event *sensu* Sánchez-García et al. (2003) from the Cambrian Epoch 2 of the Ossa-Morena Rift.

In the parautochthon of the Galicia-Trás-os-Montes Zone, the appearance of tholeiitic and alkaline-peralkaline magmatism in the Mid Ordovician would signal the first steps toward extensional conditions (Díez Fernández et al., 2012; Dias da Silva et al., 2016). In the Montagne Noire and the Mouthoumet massifs contemporaneous tholeiitic lavas indicate a similar change in the tectonic regimen (Álvaro et al., 2016). This gradual change in geodynamic conditions is also marked by the appearance of rocks with extensional characteristics in some of subgroups considered here, such as the Central Iberian Zone (San Sebastián orthogneisses), eastern Pyrenees (Casemí

803 orthoneisses, and G1), volcanic rocks of the Occitan Domain, and the orthogneises
804 and volcanic rocks from Sardinia.
805
806 *Sardic Phase*
807
808 In the eastern Pyrenees, two peaks of Ordovician magmatic activity are observed
809 (Casas et al., 2019). Large Lower–Middle Ordovician peraluminous granite bodies are
810 known representing the protoliths of numerous gneissic bodies with laccolithic
811 morphologies. In the Canigó massif, the Upper Ordovician granite bodies (protholits of
812 Cadí, Casemí, *G1*) are encased in sediments of the Canaveilles and Jujols groups.
813 During this time span, there was generalized uplift and erosion that culminated with the
814 onset of the Sardic unconformity. The Sardic Phase was succeeded by an extensional
815 interval related to the formation of normal faults affecting the pre–unconformity strata
816 (Puddu et al., 2018, 2019). The volcanic arc signature can be explain by crustal
817 recycling (Navidad et al., 2010; Casas et al., 2010; Martínez et al., 2011), as in the
818 case of the Toledanian Phase in the Central Iberian Zone, although, according to
819 Casas et al. (2019), the Pyrenees and the Catalan Coastal Ranges were probably
820 fringing the Gondwana margin in a different position than that occupied by the Iberian
821 Massif. As a whole, the Ordovician magmatism in the Pyrenees lasted about 30 m.y.,
822 from ca 477 to 446 Ma, in a time span contemporaneous with the formation of the
823 Sardic unconformity (Fig. 2). Recently, Puddu et al. (2019) proposed that a thermal
824 doming, bracketted between 475 and 450 Ma, could have stretched the Ordovician
825 lithosphere. The emersion and denudation of the inherited Cambrian–Ordovician
826 palaeorelief would have given rise to the onset of the Sardic unconformity. According to
827 these authors, thermal doming triggered by hot mafic magma underplating may also be
828 responsible for the late Early–Late Ordovician coeval magmatic activity.
829 In the Occitan Domain, there was a dramatic volcanic event in early Tremadocian
830 times, with the uprising of basin floors and the subsequent effusion of abundant

831 rhyolitic activities under subaerial explosive conditions (Larroque volcanosedimentary
832 Complex in the Montagne Noire, and Davejean acidic volcanic counterpart in the
833 Mouthoumet Massif). Pouclet el al., (2017) interpreted this as a delayed Ollo de Sapo-
834 style outpouring where a massive crustal melting required a rather significant heat
835 supply. Asthenospheric upwelling leading to the interplay of lithospheric doming,
836 continental break-up, and a decompressionally driven mantle melting can explain such
837 a great thermal anomaly. The magmatic products accumulated on the mantle-crust
838 contact would provide enough heat transfer for crustal melting (Huppert and Sparks,
839 1988). Subsequently, a post–Sardic reactivation of rifting conditions is documented in
840 the Cabrières klippes (southern Montagne Noire) and the Mouthoumet massif. There, a
841 Late Ordovician fault-controlled subsidence linked to the record of rift-related tholeiites
842 (Roque de Bandies and Villerouge formations) were contemporaneous with the record
843 of the Hirnantian glaciation (Álvaro et al., 2016). Re-opening of rifting branches
844 (Montagne Noire and Mouthoumet massifs) was geometrically recorded as onlapping
845 patterns and final sealing of Sardic palaeoreliefs by Silurian and Lower Devonian
846 strata.

847 Sardinia illustrates an almost complete record of the Variscan Belt (Carmignani et
848 al., 1994; Rossi et al., 2009). Some plutonic orthogneises of the Inner Zone belong to
849 this cycle, such as the orthogneises of Golfo Aranci (Giacomini et al., 2006). Gaggero
850 et al. (2012) described three magmatic cycles. The first cycle is well represented in the
851 Sarrabus unit by Furongian–Tremadocian volcanic and subvolcanic interbeds within a
852 terrigenous sucession (San Vito Formation) which is topped by the Sardic
853 uncomformity. Some plutonic orthogneises of the Inner Zone belong to this cycle, such
854 as the orthogneises of Golfo Aranci (Giacomini et al., 2006) and the PB orthogneiss of
855 Punta Bianca). The second Mid–Ordovician cycle, about 50 m.y. postdating the
856 previous cycle, is of an arc-volcanic type with calc-alkaline affinity and acidic-to-
857 intermediate composition. The acidic metavolcanites are referred in the literature as
858 “porphyroids”, which crop out in the External Nappe Zone and some localities of the

Inner Zone. The intermediate to basic derivates are widespread in Central Sardinia (Serra Tonnai Formation). Some plutonic rocks (Mt. Filau orthogneisses and Capo Spartivento) of the second cycle are discussed above. The third cycle consists of alkalic meta-epiclastites interbedded in post–Sandbian strata and metabasites marking the Ordovician/Silurian contact and reflecting rifting conditions. In this work only the first two cycles are considered. Giacomini et al. (2006) cite coeval mafic rocks of felsic magmatism of Mid Ordovician age (Cortesogno et al., 2004; Palmeri et al., 2004; Giacomini et al., 2005), although they interpret a subduction scenario of the Hun terrain below Corsica and Sardinia in the Mid Ordovician.

*Origin of intracrustal siliceous melts*

In this scenario, the key to generate large volumes of acidic rocks in an intraplate context would be the existence of a lower-middle crust, highly hydrated, in addition to a high heat flow, possibly caused by mafic melts (Bryan et al., 2002; Díez-Montes, 2007). This could be the scenario initiated by the arrival of a thermal anomaly in a subduction-free area (Sánchez-García et al., 2003, 2008, 2019; Álvaro et al., 2016). The formation of large volumes of intracrustal siliceous melts could act as a viscous barrier, preventing the rise of mafic magmas within volcanic environments, and causing the underplating of these magmas at the contact between the lower crust and the mantle (Huppert and Sparks, 1988; Pankhurst et al., 1998; Bindeman and Valley, 2003). The cooling of these magmas could lead to crustal thickening and in this case, the volcanic arc signature can be explained by crustal recycling (Navidad et al., 2010; Díez-Montes et al., 2010; Martínez et al., 2011).

Sánchez-García et al. (2019) have proposed that the anomaly that produced the large magmatism throughout the Iberian Massif could have migrated from the rifting axis to inwards zones and the acid, peraluminous, K-rich rocks of Mid Ordovician in age should represent the initial stages of a new rifting pulse, resembling the

peraluminous rocks of the Early Rift Event *sensu* Sánchez-García et al. (2003) from the Cambrian Epoch 2 of the Ossa-Morena Rift. In the parautochthon of the Galicia-Trás-os-Montes Zone, the appearance of tholeiitic and alkaline-peralkaline magmatism in the Mid Ordovician would signal the first steps toward extensional conditions (Díez Fernández et al., 2012; Dias da Silva et al., 2016). In the Montagne Noire and the Mouthoumet massifs contemporaneous tholeiitic lavas indicate a similar change in the tectonic regimen (Álvaro et al., 2016). This change in geodynamic conditions is also marked by the appearance of rocks with extensional characteristics in some of subgroups considered here, such as the Central Iberian Zone (San Sebastián orthogneisses), eastern Pyrenees (Casemí orthogneisses, and G1), volcanic rocks of the Occitan Domain, and the orthogneises and volcanic rocks from Sardinia. In the Pyrenees, Puddu et al. (2019) proposed that a thermal doming, between 475 and 450 Ma, should have stretched the Ordovician lithosphere leading to emersion and denudation of a Cambrian–Ordovician palaeorelief, and giving rise to the onset of the Sardic unconformity. According to these authors, thermal doming triggered by hot mafic magma underplating may also be responsible for the late Early–Late Ordovician coeval magmatic activity

A major continental break-up, leading to the so-called Tremadocian Tectonic Belt, was suggested by Pouclet et al. (2017), which initiated by upwelling of the asthenosphere and tectonic thinning of the lithosphere. Mantle-derived mafic magmas were underplated at the mantle-crust transition zone and intruded the crust. These magmas provided heat for crustal melting, which supplied the rhyolitic volcanism. After emptying the rhyolitic crustal reservoirs, the underlying mafic magmas finally rose and reached the surface. According to Pouclet et al. (2017), the acidic magmatic output associated with the onset of the Larroque metarhyolites resulted in massive crustal melting requiring a rather important heat supply. Asthenospheric upwelling leading to lithospheric doming, continental break-up, and a decompressionally driven mantle

914 melting can explain such a great thermal anomaly. Magmatic products accumulated on
915 the mantle-crust contact providing enough heat transfer for crustal melting.
916
917 **6. Conclusions**
918
919 A geochemical comparison of 231 plutonic and volcanic samples of two major suites,
920 Furongian–Mid Ordovician and Late Ordovician in age, from the Central Iberian and
921 Galicia-Trás-os-Montes Zones of the Iberian Massif and in the eastern Pyrenees,
922 Occitan Domain (Albigeois, Montagne Noire and Mouthoumet massifs) and Sardinia
923 points to a predominance of materials derived from the melting of metasedimentary
924 rocks, peraluminous and rich in $SiO_2$ and $K_2O$. The total content in REE is moderate to
925 high. Most felsic rocks display similar chondritic normalized REE patterns, with an
926 enrichment of LREE relative to HREE, which should indicate the involvement of crustal
927 materials in their parental magmas.
928 $Zr/TiO_2$, Zr/Nb, Nb/Y and Zr vs. Ga/Al ratios, and REE and $\varepsilon$Nd values reflect
929 contemporaneous arc and extensional scenarios, which progressed to distinct
930 extensional conditions finally associated with outpouring of mafic tholeiitic-dominant
931 rifting lava flows. Magmatic events are contemporaneous with the formation of the
932 Toledanian (Furongian–Early Ordovician) and Sardic (Early–Late Ordovician)
933 unconformities, related to neither metamorphism nor penetrative deformation. The
934 geochemical and structural framework precludes subduction generated melts reaching
935 the crust in a magmatic arc to back-arc setting. On the contrary, it favours partial
936 melting of sediments and/or granitoids in a continental lower crust triggered by the
937 underplating of hot mafic magmas related to the opening of the Rheic Ocean as a
938 result of asthenospheric upwelling.
939
940 **7. Acknowledgements**
941

942 The authors thank the constructive and useful revisions made by Laura Gaggero
943 (Genoa, Italy) and Jochen Mezger (Fairbanks, USA). This paper is a contribution to
944 projects CGL2017-87631-P and PGC2018-093903-B-C22 from Spanish Ministry of
945 Science and Innovation. We acknowledge support of the publication fee by the CSIC
946 Open Access Publication Support Initiative through its Unit of Information Resources
947 for Research (URICI).

948

949 **Data availability** - All data included in the paper and the Repository Data.

950

951 **Author contributions** - JJA, TSG and JMC: Methodology (Lead), Supervision (Lead),
952 Writing – Original Draft (Lead), Writing – Review & Editing (Lead); CP, ADM, ML & GO:
953 Methodology (Supporting), Supervision (Supporting), Writing – Original Draft
954 (Supporting), Writing – Review & Editing (Supporting).

955

956 **Competing interests** - No competing interests

957

958 **References**

959

960 Alabouvette, B., Demange, M., Guérangé-Lozes, J., Ambert, P., 2003. Notice
961 explicative de la carte géologique de Montpellier au 1/250 000. BRGM, Orléans.
962 Álvaro, J.J., Vizcaïno, D., 2018. The Furongian break-up (rift-drift) transition in the Anti-
963 Atlas, Morocco. J. Iberian Geol. 44, 567–587.
964 Álvaro, J.J., Ferretti, F., González-Gómez, C., Serpagli, E., Tortello, M. F., Vecoli, M.,
965 Vizcaïno, D., 2007. A review of the Late Cambrian (Furongian) palaeogeography in
966 the western Mediterranean region, NW Gondwana. Earth-Sci. Rev. 85, 47–81.
967 Álvaro, J.J., Ezzouhairi, H., Ribeiro, M.L., Ramos, J.F., Solá, A.R., 2008. Early
968 Ordovician volcanism of the Iberian Chains (NE Spain) and its influence on
969 preservation of shell concentrations. Bull. Soc. géol. France 179(6), 569–581.

970 Álvaro, J.J., Bellido, F., Gasquet, D., Pereira, F., Quesada, C., Sánchez-García, T.,
971 2014a. Diachronism of late Neoproterozoic–Cambrian arc-rift transition of North
972 Gondwana: a comparison of Morocco and the Iberian Ossa-Morena Zone. J. Afr.
973 Earth Sci. 98, 113–132.
974 Álvaro, J.J., Bauluz, B., Clausen, S., Devaere, L., Gil Imaz, A., Monceret, E., Vizcaïno,
975 D., 2014b. Stratigraphy of the Cambrian–Lower Ordovician volcanosedimentary
976 complexes, northern Montagne Noire, France. Stratigraphy 11, 83–96.
977 Álvaro, J.J., Colmenar, J., Monceret, E., Pouclet, A., Vizcaïno, D., 2016. Late
978 Ordovician (post–Sardic) rifting branches in the North Gondwanan Montagne Noire
979 and Mouthoumet massifs of southern France. Tectonophysics 681, 111–123.
980 Álvaro, J.J., Casas, J.M., Clausen, S., Quesada, C., 2018. Early Palaeozoic
981 geodynamics in NW Gondwana. J. Iberian Geol. 44, 551–565.
982 Álvaro, J.J., Cortijo, I., Jensen, S., Lorenzo, S., Palacios, T., Pieren, A., 2019. Updated
983 stratigraphic framework and biota of the Ediacaran and Terreneuvian in the Alcudia-
984 Toledo Mountains of the Central Iberian Zone, Spain. Est. Geol. 75(2), e093.
985 Antunes, I.M.H.R., Neiva, A.M.R., Silva, M.M.V.G., Corfu, F., 2009. The genesis of I-
986 and S-type granitoid rocks of the Early Ordovician Oledo pluton, Central Iberian
987 Zone (central Portugal). Lithos 111, 168–185.
988 Arthaud, F., 1970. Etude tectonique et microtectonique comparée de deux domaines
989 hercyniens: les nappes de la Montagne Noire (France) et l'anticlinorium de
990 l'Iglesiente (Sardaigne). PhD, Univ. Montpellier.
991 Ayora, C., 1980. Les concentrationes metàl·liques de la Vall de Ribes. PhD, Univ.
992 Barcelona.
993 Ballèvre, M., Fourcade S., Capdevila, R., Peucat, J.J., Cocherie, A., Mark Fanning, C.,
994 2012. Geochronology and geochemistry of Ordovician felsic volcanism in the
995 Southern Armorican Massif (Variscan belt, France): Implications for the breakup of
996 Gondwana. Gondwana Res. 21, 1019–1036.

997 Barca, S., 1991. Phénomènes de resédimentation et flysch hercynien à faciès Culm
998 dans le “synclinal du Sarrabus” (SE de la Sardaigne, Italie). C. R. Acad. Sci., Paris
999 313(2), 1051–1057.
1000 Barca, S., Cherchi, A., 2004. Regional geological setting. In: Barca, S., Cherchi, A.
1001 (eds.), Sardinian Palaeozoic Basement and its Meso–Cainozoic Cover (Italy). 32nd
1002 Int. Geol. Congress. Field Trip Guide Book–P39 (5), 3–8.
1003 Barca, S., Carmignani, L., Maxia, M., Oggiano, G., Pertusati, P.C., 1986. The Geology
1004 of Sarrabus. In: Guide-Book to the Excursion on the Paleozoic Basement of Sardinia
1005 (Carmignani, L., Cocozza, T., Ghezzo, C., Pertusati, P.C., Ricci, C.A., eds.). IGCP
1006 Newsl., Spec. Iss. 5, 51–60.
1007 Barca, S., Cocozza, T., Del Rio, M., Pillola, G.L., Pittau Demelia, P., 1987. Datation de
1008 l’Ordovicien inférieur par *Dictyonema flabelliforme* et acritarches dans la partie
1009 supérieure de la formation “cambrienne” de Cabitza (SW de la Sardaigne, Italie):
1010 conséquences géodynamiques. C. R. Acad. Sci., Paris 305(2), 1109–1113.
1011 Barca, S., Del Rio, M., Pittau Demelia, P., 1988. New geological and stratigraphical
1012 data and discovery of Lower Ordovician acritarchs in the San Vito Sandstone of the
1013 Genn’Argiolas Unit (Sarrabus, Southeastern Sardinia). Riv. It. Paleontol. Stratigr. 94,
1014 339–360.
1015 Bea, F., Montero, P., Talavera, C., Zinger, T., 2006. A revised Ordovician age for the
1016 Miranda do Douro orthogneiss, Portugal. Zircon U–Pb ion-microprobe and LA–
1017 ICPMS dating. Geol. Acta 4, 395-401.
1018 Bea, F., Montero, P., González Lodeiro, F., Talavera, C., 2007. Zircon inheritance
1019 reveals exceptionally fast crustal magma generation processes in Central Iberia
1020 during the Cambro–Ordovician. J. Petrol. 48, 2327–2339
1021 Bé Mézème, E., 2005. Contribution de la géochronologie U–Th–Pb sur monazite à la
1022 compréhension de la fusion crustale dans la chaîne Hercynienne française et
1023 implication géodynamique. PhD, Univ. Orléans.

1024 Bindeman, I.N., Valley, J.W., 2003. Rapid generation of both high- and low-$\delta^{18}O$, large-
1025 volume silicic magmas at the Timber Mountain/Oasis Valley caldera complex,
1026 Nevada. Geol. Soc. Am. Bull. 115(5), 581–595.
1027 Boni, M., 1986. The Permo–Triassic vein and paleokarst ores in southwest Sardinia:
1028 contribution of fluid inclusion studies to their genesis and paleoenvironment. Mineral.
1029 Deposita 21, 53–62.
1030 Boni, M., Koeppel, V., 1985. Ore-lead isotope pattern from the Iglesiente-Sulcis area
1031 (SW Sardinia) and the problem of remobilization of metals. Mineral. Deposita 20,
1032 185–193.
1033 Bryan, S.E., Riley, T.R., Jerram, D.A., Stephens, Ch.J., Leat, Ph.T., 2002. Silicic
1034 volcanism: An undervalued component of large igneous provinces and volcanic
1035 rifted margins. In: Volcanic Rifted Margins (Menzies, M.A., Klemperer, S.L., Ebinger,
1036 C.J., Baker, J., eds.). Geol. Soc. Am., Spec. Pap. 362, 99–120.
1037 Calvet, P., Lapierre, H., Chavet, J., 1988. Diversité du volcanisme Ordovicien dans la
1038 région de Pierrefitte (Hautes Pyrénées): rhyolites calco-alcalines et basaltes
1039 alcalins. C. R. Acad. Sci., Paris 307, 805–812.
1040 Calvino, F., 1972. Note Illustrative della Carta Geologica d'Italia, Foglio 227 –
1041 Muravera. Servizio Geologico d'Italia, Roma, 60 p.
1042 Carmignani, L., Cocozza, T., Ghezzo, C., Pertusati, P.C., Ricci, C.A., 1986. Guide-
1043 book to the Excursion on the Palaeozoic Basement of Sardinia. IGCP Project no. 5,
1044 Newsl. Spec. Iss., 1–102.
1045 Carmignani, L., Pertusati, P.C., Barca, S., Carosi, R., Di Pisa, A., Gattiglio, M., et al.,
1046 1992. Struttura della Catena Ercinica in Sardegna. Guida all'escursione del Gruppo
1047 Informali di Geologia Strutturale in Sardegna, 24–29 (Maggio), 1–177.
1048 Carmignani, L., Carosi, R., Di Pisa, A., Gattiglio, M., Musumeci, G., Oggiano, G. et al.,
1049 1994. The Hercynian chain in Sardinia (Italy). Geodin. Acta 7, 31–47.
1050 Carmignani, L., Oggiano, G., Barca, S., Conti, P., Salvadori, I., Eltrudis, A. et al. 2001.
1051 Geologia della Sardegna. Note illustrative della Carta Geologica della Sardegna a

1052 scala 1:200.000. Memorie Descrittive della Carta Geologica d'Italia, Servizio
1053 Geologico 60, 1–283. Instituto Poligrafico e Zecca dello Stato, Roma.
1054 Caron, C., Lancelot, J., Omenetto, P., Orgeval, J.J., 1997. Role of the Sardic tectonic
1055 phase in the metallogenesis of SW Sardinia (Iglesiente): lead isotope evidence.
1056 European J. Miner. 9, 1005–1016.
1057 Casas, J.M., 2010. Ordovician deformations in the Pyrenees: new insights into the
1058 significance of pre–Variscan ('sardic') tectonics. Geol. Mag. 147, 674–689.
1059 Casas, J.M., Fernández, O., 2007. On the Upper Ordovician unconformity in the
1060 Pyrenees: New evidence from the La Cerdanya area. Geol. Acta 5, 193–198.
1061 Casas, J.M., Murphy, J.B. 2018. Unfolding the arc: the use of pre-orogenic constraints
1062 to assess the evolution of the Variscan belt in Western Europe. Tectonophysics 736,
1063 47–61.
1064 Casas, J.M., Palacios, T., 2012. First biostratigraphical constraints on the pre–Upper
1065 Ordovician sequences of the Pyrenees based on organic-walled microfossils. C. R.
1066 Geosci. 344, 50–56.
1067 Casas, J.M., Castiñeiras, P., Navidad, M., Liesa, M., Carreras, J., 2010. New insights
1068 into the Late Ordovician magmatism in the Eastern Pyrenees: U–Pb SHRIMP zircon
1069 data from the Canigó massif. Gondwana Res. 17, 317–324.
1070 Casas, J.M., Álvaro, J.J., Clausen, S., Padel, M., Puddu, C., Sanz-López, J., Sánchez-
1071 García, T., Navidad, M., Castiñeiras, P., Liesa, M., 2019. Palaeozoic basement of
1072 the Pyrenees. In: The Geology of Iberia: A Geodynamic Approach (Quesada, C.,
1073 Oliveira, J.T., eds.). Regional Geology Reviews, vol. 2, 229–259. Springer,
1074 Heidelberg.
1075 Castiñeiras, P., Villaseca, C., Barbero, L., Martín-Romera, C., 2008a. SHRIMP U–Pb
1076 zircon dating of anatexis in high-grade migmatite complexes of Central Spain:
1077 implications in the Hercynian evolution of Central Iberia. Int. J. Earth Sci. 97, 35–50.
1078 Castiñeiras, P., Navidad, M., Liesa, M., Carreras, J., Casas, J.M., 2008b. U–Pb zircon
1079 ages (SHRIMP) for Cadomian and Lower Ordovician magmatism in the Eastern

1080 Pyrenees: new insights in the pre–Variscan evolution of the northern Gondwana
1081 margin. Tectonophysics 46, 228–239.
1082 Castro, A., García-Casco, A., Fernández, C., Corretgé, L.G., Moreno-Ventas, I., Gerya,
1083 T., Löw, I., 2009. Ordovician ferrosilicic magmas: experimental evidence for
1084 ultrahigh temperaturas affecting a metagreywacke source. Gondwana Res. 16, 622–
1085 632
1086 Charles, N., Faure, M., Chen, Y., 2008. The emplacement of the Montagne Noire axial
1087 zone (French Massif Central): New insights from petro-textural, geochronological
1088 and AMS studies. 22ème Réunion des Sciences de la Terre, Nancy, 155.
1089 Charles, N., Faure, M., Chen, Y., 2009. The Montagne Noire migmatitic dome
1090 emplacement (French Massif Central): New insights from petrofabric and AMS
1091 studies. J. Struct. Geol. 31, 1423–1440.
1092 Clariana, P., Valverde-Vaquero, P., Rubio-Ordóñez, A., Beranoaguirre, A., García-
1093 Sansegundo, J., 2018. Pre–Variscan tectonic events and Late Ordovician
1094 magmatism in the Central Pyrenees: U–Pb age and Hf in zircon isotopic signature
1095 from subvolcanic sills in the Pallaresa massif. J. Iberian Geol. 44, 589–601.
1096 Cocco, F., Funedda, A., 2011. New data on the pre–Middle Ordovician deformation in
1097 SE Sardinia: a preliminary note. Rend. online Soc. Geol. It. 15, 34–36.
1098 Cocco, F., Funneda, A., 2017. The Sardic Phase: field evidence of Ordovician tectonics
1099 in SE Sardinia. Italy. Geol. Mag. 156, 25–38.
1100 Cocco, F., Oggiano, G. Funedda, A., Loi, A., Casini, L., 2018. Stratigraphic, magmatic
1101 and structural features of Ordovician tectonics in Sardinia (Italy): a review. J. Iberian
1102 Geol. 44, 619–639.
1103 Cocherie, A., 2003. Datation avec le SHRIMP II du métagranite oeillé du Somail-
1104 Montagne Noire. C. R. technique ANA–ISO/NT, BRGM.
1105 Cocherie, A., Baudin, T., Guerrot, C., Autran, A., Fanning, M.C., Laumonier, B., 2005.
1106 U–Pb zircon (ID–TIMS and SHRIMP) evidence for the early Ordovician intrusion of

1107 metagranites in the late Proterozoic Canaveilles Group of the Pyrenees and the
1108 Montagne Noire (France). Bull. Soc. géol. France 176, 269–282.
1109 Cortesogno, L., Gaggero, L., Oggiano, G., Paquette, J.L., 2004. Different tectono-
1110 thermal evolution paths in eclogitic rocks from the Axial Zone of the Variscan Chain
1111 in Sardinia (Italy) compared with the Ligurian Alps. Ofioliti 29, 125–144.
1112 Costamagna, L.G., Elter, F.M., Gaggero, L., Mantovani, F., 2016. Contact
1113 metamorphism in Middle Ordovician arc rocks (SW Sardinia, Italy): New
1114 paleogeographic constraints. Lithos 264, 577–593.
1115 Cruciani, G., Franceschelli, M., Musumeci, G., Spano, M.E., Tiepolo, M., 2013. U–Pb
1116 zircon dating and nature of metavolcanics and metarkoses from the Monte Grighini
1117 Unit: new insights on Late Ordovician magmatism in the Variscan belt in Sardinia,
1118 Italy. Int. J. Earth Sci. 102, 2077–2096.
1119 Cruciani, G., Franceschelli, M., Puxeddu, M., Tiepolo, M., 2018. Metavolcanics from
1120 Capo Malfatano, SW Sardinia, Italy: New insight on the age and nature of
1121 Ordovician volcanism in the Variscan foreland zone. Geol. J. 53(4), 1573–1585.
1122 Demange, M., 1999. Evolution tectonique de la Montagne noire: un modèle en
1123 transpression. C. R. Acad. Sci., Paris 329, 823–829.
1124 Demange, M., Guérangé-Lozes, J., Guérangé, B., 1996. Notice explicative de la feuille
1125 de Lacaune (987) au 1:50 000. BRGM, Orléans.
1126 Denèle, Y., Barbey, P., Deloule, E., Pelleter, E., Olivier, Ph., Gleizes, G., 2009. Middle
1127 Ordovician U–Pb age of the Aston and Hospitalet orthogneissic laccoliths: their role
1128 in the Variscan evolution of the Pyrenees. Bull. Soc. géol. France 180, 209–221.
1129 DePaolo, D.J., 1981. Neodymiun isotopes in the Colorado Front Range and crust-
1130 mantle evolution in the Proterozoic. Nature 291,193–196.
1131 DePaolo, D.J., 1988. Neodymium isotope geochemistry. An introduction. Minerals and
1132 Rocks Series 20, 1–187. Springer-Verlag, Berlin.
1133 DePaolo, D.J., Wasserburg, G.J., 1976. Nd isotopic variations and petrogenetic
1134 models. Geophys. Res. Lett. 3(5), 249–252.

1135 Dias da Silva, Í., 2014. Geología de las Zonas Centro Ibérica y Galicia-Tras-os-Montes
1136 en la pate oriental del Complejo de Morais, Portugal/España. Serie Nova Terra 45,
1137 1–424.
1138 Dias da Silva, I., Valverde-Vaquero, P., González-Clavijo, E., Díez-Montes, A.,
1139 Martínez-Catalán, J.R., 2012. Structural and stratigraphical significance of U–Pb
1140 ages from the Saldanha and Mora volcanic complexes (NE Portugal, Iberian
1141 Variscides). Géol. France 1, 105–106.
1142 Dias da Silva Í., Valverde-Vaquero, P., González Clavijo E., Díez-Montes A., Martínez
1143 Catalán J.R., 2014. Structural and stratigraphical significance of U–Pb ages from the
1144 Mora and Saldanha volcanic complexes (NE Portugal, Iberian Variscides). In:
1145 Schulmann, K., Martínez Catalán, J. R., Lardeaux, J. M., Janousek, V., Oggiano, G.,
1146 (eds.), The Variscan Orogeny: Extent, Timescale and the Formation of the
1147 European Crust. Geol. Soc., London, Spec. Publ. 405, 115–135.
1148 Dias da Silva, I., Díez Fernández, R., Díez Montes, A., González Clavijo, E., Foster,
1149 D.A., 2016. Magmatic evolution in the N-Gondwana margin related to the opening of
1150 the Rheic Ocean – evidence from the Upper Parautochthon of the Galicia-Trás-os-
1151 Montes Zone and from the Central Iberian Zone (NW Iberian Massif). Int. J. Earth
1152 Sci. 105, 1127–1151.
1153 Díaz-Alvarado, J., Fernández, C., Chichorro, M., Castro, A., Pereira, M.F., 2016.
1154 Tracing the Cambro–Ordovician ferrosilicic to calc-alkaline magmatic association in
1155 Iberia by *in situ* U–Pb SHRIMP zircon geochronology (Gredos massif, Spanish
1156 Central System batholith). Tectonophysics 681, 95–110.
1157 Díez Balda, M.A., Vegas, R., González Lodeiro, F., 1990. Part IV. Central Iberian Zone.
1158 Structures. In: (Dallmeyer, R.D. & Martínez García, E. (eds.), Pre-Mesozoic Geology
1159 of Iberia. Springer-Verlag, Berlin, pp. 172–188.
1160 Díez Fernández, R., Castiñeiras, P., Gómez Barreiro, J., 2012. Age constraints on
1161 Lower Paleozoic convection system: Magmatic events in the NW Iberian Gondwana
1162 margin. Gondwana Res. 21, 1066–1079.

1163 Díez-Montes, A., 2007. La Geología del Dominio “Ollo de Sapo” en las Comarcas de
1164 Sanabria y Terra do Bolo. PhD, Univ. Salamanca. Laboratorio Xelóxico de Laxe,
1165 Serie Nova Terra no. 34, A Coruña.
1166 Díez Montes, A., Martínez Catalán, J.R., Bellido Mulas, F., 2010. Role of the Ollo de
1167 Sapo massive felsic volcanism of NW Iberia in the Early Ordovician dynamics of
1168 northern Gondwana. Gondwana Res. 17, 363–376.
1169 Di Pisa, A., Gattiglio, M., Oggiano, G., 1992. Pre–Hercynian magmatic activity in the
1170 nappe zone (internal and external) of Sardinia: evidence of two within plate basaltic
1171 cycles. In: Contributions to the Geology of Italy with Special Regard to the Paleozoic
1172 Basements (Carmingnani, L., Sassi, F.P., eds.). Newsl. IGCP 276, 107–116.
1173 Echtler, H., Malavieille, J., 1990. Extensional tectonics, basement uplift and Stephano–
1174 Permian collapse basin in a late Variscan metamorphic core complex (Montagne
1175 Noire, southern Massif Central). Tectonophysics 177, 125–138.
1176 El Korh, A., Schmidt , S.Th., Ballèvre, M., Ulianov, A., Bruguier, O., 2012. Discovery of
1177 an albite gneiss from the Ile de Groix (Armorican Massif, France): geochemistry and
1178 LA–ICP–MS U–Pb geochronology of its Ordovician protolith. Int. J. Earth Sci. 101,
1179 1169–1190.
1180 Engel,W., Feist, R., Franke,W., 1980. Le Carbonifère anté–stéphanien de la Montagne
1181 Noire: rapports entre mise en place des nappes et sédimentation. Bull. BRGM 2,
1182 341–389.
1183 Farias, P., Ordoñez-Casado, B., Marcos, A., Rubio-Ordóñez, A., Fanning, C.M., 2014.
1184 U–Pb zircon SHRIMP evidence for Cambrian volcanism in the Schistose Domain
1185 within the Galicia-Trás-os-Montes Zone (Variscan Orogen, NW Iberian Peninsula).
1186 Geol. Acta 12(3), 209–218.
1187 Faure, M., Ledru, P., Lardeaux, J.M., Matte, P., 2004. Paleozoic orogenies in the
1188 French Massif Central. A cross section from Béziers to Lyon. 32nd Int. Geol.
1189 Congress Florence (Italy), Field-trip guide book, 40 p.

1190 Feist, R., Galtier, J., 1985. Découverte de flores d'âge namurien probable dans le
1191 flysch à olistolithes de Cabrières (Hérault). Implications sur la durée de la
1192 sédimentation synorogénique dans la Montagne Noire (France Méridionale). C. R.
1193 Acad. Sci., Paris 300, 207–212.
1194 Franz, L., Romer, R.L., 2007. Caledonian high-pressure metamorphism in the Strona-
1195 Ceneri-Zone (Southern Alps of southern Switzerland and northern Italy). Swiss J.
1196 Geosci. 100, 457–467.
1197 Friedl, G., Finger, F., Paquette, J.L., von Quadt, A., McNaughton, N.J., Fletcher, I.R.,
1198 2004. Pre–Variscan geological events in the Austrian part of the Bohemian Massif
1199 deduced from U–Pb zircon ages. Int. J. Earth Sci. 93, 802–823
1200 Funedda, A., Oggiano, G., 2009. Outline of the Variscan basement of Sardinia. In: The
1201 Silurian of Sardinia. Volume in Honour of Enrico Serpagli (Corradini, C., Ferretti, A.,
1202 Štorch, P., eds.). Rend. Soc. Paleontol. It. 3, 23–35.
1203 Gaggero L., Oggiano G., Funedda A., Buzzi L., 2012. Rifting and arc-related Early
1204 Paleozoic volcanism along the North Gondwana margin: Geochemical and
1205 geological evidence from Sardinia (Italy). J. Geol. 120, 273–292.
1206 García-Arias, M., Díez-Montes, A., Villaseca, C., Blanco-Quintero, I.F. 2018. The
1207 Cambro–Ordovician Ollo de Sapo magmatism in the Iberian Massif and its Variscan
1208 evolution: A review. Earth-Sci. Rev. 176, 345–372.
1209 Gèze, B., 1949. Etude géologique de la Montagne Noire et des Cévennes
1210 méridionales. Mém. Soc. géol. France 62, 1–215.
1211 Giacomini, F, Bomparola, R.M., Ghezzo, C., 2005. Petrology and geochronology of
1212 metabasites with eclogite facies relics from NE Sardinia: constraints for the
1213 Palaeozoic evolution of Southern Europe. Lithos 82, 221–248
1214 Giacomini, F., Bomparola, R.M., Ghezzo, C., Guldbransen, H., 2006. The geodynamic
1215 evolution of the Southern European Variscides: constraints from the U/Pb
1216 geochronology and geochemistry of the lower Palaeozoic magmatic-sedimentary
1217 sequences of Sardinia (Italy). Contrib. Miner. Petr. 152, 19–42.

1218 Guérangé-Lozes, J., Alabouvette, B., 1999. Notice explicative, Carte géol. France (1/50
1219 000), feuille Saint-Sernin-sur-Rance (960). BRGM, Orléans, 84 p.
1220 Guérangé-Lozes, J., Guérangé, B., Mouline, M.P., Delsahut, B., 1996. Notice
1221 explicative, Carte géol. France (1/50 000), feuille Réalmont (959). BRGM, Orléans,
1222 78 p.
1223 Guitard, G., 1970. Le métamorphisme hercynien mésozonal et les gneiss oeillés du
1224 masif du Canigou (Pyrénées orientales). Mém. BRGM 63, 1–353.
1225 Gutiérrez-Alonso, G., Fernández-Suárez, J., Gutiérrez-Marco, J.C., Corfu, F., Murphy,
1226 J.B., Suárez Martínez, S., 2007. U–Pb depositional age for the upper Barrios
1227 Formation (Armorican Quartzite facies) in the Cantabrian zone of Iberia: implications
1228 for stratigraphic correlation and paleogeography. In: The Evolution of the Rheic
1229 Ocean: from Avalonian–Cadomian Active Margin to Alleghenian–Variscan Collision
1230 (Linnemann, R.D., Nance, P., Kraft, G.Z., eds.). Geol. Soc. Am., London, 287–296.
1231 Gutiérrez-Alonso, G., Gutiérrez-Marco, J.C., Fernández-Suárez, J., Bernárdez, E.,
1232 Corfu, F., 2016. Was there a super-eruption on the Gondwanan coast 477 Ma ago?
1233 Tectonophysics 681, 85–94.
1234 Gutiérrez-Marco, J.C., Robardet, M., Rábano, I., Sarmiento, G., San José Lancha,
1235 M.A., Herranz Araújo, P., Pieren Vidal, A., 2002. Ordovician. In: The Geology of
1236 Spain, (Gibbons, W., Moreno, T., eds.), 31–49, Geological Society, London
1237 Gutiérrez-Marco, J.C., Piçarra, J.M., Meireles, C.A., Cózar, P., García-Bellido, D.C.,
1238 Pereira, Z. et al., 2019. Early Ordovician–Devonian Passive margin stage in the
1239 Gondwanan units of the Iberian massif. In: The Geology of Iberia: A Geodynamic
1240 Approach (Quesada, C., Oliveira, J.T., eds.). Regional Geology Reviews, vol. 2, 75–
1241 98. Springer, Heidelberg.
1242 Hartevelt, J.J.A., 1970. Geology of the upper Segre and Valira valleys, central
1243 Pyrenees, Andorra/Spain. Leid. Geol. Meded. 45, 167–236.

1244 Helbing, H., Tiepolo, M., 2005. Age determination of Ordovician magmatism in NE
1245 Sardinia and its bearing on Variscan basement evolution. J. Geol. Soc. 162, 689–
1246 700.
1247 Huppert, H.E., Sparks, R.S.J., 1988. The generation of granitic magmas by intrusion of
1248 basalt into continental crust. J. Petrol. 29, 599–624.
1249 Ibrahim, M.E., El-Kalioby, B.A., Aly, G.M., El-Tohamy, A.M., Watanabe, K., 2015.
1250 Altered granitic rocks, Nusab El Balgum Area, Southwestern Desert, Egypt.
1251 Mineralogical and geochemical aspects of REEs. Ore Geol. Rev. 70, 252–261.
1252 Irber, W., 1999. The lanthanide tetrad effect and its correlation with K/Rb, Eu/Eu*,
1253 Sr/Eu, Y/Ho, and Zr/Hf of evolving peraluminous granite suites. Geochim.
1254 Cosmochim. Acta 63, 489–508.
1255 Jégouzo, P., Peucat, J.J., Audren, C., 1986. Caractérisation et signification
1256 géodynamique des orthogneiss calco-alcalins d'âge ordovicien de Bretagne
1257 méridionale. Bull. Soc. géol. France 2, 839–848.
1258 Kröner, A., Willner, A.P., 1998. Time of formation and peak of Variscan HP–HT
1259 metamorphism of quartz-feldspar rocks in the central Erzgebirge, Saxony, Germany.
1260 Contrib. Mineral. Petrol. 132, 1–20
1261 Lancelot, J. Allegret, A., Iglesias Ponce de León, M., 1985. Outline of Upper
1262 Precambrian and Lower Paleozoic evolution of the Iberian Peninsula according to
1263 U–Pb dating of zircons. Earth Planet. Sci. Lett. 74, 325–337.
1264 Laske, R., Bechstädt, T., Boni, M., 1994. The post–Sardic Ordovician series. In:
1265 Sedimentological, stratigraphical and ore deposits field guide of the autochtonous
1266 Cambro–Ordovician of Southeastern Sardinia (Bechstädt, T., Boni, M., eds.).
1267 Memorie descrittive della carta geologica d'Italia 48, 115–146.
1268 Leat, P.T., Jackson, S.E., Thorpe, R.S., Stillman, C.J., 1986. Geochemistry of bimodal
1269 basalt-subalkaline/peralkaline rhyolite provinces within the Southern British
1270 Caledonides. J. Geol. Soc. 143, 259–273.

1271 Le Corre, C., Auvray, B., Ballèvre, M., Robardet, M., 1991. Le Massif Armoricain. Sci.
1272 Géol., Bull. 44, 31–103.
1273 Lentz, D., 1996. U, Mo and REE mineralization in late-tectonic granite pegmatites,
1274 south-west Grenville Province, Canada. Ore Geol. Rev. 11, 197–227.
1275 Leone, F., Hamman, W., Laske, R., Serpagli, E., Villas, E., 1991. Lithostratigraphic
1276 units and biostratigraphy of the post–Sardic Ordovician sequence in south-west
1277 Sardinia. Boll. Soc. Paleontol. It. 30, 201–235.
1278 Leone, F., Ferretti, A., Hammann, W., Loi, A., Pillola, G.L., Serpagli, E., 2002. A
1279 general view of the post–Sardic Ordovician sequence from SW Sardinia. Rend. Soc.
1280 Paleontol. It. 1, 51–68.
1281 Lescuyer, J.L., Cocherie, A., 1992. Datation sur monozircons des métadacites de
1282 Sériès: arguments pour un âge protérozoïque terminal des **"**schistes X**"** de la
1283 Montagne Noire (Massif central français). C. R. Acad. Sci., Paris (sér. 2) 314, 1071–
1284 1077.
1285 Liesa, M., Carreras, J., Castiñeiras, P., Casas, J.M., Navidad, M., Vilà, M., 2011. U–Pb
1286 zircon age of Ordovician magmatism in the Albera Massif (Eastern Pyrenees). Geol.
1287 Acta 9, 1–9.
1288 Linnemann, U., Gehmlich, M., Tichomirowa, M., Buschmann, B., Nasdala, L., Jonas, P.
1289 et al. 2000. From Cadomian subduction to early Palaeozoic rifting: the evolution of
1290 Saxo-Thuringia at the margin of Gondwana in the light of single zircon
1291 geochronology and basin development (Central European Variscides, Germany). In:
1292 Orogenic Processes: Quantification and Modelling in the Variscan Belt (Franke, W.,
1293 Haak, V., Oncken, O., Tanner, D., eds.). Geol. Soc., London, Spec. Publ. 179, 131–
1294 153.
1295 Loi, A., Dabard, M.P., 1997. Zircon typology and geochemistry in the palaeogeographic
1296 reconstruction of the Late Ordovician of Sardinia (Italy). Sediment. Geol. 112, 263–
1297 279.

1298 Loi, A., Barca, S., Chauvel, J.J., Dabard, M.P., Leone, F., 1992. Analyse de la
1299 sédimentation post-phase sarde les dépôts initiaux à placers du SE de la Sardaigne.
1300 C. R. Soc. géol. France (sér. 2) 315, 1357–1364.
1301 López-Sánchez, M.A., Iriondo, A., Marcos, A., Martínez, F.J., 2015. A U–Pb zircon age
1302 (479 ± 5 Ma) from the uppermost layers of the Ollo de Sapo Formation near Viveiro
1303 (NW Spain): implications for the duration of rifting-related Cambro–Ordovician
1304 volcanism in Iberia. Geol. Mag. 152, 341–350.
1305 Ludwig, K.R., Turi, B., 1989. Paleozoic age of the Capo Spartivento Orthogneiss,
1306 Sardinia, Italy. Chem. Geol. 79, 147–153.
1307 Margalef, A., Castiñeiras, P., Casas, J.M., Navidad, M., Liesa, M., Linnemann, U.,
1308 Hofmann, M., Gärtner, A., 2016. Detrital zircons from the Ordovician rocks of the
1309 Pyrenees: Geochronological constraints and provenance. Tectonophysics 681, 124–
1310 134.
1311 Marini, F., 1988. “Phase“ sarde et distension ordovicienne du domaine sud-varisque,
1312 effets de point chaud? Une hypothèse fondée sur les données nouvelles du
1313 volcanisme albigeois. C. R. Acad. Sci., Paris (sér. 2) 306, 443–450.
1314 Martí, J., Muñoz, J.A., Vaquer, R., 1986. Les roches volcaniques de l’Ordovicien
1315 supérieur de la région de Ribes de Freser-Rocabruna (Pyrénées catalanes):
1316 caractères et signification. C. R. Acad. Sci., Paris 302, 1237–1242.
1317 Martí, J., Solari, L., Casas, J.M., Chichorro, M., 2019. New late Middle to early Late
1318 Ordovician U–Pb zircon ages of extension-related felsic volcanic rocks in the
1319 Eastern Pyrenees (NE Iberia): tectonic implications. Geol. Mag. 156(10), 1783–
1320 1792.
1321 Martínez, F., Iriondo, A., Dietsch, C., Aleinikoff, J.N., Peucat, J.J., Cirès, J., Reche, J.,
1322 Capdevila, R., 2011. U–Pb SHRIMP–RG zircon ages and Nd signature of lower
1323 Paleozoic rifting-related magmatism in the Variscan basement of the Eastern
1324 Pyrenees. Lithos 127, 10–23.

1325 Martínez Catalán, J.R., Hacar Rodríguez, M.P., Villar Alonso, P., Peréz-Estaún, A.,
1326 González Lodeiro, F., 1992. Lower Paleozoic extensional tectonics in the limit
1327 between the West Asturian-Leonese and Central Iberian Zones of the Variscan
1328 Fold-Belt in NW Spain. Geologische Rundschau 81(2), 546–560.
1329 Martínez Catalán, J.R., Arenas, R., Díaz García, F., Gómez Barreiro, J.,
1330 González Cuadra, P., Abati, J. et al. 2007. Space and time in the tectonic
1331 evolution of the northwestern Iberian Massif. Implications for the
1332 comprehension of the Variscan belt. In: 4–D Framework of Continental Crust
1333 (Hatcher, R.D.Jr., Carlson, M.P., McBride, J.H., Martínez Catalán, J.R., eds.).
1334 Geol. Soc. Am., Mem. 200, 403–423.
1335 Martini, I.P., Tongiorgi, M., Oggiano, G., Cocozza, T., 1991. Ordovician alluvial fan to
1336 marine shelf transition in SW Sardinia, Western Mediterranean Sea: tectonically
1337 ("Sardic" phase") influenced clastic sedimentation. Sediment. Geol. 72, 97–115.
1338 Masuda, A., Akagi, T., 1989. Lanthanide tetrad effect observed in leucogranites from
1339 China. Geochem. J. 23, 245–253.
1340 McDougall, N., Brenchley, P.J., Rebelo, J.A., Romano, M., 1987. Fans and fan deltas –
1341 precursors to the Armorican Quartzite (Ordovician) in western Iberia. Geol. Mag.
1342 124, 347–359.
1343 McLennan, S.M., 1994. Rare earth element geochemistry and the "tetrad" effect.
1344 Geochim.Cosmochim. Acta 58, 2025–2033.
1345 Mezger, J., Gerdes, A., 2016. Early Variscan (Visean) granites in the core of central
1346 Pyrenean gneiss domes: implications from laser ablation U–Pb and Th–Pb studies.
1347 Gondwana Res. 29, 181–198.
1348 Mingram, B., Kröner, A., Hegner, E., Krentz, O., 2004. Zircon ages, geochemistry, and
1349 Nd isotopic systematics of pre–Variscan orthogneisses from the Erzgebirge, Saxony
1350 (Germany), and geodynamic interpretation. Int. J. Earth Sci. 93, 706–727.

1351 Monecke, T., Dulski, P., Kempe, U., 2007. Origin of convex tetrads in rare earth
1352 element patterns of hydrothermally altered siliceous igneous rocks from the
1353 Zinnwald Sn–W deposit, Germany. Geochim. Cosmochim. Acta 71, 335–353.
1354 Montero, P., Bea, F., González-Lodeiro, F., Talavera, C., Whitehouse, M.J., 2007.
1355 Zircon ages of the metavolcanic rocks and metagranites of the Ollo de Sapo Domain
1356 in central Spain: implications for the Neoproterozoic to Early Palaeozoic evolution of
1357 Iberia. Geol. Mag. 144, 963–976.
1358 Montero, P., Talavera, C., Bea, F., Lodeiro, F.G., Whitehouse, M.J., 2009. Zircon
1359 geochronology of the Ollo de Sapo Formation and the age of the Cambro–
1360 Ordovician rifting in Iberia. J. Geol. 117, 174–191.
1361 Murphy, J.B., Gutiérrez-Alonso, G., Nance, R.D., Fernández-Suárez, J., Keppie, J.D.,
1362 Quesada, C. et al., 2006. Origin of the Rheic Ocean: rifting along a Neoproterozoic
1363 suture? Geology 34, 325–328.
1364 Nance, R.D., Gutiérrez-Alonso, G., Keppie, J.D., Linnemann, U., Murphy, J.B.,
1365 Quesada, C. et al., 2010. Evolution of the Rheic Ocean. Gondwana Res.17, 194–
1366 222.
1367 Navidad, M., Castiñeiras, P., 2011. Early Ordovician magmatism in the northern
1368 Central Iberian Zone (Iberian Massif): new U–Pb (SHRIMP) ages and isotopic Sr–
1369 Nd data. 11th ISOS, Alcalá de Henares, May 2011.
1370 Navidad, M., Castiñeiras, P., Casas, J.M., Liesa, M., Fernández-Suárez, J., Barnolas,
1371 A., Carreras, J., Gil-Peña, I., 2010. Geochemical characterization and isotopic ages
1372 of Caradocian magmatism in the northeastern Iberia: insights into the Late
1373 Ordovician evolution of the northern Gondwana margin. Gondwana Res. 17, 325–
1374 337.
1375 Navidad, M., Castiñeiras, P., Casas, J.M., Liesa, M., Belousova, E., Proenza, J.,
1376 Aiglsperger, T., 2018. Ordovician magmatism in the Eastern Pyrenees: Implications
1377 for the geodynamic evolution of northern Gondwana. Lithos 314–315, 479–496.

1378 Neiva, A.M.R., Williams, I.S., Ramos, J.M.F., Gomes, M.E.P., Silva, M.M.V.G.,
1379 Antunes, I.M.H.R., 2009. Geochemical and isotopic constraints on the petrogenesis
1380 of Early Ordovician granodiorite and Variscan two-mica granites from the Gouveia
1381 area, central Portugal. Lithos 111, 186–202.
1382 Oggiano, G., Gaggero, L., Funedda, A., Buzzi, L., Tiepolo, M., 2010. Multiple early
1383 Paleozoic volcanic events at the northern Gondwana margin: U–Pb age evidence
1384 from the southern Variscan branch (Sardinia, Italy). Gondwana Res. 17, 44–58.
1385 Padel, M., Álvaro, J.J., Clausen, S., Guillot, F., Poujol, M., Chichorro, M., Monceret, E.,
1386 Pereira, M.F., Vizcaïno, D., 2017. U–Pb laser ablation ICP–MS zircon dating across
1387 the Ediacaran–Cambrian transition of the Montagne Noire, southern France. C. R.
1388 Geosci. 349, 380–390.
1389 Padel, M., Clausen, S., Álvaro, J.J., Casas, J.M., 2018. Review of the Ediacaran–
1390 Lower Ordovician (pre-Sardic) stratigraphic framework of the Eastern Pyrenees,
1391 southwestern Europe. Geol. Acta 16**,** 339–355
1392 Palme, H., O'Neill, H.S.C., 2004. Cosmochemical estimates of mantle composition. In:
1393 Treatise on Geochemistry 2 (Holland, H.D., Turekian, K.K., eds.), 1–38. Elsevier-
1394 Pergamon, Oxford.
1395 Palmeri, R., Fanning, M., Franceschelli, M., Memmi, I., Ricci, C.A., 2004. SHRIMP
1396 dating of zircons in eclogite from the Variscan basement in northeastern Sardinia
1397 (Italy). N. Jb. Miner., Mh. 6, 275–288.
1398 Pan, Y., 1997. Controls on the fractionation of isovalent trace elements in magmatic
1399 and aqueous systems: evidence from Y/Ho, Zr/Hf, and lanthanide tetrad effect – a
1400 discussion of the article by M. Bau, 1996. Contrib. Mineral. Petrol. 128, 405–408.
1401 Pankhurst, R.J., Rapela, C.W., Saavedra, J., Baldo, E., Dahlquist, J., Pascua, I.,
1402 Fanning, C.M., 1998. The Famatinian magmatic arc in the central Sierras
1403 Pampeanas, and Early to Middle Ordovician continental arc on the Gondwana
1404 margin. In: The Proto-Andean Margin of Gondwana (Pankhurst, R.J., Rapela, C.E.,
1405 eds.). Geol. Soc., London, Spec. Publ. 142, 343–367.

1406 Pavanetto, P., Funedda, A., Northrup, C. J., Schmitz, M., Crowley, J., Loi, A., 2012.
1407 Structure and U–Pb zircon geochronology in the Variscan foreland of SW Sardinia,
1408 Italy. Geol. J. 47, 426–445.
1409 Pearce, J.A., 1996. Sources and settings of granitic rocks. Episodes 19,120–125.
1410 Pearce, J.A., Harris, N.B.W., Tindle, A.G., 1984. Trace element discrimination
1411 diagrams for the tectonic interpretation of granitic rocks. J. Petrol. 25, 956–983.
1412 Pereira, M.F., Solá, A.R., Chichorro, M., Lopes, L., Gerdes, A., Silva, J.B., 2012. North-
1413 Gondwana assembly, break-up and paleogeography: U–Pb isotope evidence from
1414 detrital and igneous zircons of Ediacaran and Cambrian rocks of SW Iberia.
1415 Gondwana Res. 22(3–4), 866–881.
1416 Piercey, S.J., 2011. The setting, style, and role of magmatism in the formation of
1417 volcanogenic massive sulphide deposits. Miner. Deposita 46, 449–471.
1418 Pistis, M., Loi, A., Dabard, M.P., 2016. Influence of relative sea-level variations on the
1419 genesis of palaeoplacers, the examples of Sarrabus (Sardinia, Italy) and the
1420 Armorican Massif (western France). C. R. Geosci. 348(2), 150–157.
1421 Pillola, G.L., Leone, F., Loi, A., 1998. The Cambrian and Early Ordovician of SW
1422 Sardinia. Gior. Geol. (ser. 3), Spec. Iss. 60, 25–38.
1423 Pitra, P., Poujol, M., Den Driessche, J.V., Poilvet, J. C., Paquette, J.L., 2012. Early
1424 Permian extensional shearing of an Ordovician granite: the Saint-Eutrope ‘‘C/S-like’’
1425 orthogneiss (Montagne Noire, French Massif Central). C. R. Geosci. 344, 377–384.
1426 Pouclet, A., Álvaro, J.J., Bardintzeff, J.M., Gil Imaz, A., Monceret, E., Vizcaïno D.,
1427 2017. Cambrian–Early Ordovician volcanism across the South Armorican and
1428 Occitan Domains of the Variscan Belt in France: Continental break-up and rifting of
1429 the northern Gondwana margin. Geosci. Frontiers 8, 25–64.
1430 Puddu, C., Álvaro, J.J., Casas, J.M., 2018. The Sardic unconformity and the Upper
1431 Ordovician successions of the Ribes de Freser area, Eastern Pyrenees. J. Iberian
1432 Geol. 44, 603–617.

1433 Puddu, C., Álvaro, J.J., Carrera, N., Casas, J.M., 2019. Deciphering the Sardic
1434 (Ordovician) and Variscan deformations in the Eastern Pyrenees. J. Geol. Soc.
1435 176(6), 1191–1206.
1436 Quesada, C., 1991. Geological constraints on the Paleozoic tectonic evolution of
1437 tectonostratigraphic terranes in the Iberian Massif. Tectonophysics 185, 225–245.
1438 Rabin, M., Trap, P., Carry, N. Fréville, K. Cenki-Tok, B. Lobjoie, C. Gonçalves, P.,
1439 Marquer, D., 2015. Strain partitioning along the anatectic front in the Variscan
1440 Montagne Noire massif (southern French Massif Central). Tectonics 34, 1709–1735.
1441 Robert, J. F. 1980. Étude géologique et métallogénique du val de Ribas sur le versant
1442 espagnol des Pyrénées catalanes. PhD, Univ. Franche-Comté.
1443 Robert, J.F., Thiebaut, J., 1976. Découverte d'un volcanisme acide dans le Caradoc de
1444 la région de Ribes de Freser (Prov. de Gérone). C. R. Acad. Sci., Paris 282, 2050–
1445 2079.
1446 Roger, F., Respaut, J.P., Brunel, M., Matte, Ph., Paquette, J.L., 2004. Première
1447 datation U–Pb des orthogneiss oeillés de la zone axiale de la Montagne Noire (Sud
1448 du Massif central): nouveaux témoins du magmatisme ordovicien dans la chaîne
1449 varisque. C. R. Geosci. 336, 19–28
1450 Roger, F., Teyssier, C., Respaut, J.P., Rey, P.F., Jolivet, M., Whitney, D.L., Paquette,
1451 J.L., Brunel, M., 2015. Timing of formation and exhumation of the Montagne Noire
1452 double dome, French massif Central. Tectonophysics 640–641, 53–69.
1453 Rollison, H.R., 1993. Using Geochemical Data: Evaluation, Presentation, Interpretation.
1454 Longman Group, London, 352 p.
1455 Romão, J., Dunning, G., Marcos, A., Dias, R., Ribeiro, A., 2010. O lacólito granítico de
1456 Mação-Penhascoso: idade e as suas implicações (SW da Zona Centro-Ibérica). e-
1457 Terra 16, 1–4.
1458 Rossi, P., Oggiano, G., Cocherie, A., 2009. A restored section of the "southern
1459 Variscan realm" across the Corsica-Sardinia microcontinent. C. R. Geosci. 34, 224–
1460 238.

1461 Rubio-Ordóñez, A., Valverde-Vaquero, P., Corretgé, L. G., Cuesta-Fernández, A.,
1462 Gallastegui, G., Fernández-González, M., Gerdes, A., 2012. An Early Ordovician
1463 tonalitic-granodioritic belt along the Schistose-Greywacke Domain of the Central
1464 Iberian Zone (Iberian Massif, Variscan Belt). Geol. Mag. 149, 927–939.
1465 Rudnick, R.L., Gao, S., 2003. Composition of the Continental Crust. In: Treatise on
1466 Geochemistry (Holland, H.D., Turekian, K.K., eds.), vol. 3, 1–64. Elsevier-
1467 Pergamon, Oxford.
1468 Sánchez-García, T., Bellido, F., Quesada, C., 2003. Geodynamic setting and
1469 geochemical signatures of Cambrian–Ordovician rift-related igneous rocks (Ossa-
1470 Morena Zone, SW Iberia). Tectonophysics 365, 233–255.
1471 Sánchez-García, T., Quesada, C., Bellido, F., Dunning, G., González de Tánago, J.,
1472 2008. Two-step magma flooding of the upper crust during rifting: the Early Paleozoic
1473 of the Ossa-Morena Zone (SW Iberia). Tectonophysics 461, 72–90.
1474 Sánchez-García, T., Bellido, F., Pereira, M.F., Chichorro, M., Quesada, C., Pin, Ch.,
1475 Silva, J.B., 2010. Rift-related volcanism predating the birth of the Rheic Ocean
1476 (Ossa-Morena zone, SW Iberia). Gondwana Res. 17, 392–407.
1477 Sánchez-García, T., Quesada, C., Bellido, F., Dunning, G.R., Pin, Ch., Moreno-Eiris,
1478 E., Perejón, A., 2016. Age and characteristics of the Loma del Aire unit (SW Iberia):
1479 Implications for the regional correlation of the Ossa-Morena Zone. Tectonophysics
1480 681, 58–72.
1481 Sánchez-García, T., Chichorro, M., Solá, R., Álvaro, J.J., Díez Montes, A., Bellido, F. et
1482 al. 2019. The Cambrian–Early Ordovician Rift Stage in the Gondwanan Units of the
1483 Iberian Massif. In: The Geology of Iberia: A Geodynamic Approach (Quesada, C.,
1484 Oliveira, J.T., eds.). Regional Geol. Rev. 1, 27–74.
1485 Sarmiento, G.N., Gutiérrez-Marco, J.C., Robardet, M., 1999. Conodontos ordovícicos
1486 del noroeste de España. Aplicación al modelo de sedimentación de la región
1487 limítrofe entre las zonas Asturoccidental-Leonesa y Centroibérica durante el
1488 Ordovícico Superior. Rev. Soc. Geol. España 12, 477–500.

1489 Schaltegger, U., Abrecht, J., Corfu, F., 2003. The Ordovician orogeny in the Alpine
1490 basement: constraints from geochronology and geochemistry in the Aar Massif
1491 (Central Alps). Schweizerische Miner. Petrogr. Mitteil. 83, 183–195.
1492 Shaw, J., Johnston, S., Gutiérrez-Alonso, G., Weil, A.B., 2012. Oroclines of the
1493 Variscan orogen of Iberia: paleocurrent analysis and paleogeographic implications.
1494 Earth Planet. Sci. Lett. 329–330, 60–70.
1495 Shaw, J., Gutiérrez-Alonso, G., Johnston, S., Pastor Galán, D., 2014. Provenance
1496 variability along the early Ordovician north Gondwana margin: paleogeographic and
1497 tectonic implications of U–Pb detrital zircon ages from the Armorican Quartzite of
1498 the Iberian Variscan belt. Geol. Soc. Am. Bull. 126(5–6), 702–719.
1499 Solá, A.R., 2007. Relações Petrogeoquímicas dos Maciços Graníticos do NE
1500 Alentejano. PhD, Univ. Coimbra.
1501 Solá, A.R., Pereira, M.F., Williams, I.S., Ribeiro, M.L., Neiva, A.M.R., Montero, P., Bea,
1502 F., Zinger, T., 2008. New insights from U–Pb zircon dating of Early Ordovician
1503 magmatism on the northern Gondwana margin: the Urra formation (SW Iberian
1504 Massif, Portugal). Tectonophysics 461, 114–129.
1505 Stern, R.J., 2002. Crustal evolution in the East African Orogen: a neodymium isotopic
1506 perspective. J. African Earth Sci. 34, 109–117.
1507 Stille, H., 1939. Bemerkungen betreffend die “Sardische” Faultung und den Ausdruck
1508 “Ophiolitisch”. Zeits. Deuts. Gess. Geowiss. 91, 771–773.
1509 Sun, S.S., McDonough, W.F., 1989. Chemical and isotopic systematics of oceanic
1510 basalts: implications for mantle composition and processes. In: Magmatism in the
1511 Ocean Basins (Saunders, A.D., Norry, M.J., eds.). Geol. Soc., Spec. Publ. 42, 13–
1512 345.
1513 Syme, E.C., 1998. Ore-Associated and Barren Rhyolites in the central Flin Flon Belt:
1514 Case Study of the Flin Flon Mine Sequence. Manitoba Energy and Mines, Open File
1515 Report OF98–9, 1–32

1516 Takahashi, Y., Yoshida, H., Sato, N., Hama, K., Yusa, Y., Shimizu, H., 2002. W- and
1517 M–type tetrad effects in REE patterns for water-rock systems in the Tono uranium
1518 deposit, central Japan. Chem. Geol. 184, 311–335.
1519 Talavera, C., 2009. Pre–Variscan magmatism of the Central Iberian Zone: chemical
1520 and isotope composition, geochronology and geodynamic significance. PhD, Univ.
1521 Granada.
1522 Talavera, C., Bea F, Montero P., Whitehouse, M., 2008. A revised Ordovician age for
1523 the Sisargas orthogneiss, Galicia (Spain). Zircon U–Pb ion-microprobe and LA–
1524 ICPMS dating. Geol. Acta 8, 313–317.
1525 Talavera, C., Montero, P., Bea, F., González Lodeiro, F., Whitehouse, M., 2013. U–Pb
1526 Zircon geochronology of the Cambro–Ordovician metagranites and metavolcanic
1527 rocks of central and NW Iberia. Int. J. Earth. Sci. 102, 1–23.
1528 Taylor, S.R., McLennan, S.M., 1985. The Continental Crust: Its Composition and
1529 Evolution. Blackwell, London, 312 pp.
1530 Teichmüller, R., 1931. Zur Geologie des Thyrrhenisgebietes, Teil 1: Alte und junge
1531 Krustenbewegungen im südlinchen Sardinien. Abh. Der wissen. Gess. Göttingen
1532 (Math.-Phys. Kl) 3, 857–950.
1533 Teipel, U., Eichhorn, R., Loth, G., Rohrmüller, J., Höll, R., Kennedy, A., 2004. U–Pb
1534 SHRIMP and Nd isotopic data from the western Bohemian Massif (Bayerischer
1535 Wald, Germany): Implications for Upper Vendian and Lower Ordovician magmatism.
1536 Int. J. Earth Sci. 93, 782–801.
1537 Thompsom, M.D., Grunow, A.M., Ramezani, J., 2010. Cambro–Ordovician
1538 paleogeography of the Southeastern New England Avalon Zone: Implications for
1539 Gondwana breakup. Geol. Soc. Am. Bull. 122, 76–88.
1540 Tichomirowa, M., Berger, H.J., Koch, E.A,, Belyatski, B., Götze, J., Kempe, U.,
1541 Nasdala, L., Schaltegger, U., 2001. Zircon ages of high-grade gneisses in the
1542 Eastern Erzgebirge (Central European Variscides) – constraints on origin of the

1543 rocks and Precambrian to Ordovician magmatic events in the Variscan foldbelt.
1544 Lithos 56, 303–332.
1545 Tichomirowa, M., Sergeev, S., Berger, H.J., Leonhardt, D., 2012. Inferring protoliths of
1546 high-grade metamorphic gneisses of the Erzgebirge using zirconology,
1547 geochemistry and comparison with lower-grade rocks from Lusatia (Saxothuringia,
1548 Germany). Contrib. Mineral. Petrol. 164, 375–396.
1549 Valverde-Vaquero, P., Dunning, G.R., 2000. New U–Pb ages for Early Ordovician
1550 magmatism in Central Spain. J. Geol. Soc. London 157, 15–26.
1551 Valverde-Vaquero, P., Marcos, A., Farias, P., Gallastegui, G., 2005. U–Pb dating of
1552 Ordovician felsic volcanism in the Schistose Domain of the Galicia-Trás-os-Montes
1553 Zone near Cabo Ortegal (NW Spain). Geol. Acta 3, 27–37.
1554 Valverde-Vaquero, P., Farias, P., Marcos, A., Gallastegui, G., 2007. U–Pb dating of
1555 Siluro–Ordovician volcanism in the Verín synform (Orense, Schistose Domain,
1556 Galicia-Trás-os-montes Zone). Geogaceta 41, 247–250.
1557 Vilà, M., Pin, C., Enrique, P., Liesa, M., 2005. Telescoping of three distinct magmatic
1558 suites in an orogenic setting: Generation of Hercynian igneous rocks of the Albera
1559 Massif (Eastern Pyrenees). Lithos 83, 97–127.
1560 Villaseca, C., Castiñeiras, P., Orejana, D., 2013. Early Ordovician metabasites from the
1561 Spanish Central System: A remnant of intraplate HP rocks in the Central Iberian
1562 Zone. Gondwana Res. 27, 392–409.
1563 Villaseca, C., Merino Martínez, E., Orejana, D., Andersen, T., Belousova, E., 2016.
1564 Zircon Hf signatures from granitic orthogneisses of the Spanish Central System:
1565 Significance and sources of the Cambro–Ordovician magmatism in the Iberian
1566 Variscan Belt. Gondwana Res. 34, 60–83.
1567 Von Quadt, A., 1997. U–Pb zircon and Sr–Nd–Pb whole-rock investigations from the
1568 continental deep drilling (KTB). Geol. Rundsch. 86 (suppl.), S258–S271.

1569 Von Raumer, J.F., Stampfli, G.M., 2008. The birth of the Rheic Ocean – early
1570 Palaeozoic subsidence patterns and tectonic plate scenarios. Tectonophysics 461,
1571 9–20.
1572 Von Raumer, J.F., Stampfli, G.M., Borel, G., Bussy, F., 2002. The organization of pre–
1573 Variscan basement areas at the Gondwana margin. Int. J. Earth Sci. 91, 35–52.
1574 Von Raumer, J.F., Bussy, F., Schaltegger, U., Schulz, B., Stampfli, G., 2013. Pre–
1575 Mesozoic Alpine basements: their place in the European Paleozoic framework.
1576 Geol. Soc. Am. Bull. 125, 89–108.
1577 Von Raumer, J.F., Stampfli, G.M., Arenas, R., Sánchez Martínez, S., 2015. Ediacaran
1578 to Cambrian oceanic rocks of the Gondwanan margin and their tectonic
1579 interpretation. Int. J. Earth Sci. 104, 1107–1121.
1580 Whalen, J.B., Currie, K.L., Chappell, B.W., 1987. A-type granites: Geochemical
1581 characteristics, discrimination and petrogenesis. Contr. Miner. Petrol. 95, 407–419.
1582 Winchester, J.A., Floyd, P.A., 1977. Geochemical discrimination of different magma
1583 series and their differentiation products using immobile elements. Chem. Geol. 20,
1584 325–343.
1585 Zeck, H.P., Whitehouse, M.J., Ugidos, J.M., 2007. 496 ± 3 Ma zircon ion microprobe
1586 age for pre–Hercynian granite, Central Iberian Zone, NE Portugal (earlier claimed
1587 618 ± 9 Ma). Geol. Mag. 144, 21-31.
1588 Zurbriggen, R., 2015. Ordovician orogeny in the Alps – a reappraisal. Int. J. Earth Sci.
1589 104, 335–350.
1590 Zurbriggen, R., 2017. The Cenerian orogeny (early Paleozoic) from the perspective of
1591 the Alpine region. Int. J. Earth Sci. 106, 517–529.
1592 Zurbriggen, R., Franz, L., Handy, M.R., 1997. Pre–Variscan deformation,
1593 metamorphism and magmatism in the Strona-Ceneri Zone (southern Alps of
1594 northern Italy and southern Switzerland). Schweiz. Miner. Petrograph. Mitteil. 77,
1595 361–380.
1596

## FIGURE CAPTIONS

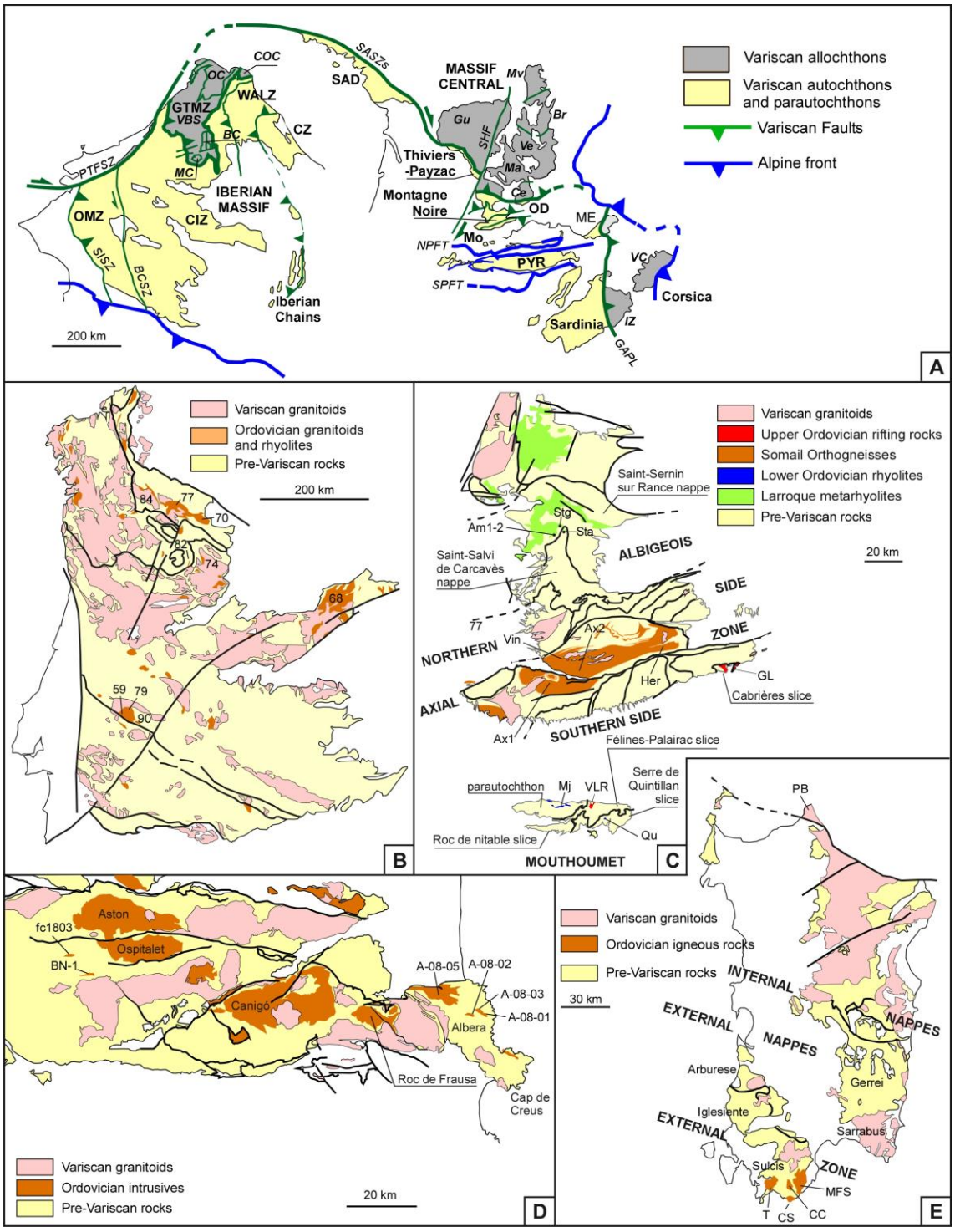


**Figure 1.** A. Reconstruction of the south-western European margin of Gondwana in Late Carboniferous–Early Permian times; modified from Pouclet et al. (2017). B. Setting of samples in the Central Iberian and Galicia-Trás-os-Montes Zones; *59* Carrascal, *68* Guadarrama, *70* Sanabria, *74* Miranda do Douro, *77* Ollo de Sapo, *79*

Portalegre, *82* Saldanha, *84* San Sebastián, *90* Urra, *Bc* Bragança Complex, *BCSZ* Badajoz-Córdoba Shear Zone, *Br* Brévenne, *Ce* Cévennes massif, *CIZ* Central Iberian Zone, *COC* Cabo Ordenes Complex, *CZ* Cantabrian Zone, *GAPL* Grimaud-Asinara-Posada Line, *Gu* Guéret, *GTMZ* Galicia-Trás-os-Montes Zone, *IZ* Inner Zone, *Ma* Margueride, *MC* Morais Complex *ME* Maures-Estérel massif, *Mo* Mouthoumet massif, *Mv* Morvan, *NPFT* North Pyrenean Fault Thrust, *OC* Ordenes Complex, *OD* Occitan Domain, *OMZ* Ossa-Morena Zone, *PTFSZ* PYR Porto-Tomar-Ferreira do Alentejo Shear Zone, Pyrenean Domain, *Sa* Sanabria, *SAD* South Armorican Domain, *SASZs* South-Armorican Shear-Zone southern branch, *SHF* Sillon Houiller Fault, *SISZ* South-Iberian Shear Zone, *SPFT* South Pyrenean Fault Thrust, *Vc* Variscan Corsica, *Ve* Velay, *VBS* Verin-Bragança Synform and *WALZ* West Asturian-Leonese Zone; modified from Sánchez-García et al. (2019). C. Setting of samples in the Montagne Noire and Mouthoumet massifs; *Am1-2* Larroque hamlet (Ambialet), *Stg* St.Géraud, *Sta* St. André, *Mj* Montjoi, *Qu* Quintillan, *GL* Roque de Bandies, *VLR* Villerouge-Termenès, *VIN* Le Vintrou, *HER* Gorges d'Héric (Caroux massif), *Ax1* S Mazamet (Nore massif), *Ax2* (Rou) S Rouayroux (Agout massif); modified from Álvaro et al. (2016). D. Setting of Pyrenean samples; *AB-08-01, 02, 03* Albera metavolcanics, *AB-08-05* Albera orthogneisses, *BN-1* Andorra rhyolites, *fc-1803* Pallaresa rhyolites; modified from Casas et al. (2019). E. Setting of Sardinian samples; *CS 2,3,4,8* Spartivento Cap, *T2* Tuerreda, *CC5* Cuile Culurgioni, *MF1* Monte Filau, *MFS1* Monte Settiballas, *PB* Punta Bianca; modified from Oggiano et al. (2010).

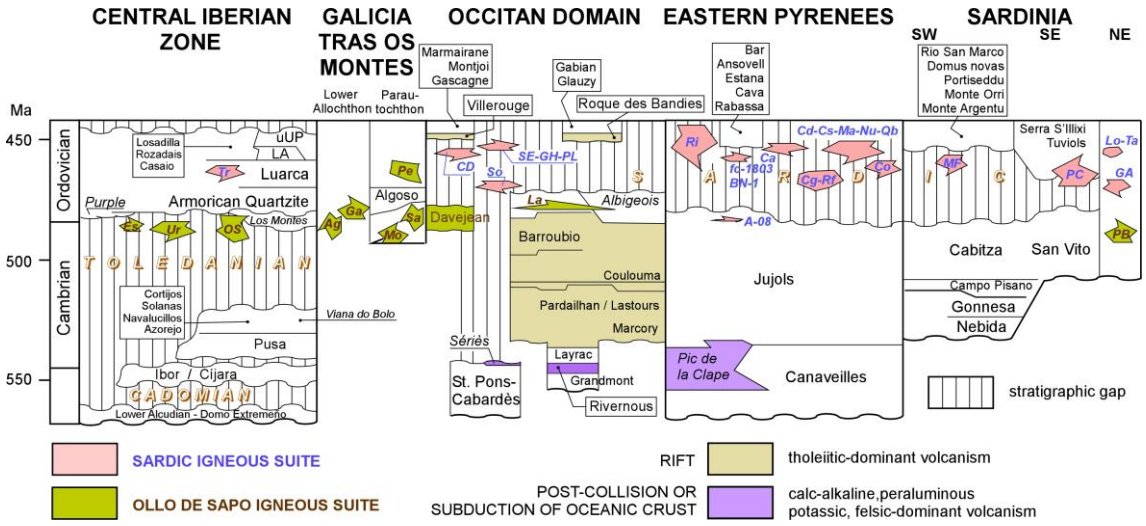


**Figure 2.** Stratigraphic comparison of the Cambro-Ordovician successions from the Central Iberian Zone, Galicia Trás-os-Montes Zone, Occitan Domain, Eastern Pyrenees and Sardinia; modified from Álvaro et al. (2014b, 2016, 2018), Pouclet et al. (2017) and Sánchez-García et al. (2019); the northern Central Iberian Zone, in the vicinity of Salamanca, is not included here (Díez Balda et al., 1990); abbreviations: *A-08* Albera orthogneisses and metavolcanics (ca. 465–472 Ma; Liesa et al., 2011), *Ag* Agualada, *BN-1* Andorra rhyolites, *Ca* Campelles ignimbrites (ca. 455 Ma, Martí et al., 2014), *CD* Cadí gneiss (456 ± 5 Ma, Casas et al., 2010), *Cg* Canigó gneiss (472–462 Ma, Cocherie et al., 2005; Navidad et al., 2018), *Co* Cortalets metabasite (460 ± 3 Ma, Navidad et al., 2018), *Cs* Casemí gneiss (446 ± 5 and 452 ± 5 Ma, Casas et al., 2010), *Es* Estremoz rhyolites (499 Ma, Pereira et al., 2012), *fc-1803* Pallaresa rhyolites (ca. 453 Ma; Clariana et al., 2018), *Ga* Galiñero, *GA* Golfo Aranci orthogneiss (469 ± 3.7 Ma, Giacomini et al., 2006), *GH* Gorges d'Heric orthogneiss (450 ± 6 Ma, Roger et al., 2004), *La* Larroque Volcanic Complex, *LA* La Aquiana Limestone, *Ma* Marialles microdiorite (453 ± 4 Ma, Casas et al., 2010), *Lo* Lodè orthogneiss (456 ± 14 Ma, Helbing and Tiepolo, 2005), *MF* Monte Filau-Capo Spartivento orthogneiss (449 ± 6 Ma, Ludwing and Turi, 1989; 457.5 ± 0,3 and 458.2 ± 0.3 Ma, Pavanetto et al., 2012), *Mo* Mora (493.5 ± 2 Ma, Dias Da Silva et al., 2014), *Nu* Núria gneiss (457 ± 4 Ma, Martínez et al., 2011), *OS* Ollo de Sapo rhyolites and ash-fall tuff beds (ca. 477 Ma.,

Gutiérrez-Alonso et al., 2016), *Pe* Peso Volcanic Complex, *PL* Pont de Larn orthogneiss (456 ± 3 Ma, Roger et al., 2004), *Qb* Queralbs gneiss (457 ± 5 Ma, Martínez et al., 2011), *PB* Punta Bianca orthogneiss (broadly Furongian–Tremadocian in age), *PC* Porto Corallo dacites (465.4 ± 1.9 and 464 ± 1 Ma, Giacomini et al., 2006; Oggiano et al., 2010), *Ri* Ribes granophyre (458 ± 3 Ma, Martínez et al., 2011), *Rf* Roc de Frausa gneiss (477 ± 4, 476 ± 5 Ma, Cocherie et al., 2005; Castiñeiras et al., 2008), *So* Somail orthogneiss (471 ± 4 Ma, Cocherie et al. 2005), *Sa* Saldanha (483.7 ± 1.5; Dias da Silva, 2014), *SE* Saint Eutrope gneiss (455 ± 2 Ma, Pitra et al., 2012), *Ta* Tanaunella orthogneiss 458 ± 7 Ma (Helbing and Tiepolo, 2005), *Tr* Turchas, *Ur* Urra rhyolites and *uUP* undifferentiated Upper Ordovician.

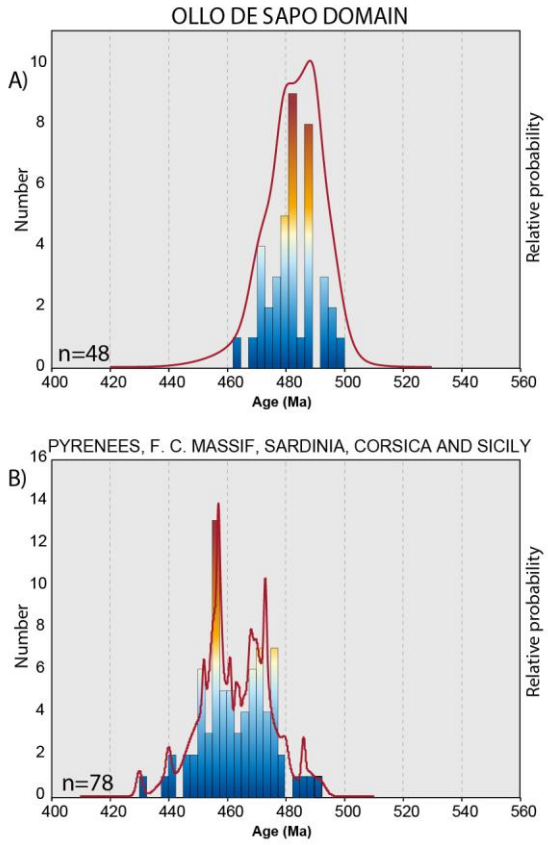


**Figure 3**. Relative probability plots of the age of the Cambrian–Ordovician magmatism for (A) the Ollo de Sapo domain from the Central Iberian Zone; and (B) Pyrenees (Guilleries and Gavarres massifs), French Central Massif (including Montagne Noire), Sardinia, Corsica and Sicily (*n* = number of analyses). Data obtained from references cited in the text.

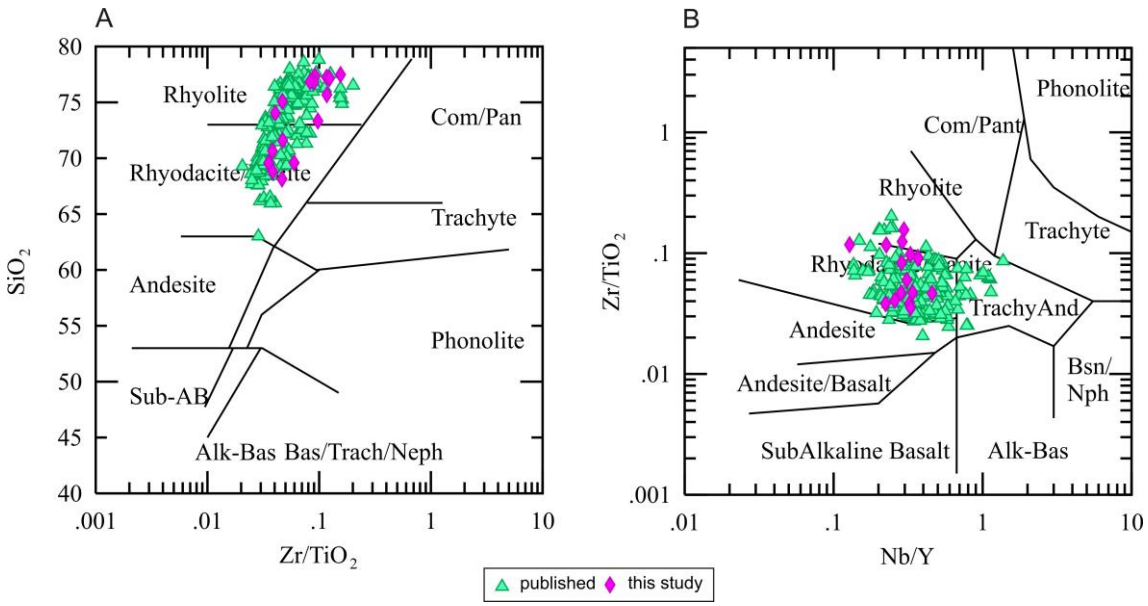


1666

1667

1668 **Figure 4.** $SiO_2$ vs. $Zr/TiO_2$ and $Zr/TiO_2$ vs. Nb/Y plots (Winchester and Floyd, 1977)
1669 showing the composition of new samples (purple diamonds) and those taken from the
1670 literature (green triangles).

1671

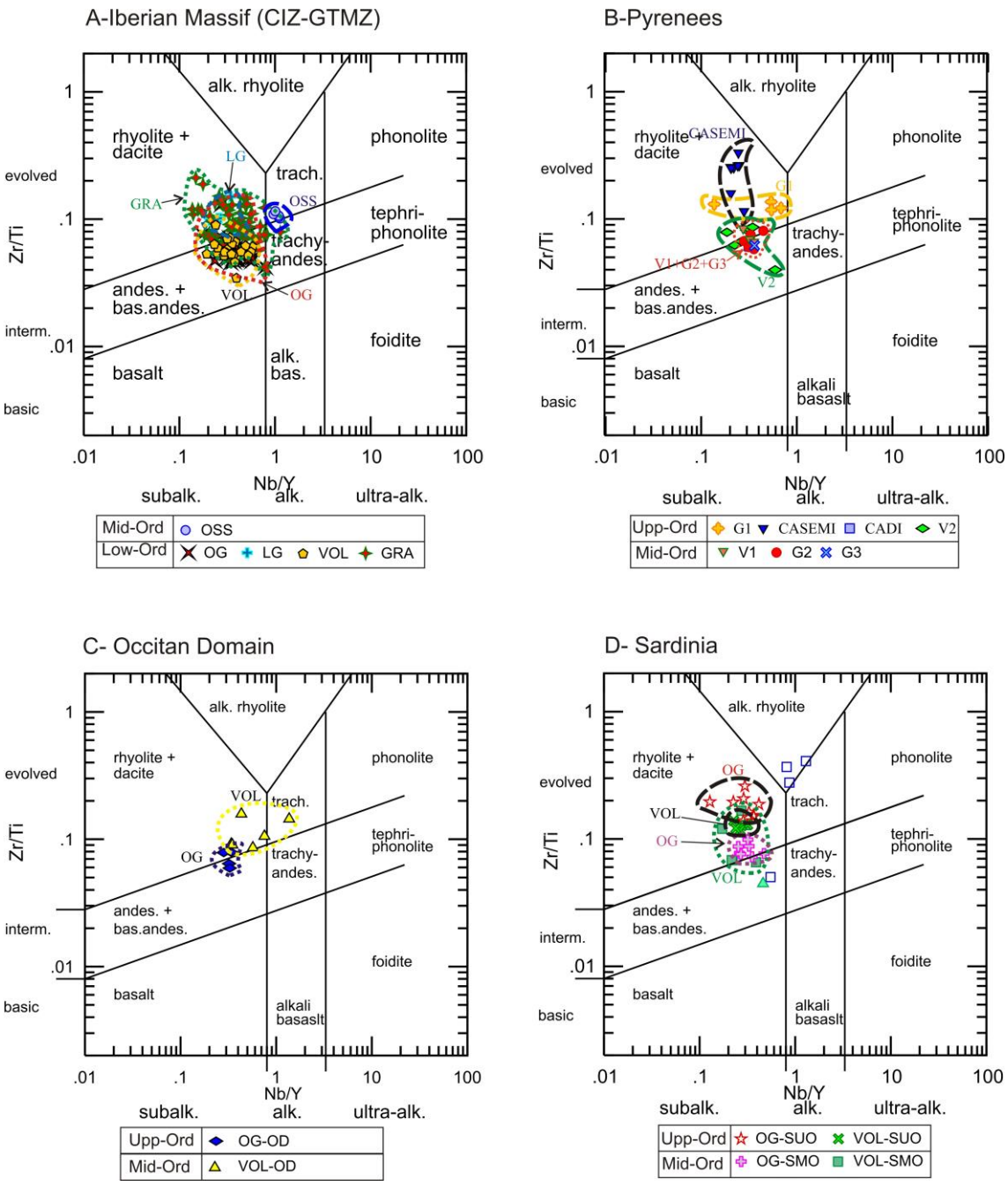


1672

1673

1674 **Figure 5.** Zr/Ti vs. Nb/Y discrimination diagram (after Winchester and Floyd, 1977;
1675 Pearce, 1996). A. Lower–Middle Ordovician rocks of Iberian Massif (Central Iberian
1676 and Galicia-Trás-os-Montes zones). B. Middle–Upper Ordovician rocks of the eastern
1677 Pyrenees. C) Middle Ordovician rocks of the Occitan Domain. C–D. Middle–Upper
1678 Ordovician rocks of Sardinia.

1679

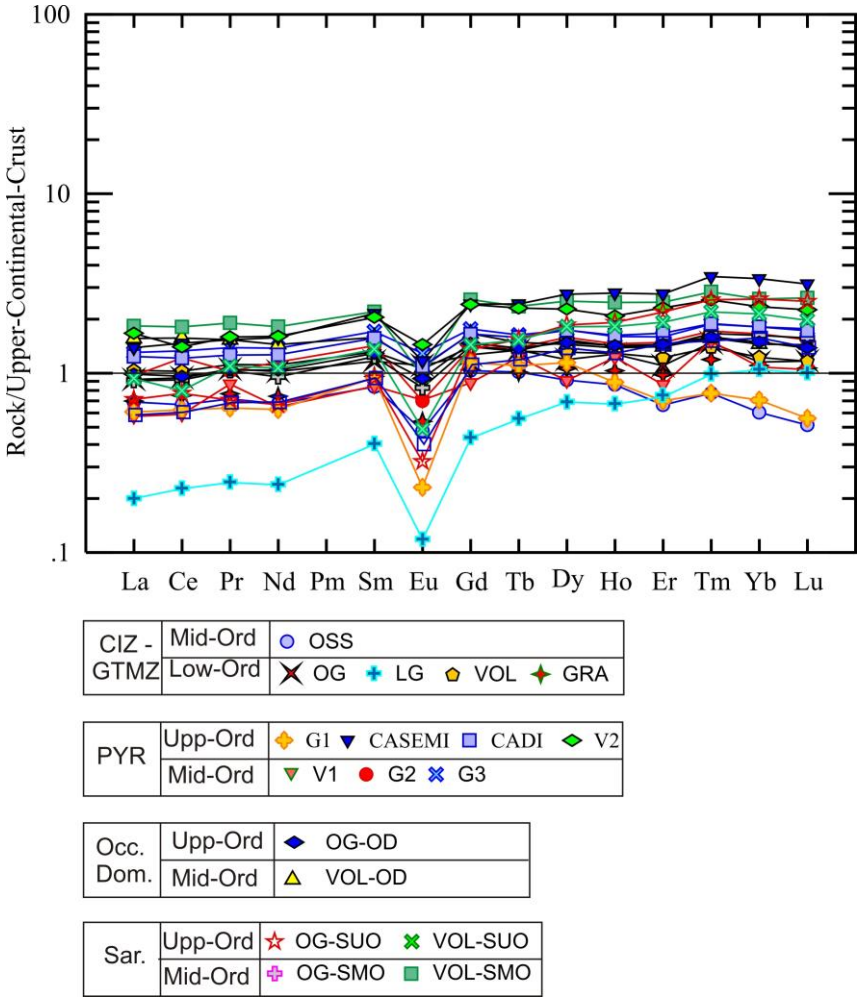


1680

1681

1682 **Figure 6.** Upper Crustal-normalized REE patterns (Rudnick and Gao, 2003) with

1683 average values for all distinguished groups; symbols as in Figure 4.

1684

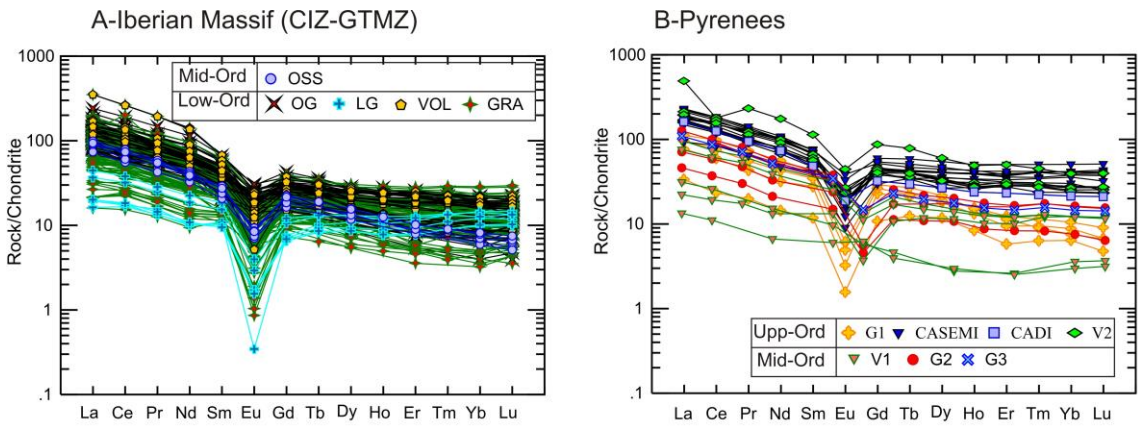


| Iberian Massif | $(La/Yb)_n$ | $(La/Sm)_n$ | Eu/Eu* | $(Gd/Yb)_n$ | REE |
|---|---|---|---|---|---|
| OSS (n=5) | 12,09 | 3,41 | 0,36 | 2,78 | 110,1 |
| OG (n=47) | 9,34 | 3,35 | 0,66 | 1,93 | 176,4 |
| LG (n=6) | 2,01 | 2,01 | 0,19 | 0,68 | 57,1 |
| GRA (n=71) | 8,07 | 2,84 | 0,36 | 1,79 | 141,7 |
| V1 (n=29) | 10,24 | 3,18 | 0,55 | 2,02 | 191,8 |




| Pyrenees | $(La/Yb)_n$ | $(La/Sm)_n$ | Eu/Eu* | $(Gd/Yb)_n$ | REE |
|---|---|---|---|---|---|
| V1 (n=6) | 5,85 | 2,65 | 0,68 | 1,32 | 110,4 |
| G2 (n=6) | 6,14 | 3,14 | 0,35 | 1,38 | 190,1 |
| G3 (n=1) | 7,54 | 3,17 | 0,51 | 1,58 | 242,9 |
| CADÍ (n=2) | 7,15 | 3,28 | 0,47 | 1,48 | 230,2 |
| G1 (n=4) | 8,92 | 2,70 | 0,15 | 2,60 | 120,7 |
| CASEMÍ (n=8) | 4,42 | 2,65 | 0,35 | 1,18 | 301,3 |
| V2 (n=11) | 7,18 | 3,29 | 0,45 | 1,64 | 287,7 |

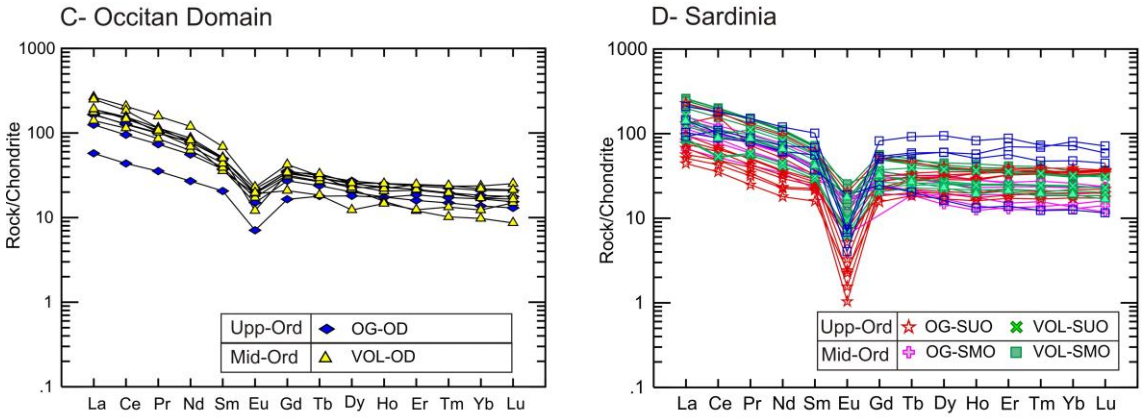


| Occitain D. | $(La/Yb)_n$ | $(La/Sm)_n$ | Eu/Eu* | $(Gd/Yb)_n$ | REE |
|---|---|---|---|---|---|
| OG-OD (n=4) | 6,93 | 3,12 | 0,46 | 1,60 | 186,0 |
| VOL-OD (n=6) | 13,04 | 4,24 | 0,48 | 2,06 | 254,4 |




| Sardinia | $(La/Yb)_n$ | $(La/Sm)_n$ | Eu/Eu* | $(Gd/Yb)_n$ | REE |
|---|---|---|---|---|---|
| SUO-OG (n=9) | 2,94 | 3,00 | 0,18 | 0,87 | 170,2 |
| SUO-VOL (n=5) | 4,52 | 2,84 | 0,24 | 1,08 | 188,1 |
| SMO-OG (n=7) | 6,21 | 3,07 | 0,48 | 1,46 | 190,4 |
| SMO-VOL (n=6) | 7,62 | 3,46 | 0,29 | 1,63 | 334,6 |
| SLO-VOL (n=5) | 4,72 | 2,44 | 0,27 | 1,28 | 271,8 |

**Figure 7.** Chondrite-normalized REE patterns (Sun and McDonough, 1989) for all study samples.

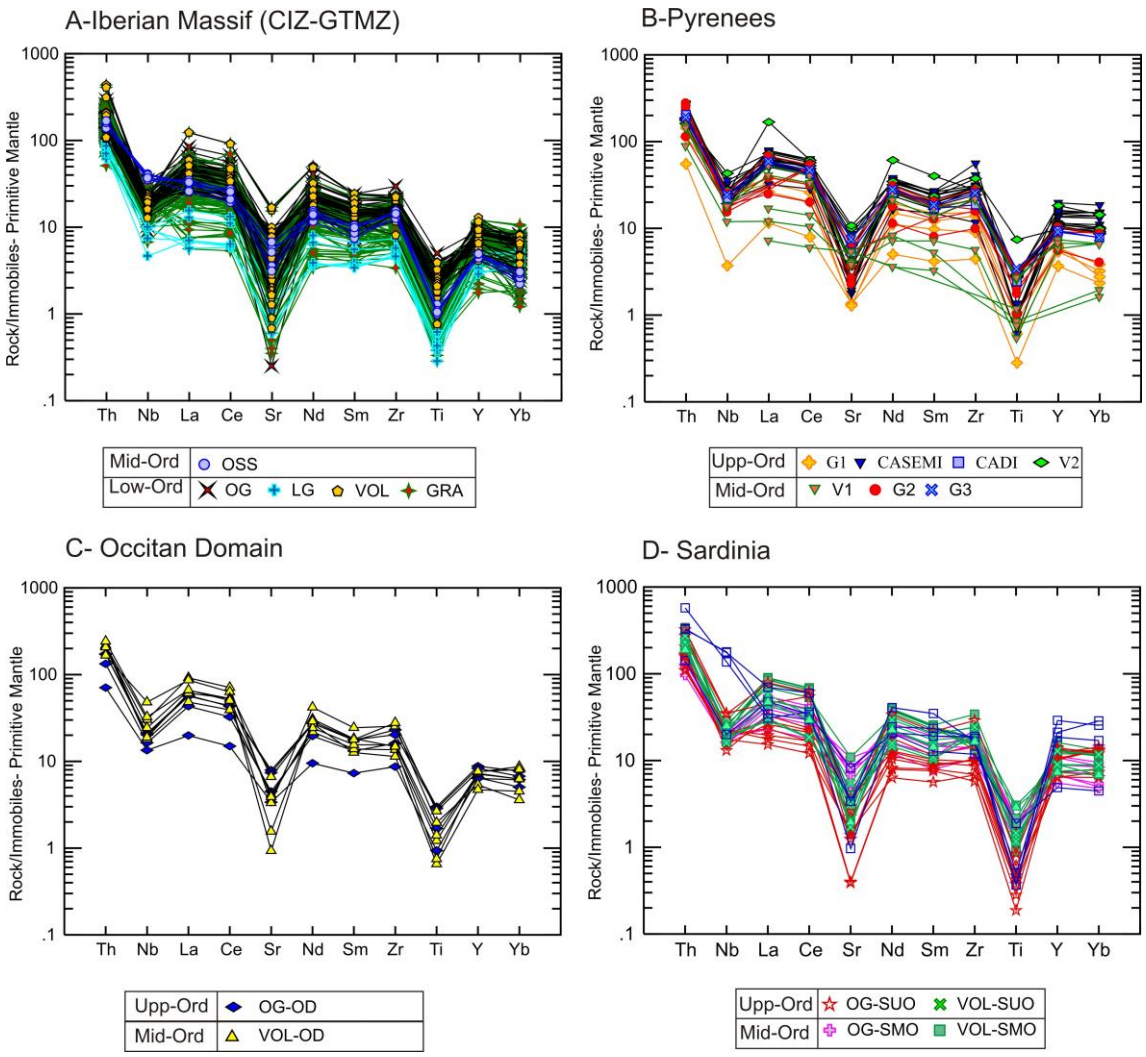


1690

1691

1692 **Figure 8.** Multi-element diagram normalised to Primitive Mantle of Palme and O'Neill

1693 (2004) for all study samples.

1694

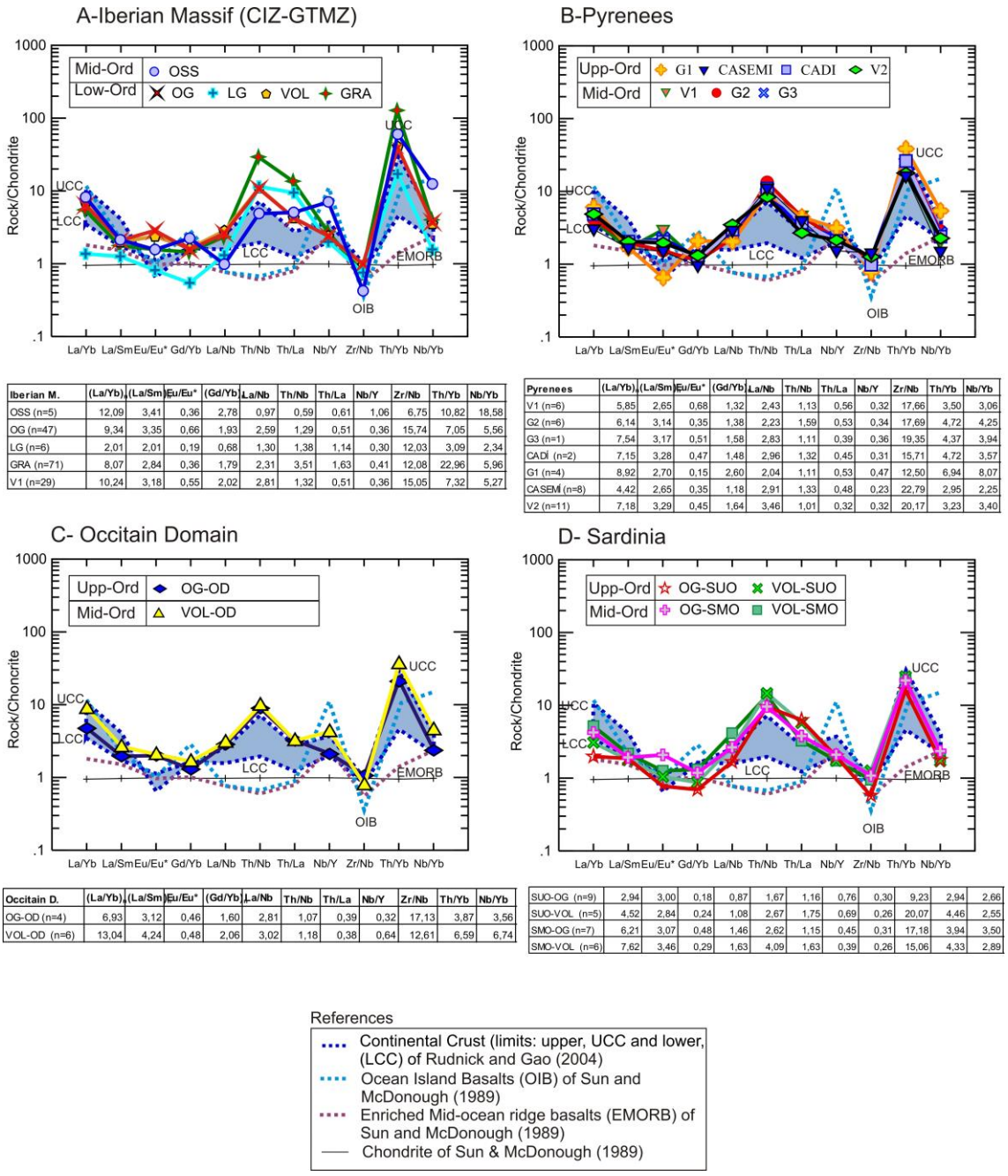


| Iberian M. | (La/Yb)$_N$ | (La/Sm)$_N$ | Eu/Eu* | (Gd/Yb)$_N$ | La/Nb | Th/Nb | Th/La | Nb/Y | Zr/Nb | Th/Yb | Nb/Yb |
|---|---|---|---|---|---|---|---|---|---|---|---|
| OSS (n=5) | 12,09 | 3,41 | 0,36 | 2,78 | 0,97 | 0,59 | 0,61 | 1,06 | 6,75 | 10,82 | 18,58 |
| OG (n=47) | 9,34 | 3,35 | 0,66 | 1,93 | 2,59 | 1,29 | 0,51 | 0,36 | 15,74 | 7,05 | 5,56 |
| LG (n=6) | 2,01 | 2,01 | 0,19 | 0,68 | 1,30 | 1,38 | 1,14 | 0,30 | 12,03 | 3,09 | 2,34 |
| GRA (n=71) | 8,07 | 2,84 | 0,36 | 1,79 | 2,31 | 3,51 | 1,63 | 0,41 | 12,08 | 22,96 | 5,96 |
| V1 (n=29) | 10,24 | 3,18 | 0,55 | 2,02 | 2,81 | 1,32 | 0,51 | 0,36 | 15,05 | 7,32 | 5,27 |

| Pyrenees | (La/Yb)$_N$ | (La/Sm)$_N$ | Eu/Eu* | (Gd/Yb)$_N$ | La/Nb | Th/Nb | Th/La | Nb/Y | Zr/Nb | Th/Yb | Nb/Yb |
|---|---|---|---|---|---|---|---|---|---|---|---|
| V1 (n=6) | 5,85 | 2,65 | 0,68 | 1,32 | 2,43 | 1,13 | 0,56 | 0,32 | 17,66 | 3,50 | 3,06 |
| G2 (n=6) | 6,14 | 3,14 | 0,35 | 1,38 | 2,23 | 1,59 | 0,53 | 0,34 | 17,69 | 4,72 | 4,25 |
| G3 (n=1) | 7,54 | 3,17 | 0,51 | 1,58 | 2,83 | 1,11 | 0,39 | 0,36 | 19,35 | 4,37 | 3,94 |
| CADI (n=2) | 7,15 | 3,28 | 0,47 | 1,48 | 2,96 | 1,32 | 0,45 | 0,31 | 15,71 | 4,72 | 3,57 |
| G1 (n=4) | 8,92 | 2,70 | 0,15 | 2,60 | 2,04 | 1,11 | 0,53 | 0,47 | 12,50 | 6,94 | 8,07 |
| CASEMI (n=8) | 4,42 | 2,65 | 0,35 | 1,18 | 2,91 | 1,33 | 0,48 | 0,23 | 22,79 | 2,95 | 2,25 |
| V2 (n=11) | 7,18 | 3,29 | 0,45 | 1,64 | 3,46 | 1,01 | 0,32 | 0,32 | 20,17 | 3,23 | 3,40 |

| Occitain D. | (La/Yb)$_N$ | (La/Sm)$_N$ | Eu/Eu* | (Gd/Yb)$_N$ | La/Nb | Th/Nb | Th/La | Nb/Y | Zr/Nb | Th/Yb | Nb/Yb |
|---|---|---|---|---|---|---|---|---|---|---|---|
| OG-OD (n=4) | 6,93 | 3,12 | 0,46 | 1,60 | 2,81 | 1,07 | 0,39 | 0,32 | 17,13 | 3,87 | 3,56 |
| VOL-OD (n=6) | 13,04 | 4,24 | 0,48 | 2,06 | 3,02 | 1,18 | 0,38 | 0,64 | 12,61 | 6,59 | 6,74 |

| | | | | | | | | | | | |
|---|---|---|---|---|---|---|---|---|---|---|---|
| SUO-OG (n=9) | 2,94 | 3,00 | 0,18 | 0,87 | 1,67 | 1,16 | 0,76 | 0,30 | 9,23 | 2,94 | 2,66 |
| SUO-VOL (n=5) | 4,52 | 2,84 | 0,24 | 1,08 | 2,67 | 1,75 | 0,69 | 0,26 | 20,07 | 4,46 | 2,55 |
| SMO-OG (n=7) | 6,21 | 3,07 | 0,48 | 1,46 | 2,62 | 1,15 | 0,45 | 0,31 | 17,18 | 3,94 | 3,50 |
| SMO-VOL (n=6) | 7,62 | 3,46 | 0,29 | 1,63 | 4,09 | 1,63 | 0,39 | 0,26 | 15,06 | 4,33 | 2,89 |

References

- Continental Crust (limits: upper, UCC and lower, (LCC) of Rudnick and Gao (2004)
- Ocean Island Basalts (OIB) of Sun and McDonough (1989)
- Enriched Mid-ocean ridge basalts (EMORB) of Sun and McDonough (1989)
- Chondrite of Sun & McDonough (1989)

**Figure 9.** Chondrite-normalised isotope ratio patterns (Sun and McDonough, 1989) for standard comparison for all study samples. Blue area: limits of continental crustal values (Lower and Upper) of Rudnick and Gao (2003).

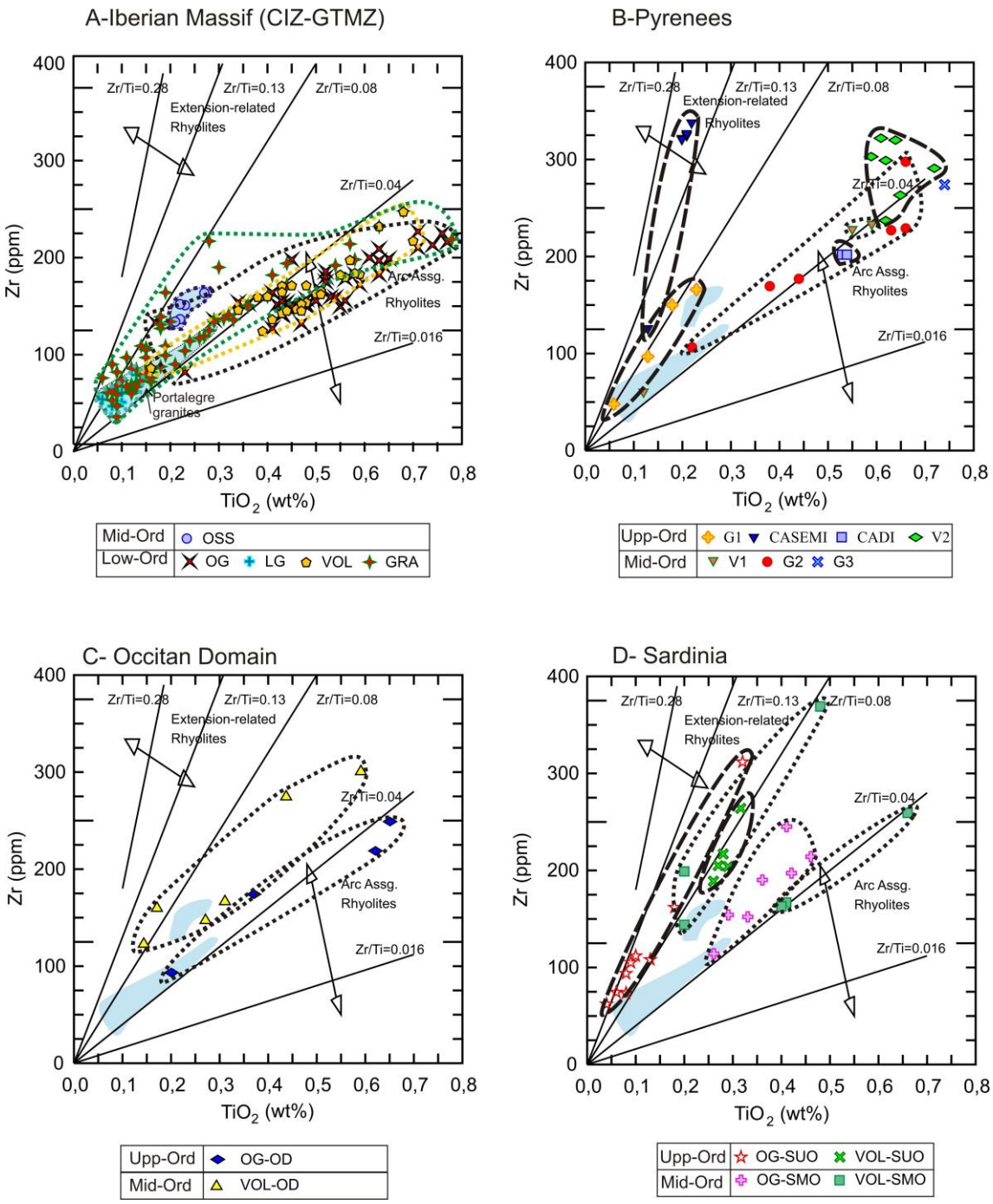


**Figure 10.** Tectonic discriminating diagram of Zr vs. $TiO_2$ (Syme, 1998) for all study samples. Double-sided arrows indicate ranging of differents fields: rhyolites in tholeiitic and calc-alkaline arc suites have $Zr/TiO_2$ ratios ranging from about 0.016 to 0.04, and extension-related rhyolites from about 0.13 to 0.28 (Syme, 1989).

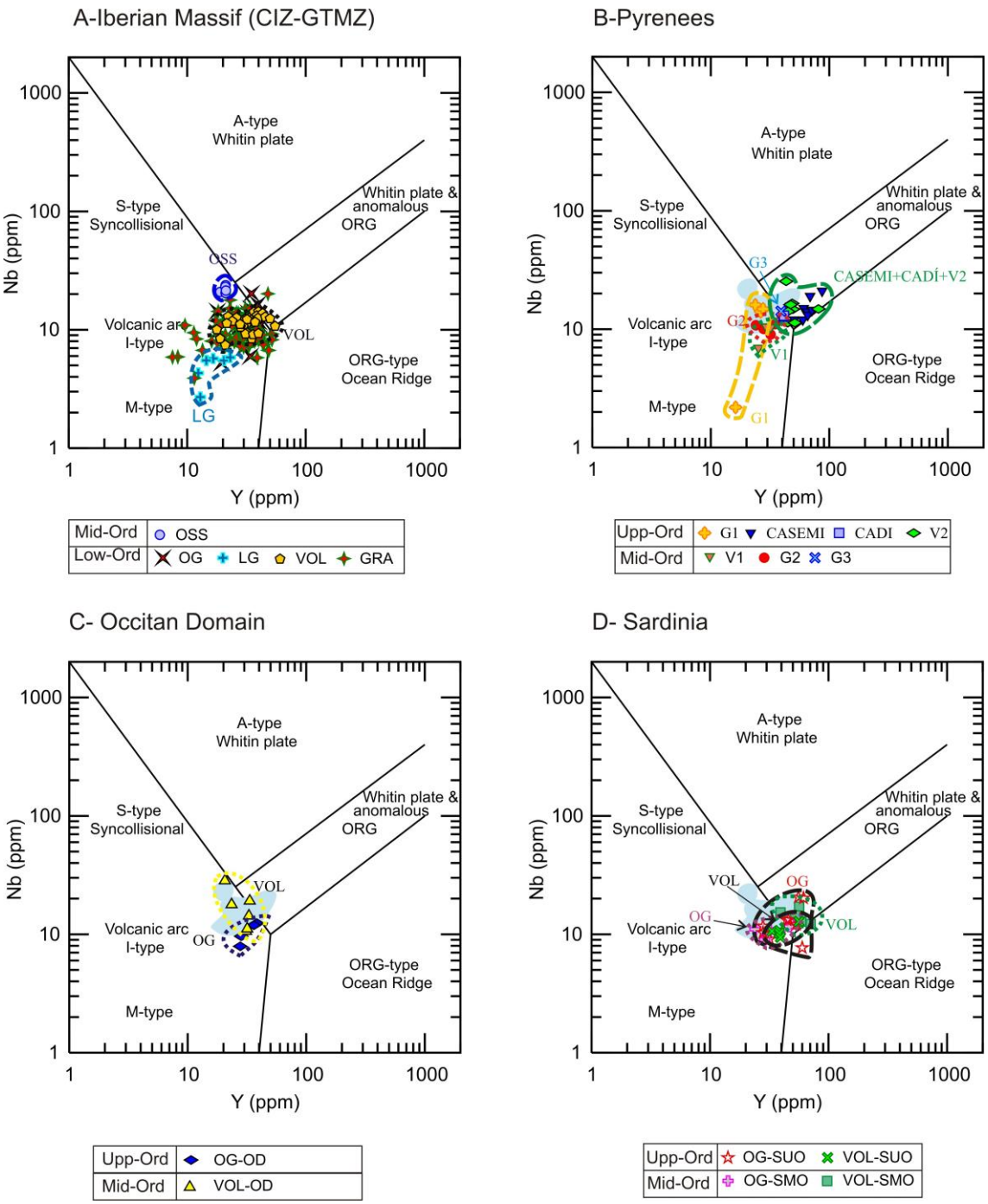


1708

1709 **Figure 11.** Tectonic discriminating diagram of Y vs. Nb (Pearce et al., 1984) for all

1710 study samples.

1711

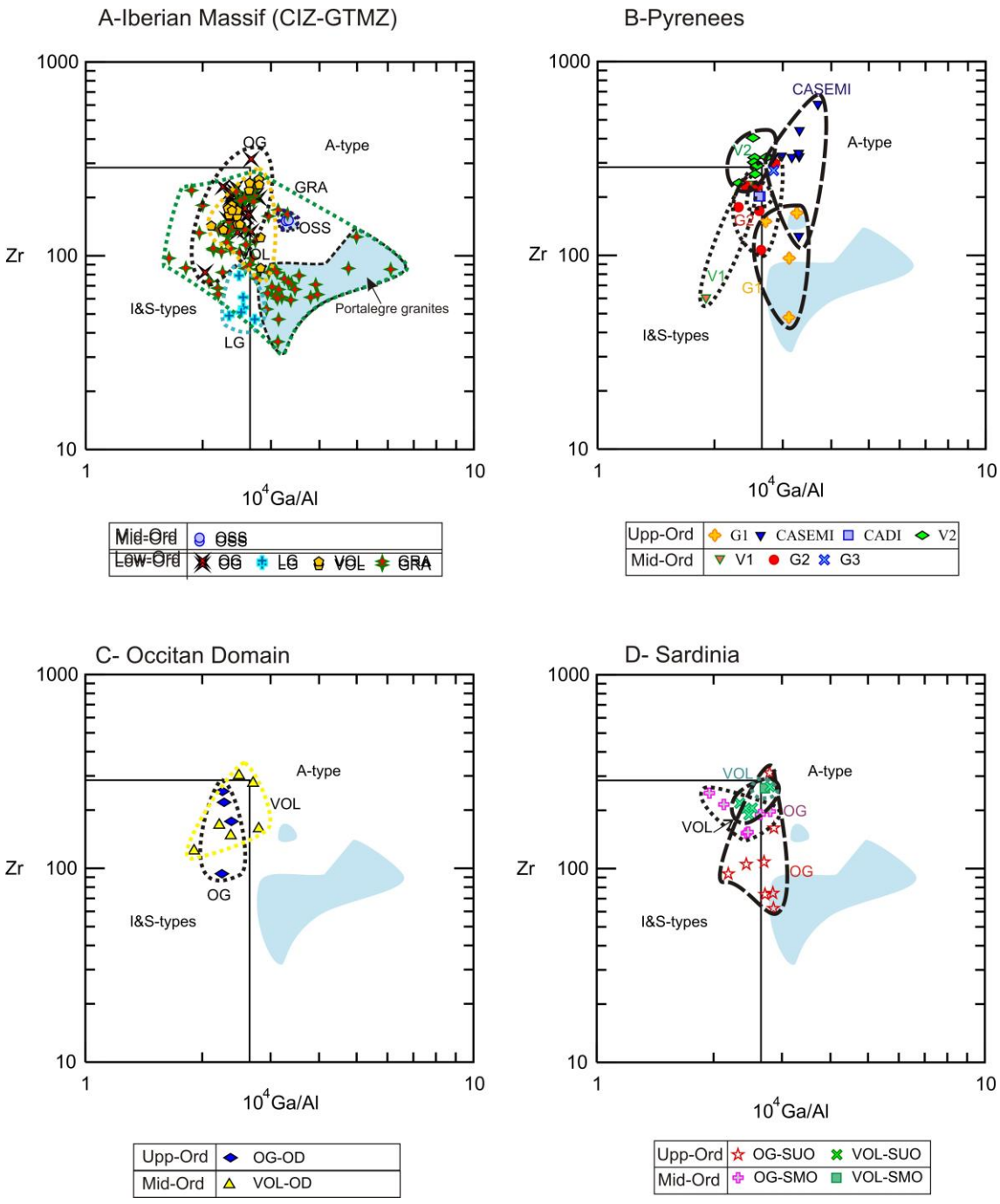


1712

1713

1714 **Figure 12.** Zr vs. $10^4$ Ga/Al discrimination diagram (Whalen et al., 1987).

1715

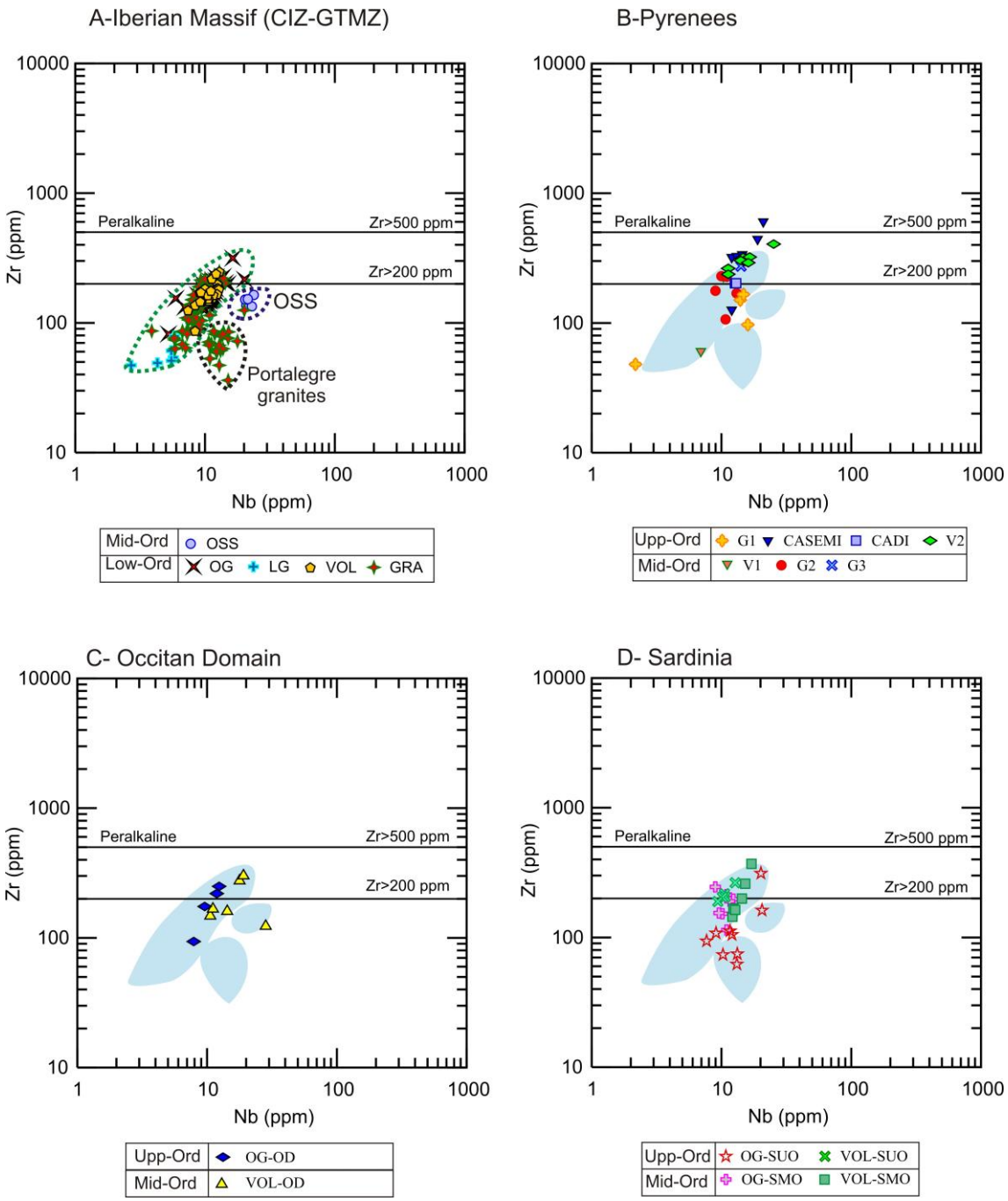


1716

1717

1718 **Figure 13.** Zr–Nb plot diagram (Leat et al.,1986; modified by Piercey, 2011) for all

1719 study samples.

1720

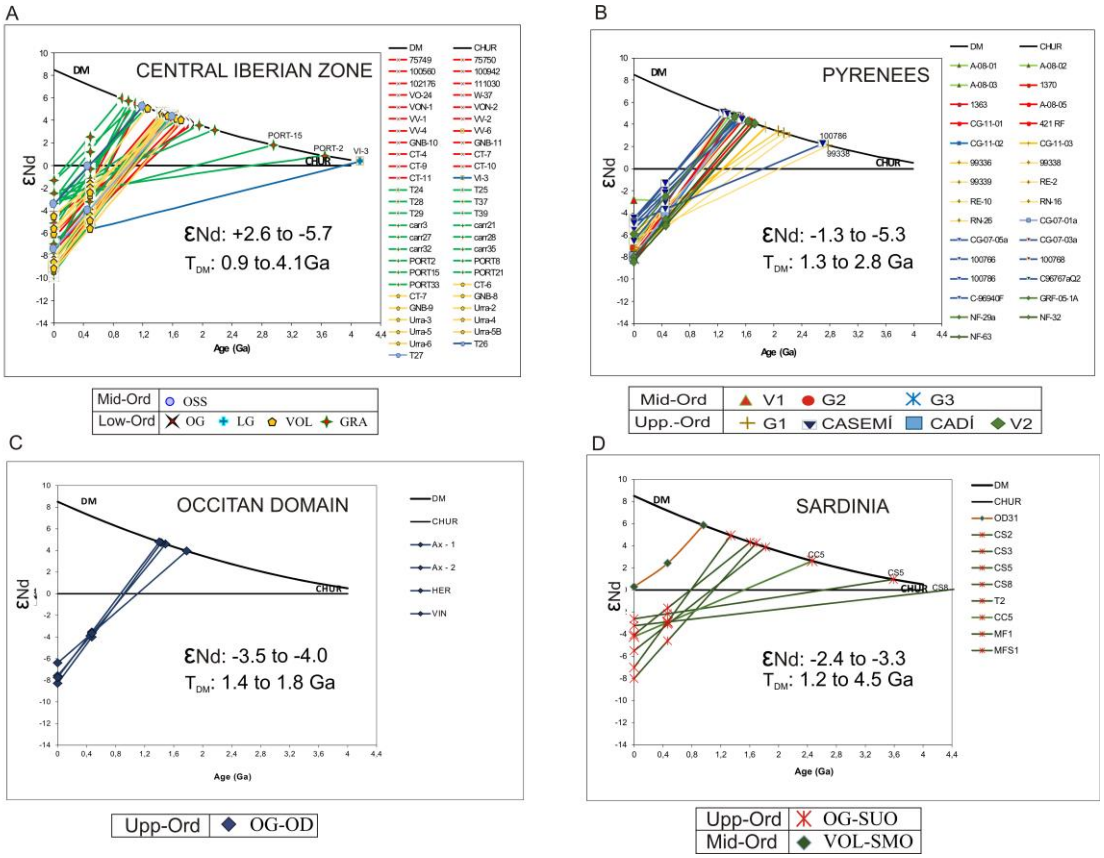


**Figure 14**. $\varepsilon Nd_{(t)}$ vs. age diagram (DePaolo and Wasserburg, 1976; DePaolo, 1981) for study sampled. A. Central Iberian and Galicia-Trás-os-Montes Zones. B. Eastern Pyrenees. C. Occitan Domain. D. Sardinia; see references in the text.

| | PYRENEES | | | MONTAGNE NOIRE | | | | SARDINIA | | | | | | | | | |
|---|---|---|---|---|---|---|---|---|---|---|---|---|---|---|---|---|---|
| | Albera | Pallaresa | Andorra | | Axial | Zone | | | | | External | Zone | | | | Inner | Zone |
| **Sample** | **A-08-03** | **fC1803** | **BN 1** | **Ax - 1** | **Ax - 2** | **HER** | **VIN** | **CC 5** | **CS 2** | **CS 3** | **CS 5** | **CS 8** | **MF 1** | **MFS 1** | **T 2** | **PB50** | **PB100** |
| **Long. (E)** | 3°7'39'' | 1°27'43'' | 1°33'29'' | 2°13'50'' | 2°33'58'' | 2°57'58'' | 2°13'50'' | 8°50'37'' | 8°50'35'' | 8°50'35'' | 8°50'40'' | 8°50'35'' | 8°50'47'' | 8°52'02'' | 8°48'54'' | 9°09'32'' | 9°09'32'' |
| **Lat. (N)** | 42°25'2'' | 42°36'1'' | 42°32'30'' | 43°34'32'' | 43°29'3'' | 43°34'32'' | 43°17'45'' | 38°54'16'' | 38°52'38'' | 38°52'38'' | 38°52'36'' | 38°52'39'' | 38°54'58'' | 38°53'57'' | 38°53'57'' | 41°11'' | 41°11'04'' |
| **$SiO_2$** | 68.38 | 71.67 | 69.18 | 70.38 | 67.43 | 68.31 | 73.97 | 76.43 | 75.14 | 76.52 | 76.61 | 76.36 | 72.13 | 75.94 | 75.55 | 68.93 | 67.24 |
| **$TiO_2$** | 0.57 | 0.63 | 0.61 | 0.36 | 0.64 | 0.61 | 0.20 | 0.08 | 0.08 | 0.09 | 0.04 | 0.06 | 0.31 | 0.13 | 0.18 | 0.41 | 0.46 |
| **$Al_2O_3$** | 15.68 | 14.24 | 15.05 | 14.90 | 15.76 | 15.39 | 13.82 | 13.28 | 12.81 | 11.80 | 12.71 | 12.63 | 13.80 | 13.16 | 12.94 | 16.32 | 15.79 |
| **$Fe_2O_3$** | 4.09 | 4.54 | 4.20 | 3.04 | 4.11 | 4.19 | 2.05 | 0.69 | 1.39 | 1.44 | 1.28 | 1.35 | 2.96 | 1.55 | 1.62 | 3.19 | 4.78 |
| **MnO** | 0.07 | 0.06 | 0.05 | 0.04 | 0.04 | 0.04 | 0.04 | 0.01 | 0.01 | 0.01 | 0.01 | 0.01 | 0.02 | 0.03 | 0.04 | 0.08 | 0.08 |
| **MgO** | 1.35 | 0.78 | 1.16 | 0.78 | 1.33 | 1.34 | 0.43 | 0.08 | 0.15 | 0.16 | 0.06 | 0.05 | 0.36 | 0.19 | 0.08 | 1.15 | 1.58 |
| **CaO** | 0.21 | 0.53 | 1.78 | 1.22 | 1.44 | 1.58 | 0.62 | 0.32 | 0.25 | 0.15 | 0.20 | 0.35 | 0.61 | 0.38 | 0.17 | 3.05 | 2.70 |
| **$Na_2O$** | 4.07 | 1.67 | 3.40 | 3.33 | 2.78 | 2.93 | 2.87 | 3.04 | 1.71 | 1.58 | 2.91 | 3.35 | 2.89 | 2.57 | 2.53 | 3.85 | 3.43 |
| **$K_2O$** | 2.84 | 2.91 | 2.71 | 4.35 | 4.68 | 4.03 | 4.55 | 4.79 | 7.84 | 7.43 | 5.16 | 4.91 | 5.47 | 4.94 | 5.36 | 2.26 | 2.96 |
| **$P_2O_5$** | 0.17 | 0.24 | 0.20 | 0.21 | 0.2 | 0.19 | 0.18 | 0.15 | 0.05 | 0.05 | 0.03 | 0.04 | 0.12 | 0.11 | 0.07 | 0.15 | 0.14 |
| **L.O.I.** | 2.03 | 2.60 | 1.50 | 1.2 | 1.3 | 1.2 | 1.2 | 1.1 | 0.4 | 0.7 | 0.9 | 0.8 | 1.1 | 0.9 | 1.4 | 0.90 | 0.70 |
| **Total** | 99.05 | 99.42 | 99.42 | 99.51 | 99.30 | 99.39 | 99.73 | 99.90 | 99.69 | 99.79 | 99.78 | 99.78 | 99.47 | 99.75 | 99.78 | 99.97 | 99.37 |
| **As** | 77.20 | 1.70 | 6.80 | 2.50 | 6.00 | 1.80 | 1.90 | 0.70 | 1.00 | 0.50 | 2.80 | 1.10 | 1.80 | 101.10 | 4.00 | 5.00 | 5.00 |
| **Ba** | 742.50 | 388.00 | 398.00 | 499 | 1050 | 767 | 256 | 60 | 467 | 109 | 21 | 27 | 784 | 194 | 192 | 689.00 | 600.00 |
| **Be** | 2.44 | 3.00 | 2.00 | 4.00 | 2.00 | 5.00 | 3.00 | 6.00 | 3.00 | 1.00 | 9.00 | 2.00 | 7.00 | 3.00 | 7.00 | 3.00 | 5.00 |
| **Bi** | 0.30 | 0.20 | 0.10 | 0.20 | 0.20 | 0.20 | 0.40 | 0.30 | 0.10 | 0.10 | 0.10 | 0.10 | 0.10 | 0.70 | 0.40 | 4.00 | 4.00 |
| **Cd** | 0.18 | 0.10 | 0.10 | 0.10 | 0.10 | 0.10 | 0.10 | 0.10 | 0.10 | 0.10 | 0.10 | 0.10 | 0.10 | 0.10 | 0.10 | | |
| **Co** | 5.84 | 4.60 | 6.20 | 5.20 | 5.20 | 5.40 | 2.70 | 0.50 | 1.60 | 1.00 | 0.80 | 0.60 | 2.30 | 1.50 | 1.20 | 5.00 | 14.00 |
| **Cs** | 9.79 | 5.60 | 4.90 | 14.30 | 7.10 | 6.80 | 7.30 | 4.20 | 3.40 | 1.60 | 4.50 | 4.60 | 6.40 | 3.90 | 4.10 | 4.20 | 9.40 |
| **Cu** | 16.34 | 13.20 | 10.30 | 7.20 | 7.40 | 10.10 | 8.70 | 4.70 | 4.60 | 8.20 | 26.80 | 2.50 | 5.00 | 5.50 | 5.00 | 10.00 | 60.00 |
| **Ga** | 21.03 | 19.80 | 18.80 | 19.10 | 19.20 | 18.90 | 16.70 | 19.30 | 14.90 | 15.30 | 19.40 | 19.20 | 20.70 | 19.00 | 19.90 | 17.00 | 18.00 |
| **Hf** | 6.40 | 7.30 | 6.40 | 5.00 | 6.90 | 5.70 | 3.10 | 3.10 | 4.10 | 4.30 | 3.50 | 3.80 | 8.80 | 3.70 | 5.80 | 5.90 | 5.30 |
| **Mo** | 1.20 | 0.90 | 1.00 | 0.60 | 0.90 | 0.60 | 0.30 | 0.70 | 0.70 | 0.70 | 0.80 | 0.50 | 1.70 | 0.80 | 1.60 | 2.00 | 2.00 |
| **Nb** | 10.49 | 11.30 | 11.30 | 9.60 | 12.40 | 11.90 | 7.90 | 10.30 | 7.70 | 12.10 | 13.20 | 13.30 | 20.20 | 9.10 | 20.60 | 9.00 | 11.00 |
| **Ni** | 16.56 | 8.00 | 7.70 | 20.00 | 20.00 | 20.00 | 20.00 | 20.00 | 20.00 | 20.00 | 20.00 | 20.00 | 20.00 | 20.00 | 20.00 | 20.00 | 80.00 |
| **Pb** | 7.94 | 9.80 | 22.90 | 3.50 | 4.60 | 5.10 | 3.60 | 2.90 | 7.40 | 8.60 | 4.50 | 5.50 | 5.10 | 6.30 | 5.50 | 21.00 | 24.00 |
| **Rb** | 124.40 | 123.70 | 137.20 | 204.6 | 161.6 | 142.2 | 188.2 | 289.9 | 206.1 | 187.4 | 294.1 | 275.1 | 208.7 | 256.4 | 227.1 | 85.00 | 118.00 |
| **Sb** | 2.27 | 0.10 | 0.30 | 0.10 | 0.10 | 0.10 | 0.10 | 0.10 | 0.10 | 0.10 | 0.10 | 0.10 | 0.10 | 0.10 | 0.10 | 5.00 | 5.00 |
| **Sc** | | 10.00 | 10.00 | 6.00 | 9.00 | 9.00 | 4.00 | 3.00 | 3.00 | 4.00 | 4.00 | 4.00 | 15.00 | 4.00 | 8.00 | 9.00 | 12.00 |
| **Sn** | 2.11 | 5.00 | 5.00 | 9.00 | 3.00 | 3.00 | 7.00 | 9.00 | 4.00 | 3.00 | 13.00 | 15.00 | 7.00 | 15.00 | 12.00 | 3.00 | 3.00 |
| **Sr** | 158.00 | 201.80 | 83.70 | 91.20 | 160.30 | 150.10 | 68.70 | 30.70 | 73.90 | 25.20 | 7.90 | 8.10 | 59.90 | 45.60 | 25.00 | 217.00 | 167.00 |
| **Ta** | 1.07 | 1.10 | 1.10 | 0.80 | 1.00 | 0.80 | 0.70 | 2.10 | 0.90 | 1.10 | 3.40 | 1.70 | 1.60 | 1.70 | 2.30 | 1.00 | 1.20 |
| **Th** | 11.90 | 15.70 | 13.50 | 11.10 | 14.40 | 14.30 | 5.90 | 9.10 | 14.10 | 17.00 | 13.50 | 13.10 | 22.80 | 10.20 | 26.90 | 13.30 | 11.50 |
| **U** | 3.70 | 5.10 | 4.60 | 4.10 | 3.60 | 3.20 | 4.80 | 3.30 | 2.90 | 3.20 | 3.50 | 3.50 | 4.60 | 8.10 | 4.90 | 4.50 | 2.20 |
| **V** | 44.49 | 49.00 | 36.00 | 36.00 | 63.00 | 68.00 | 22.00 | 8.00 | 8.00 | 8.00 | 8.00 | 8.00 | 15.00 | 8.00 | 10.00 | 62.00 | 53.00 |
| **W** | 1.80 | 1.90 | 2.50 | 3.20 | 2.60 | 1.60 | 3.00 | 5.60 | 0.90 | 2.10 | 5.20 | 3.00 | 2.40 | 4.40 | 3.50 | 1.00 | 20.00 |
| **Y** | 29.29 | 43.90 | 50.60 | 28.30 | 38.40 | 36.20 | 27.80 | 28.00 | 60.10 | 53.60 | 44.40 | 46.00 | 61.60 | 31.80 | 55.80 | 29.00 | 24.00 |
| **Zn** | 63.71 | 52.00 | 70.00 | 55.00 | 71.00 | 78.00 | 46.00 | 7.00 | 35.00 | 39.00 | 15.00 | 24.00 | 37.00 | 30.00 | 22.00 | 70.00 | 70.00 |
| **Zr** | 233.30 | 263.20 | 237.10 | 174.40 | 249.20 | 219.10 | 93.70 | 73.50 | 93.80 | 105.10 | 62.20 | 74.50 | 311.80 | 108.10 | 161.90 | 245.00 | 214.00 |
| **La** | 27.90 | 45.30 | 38.00 | 29.60 | 39.50 | 38.70 | 13.60 | 10.50 | 22.70 | 19.50 | 12.10 | 13.40 | 54.20 | 17.90 | 31.30 | 26.90 | 34.30 |
| **Ce** | 59.00 | 86.90 | 75.50 | 58.10 | 77.00 | 78.20 | 26.70 | 21.60 | 42.10 | 39.70 | 26.20 | 29.90 | 109.80 | 37.40 | 97.60 | 53.20 | 70.50 |
| **Pr** | 7.26 | 9.80 | 8.47 | 6.99 | 9.41 | 9.55 | 3.36 | 2.36 | 4.73 | 4.85 | 3.00 | 3.24 | 11.94 | 4.07 | 6.86 | 5.88 | 8.20 |
| **Nd** | 27.83 | 35.60 | 31.20 | 26.00 | 36.40 | 36.40 | 12.60 | 8.40 | 16.60 | 17.10 | 10.50 | 10.90 | 44.70 | 15.00 | 24.00 | 21.60 | 29.40 |
| **Sm** | 5.80 | 7.69 | 7.16 | 5.70 | 7.55 | 7.63 | 3.15 | 2.43 | 4.10 | 4.41 | 3.28 | 3.44 | 9.37 | 3.88 | 4.93 | 4.70 | 6.00 |
| **Eu** | 0.98 | 1.05 | 1.03 | 0.87 | 1.27 | 1.15 | 0.41 | 0.14 | 0.43 | 0.13 | 0.06 | 0.09 | 1.17 | 0.30 | 0.19 | 0.95 | 0.93 |
| **Gd** | 5.22 | 8.32 | 7.89 | 5.59 | 7.28 | 7.05 | 3.38 | 3.20 | 5.60 | 5.50 | 4.42 | 4.69 | 10.60 | 4.50 | 6.34 | 4.00 | 5.10 |
| **Tb** | 0.87 | 1.26 | 1.27 | 0.89 | 1.17 | 1.10 | 0.67 | 0.69 | 1.13 | 1.18 | 1.03 | 1.07 | 1.70 | 0.82 | 1.27 | 0.70 | 0.80 |
| **Dy** | 5.30 | 6.68 | 8.00 | 5.09 | 6.89 | 6.39 | 4.59 | 4.30 | 7.69 | 8.23 | 7.31 | 7.66 | 10.28 | 5.24 | 9.00 | 3.70 | 4.30 |
| **Ho** | 1.06 | 1.52 | 1.73 | 0.99 | 1.42 | 1.30 | 0.98 | 0.91 | 1.91 | 1.91 | 1.59 | 1.65 | 2.13 | 1.12 | 2.01 | 0.70 | 0.80 |
| **Er** | 2.98 | 4.52 | 4.96 | 2.64 | 3.92 | 3.56 | 3.07 | 2.85 | 5.80 | 6.46 | 5.35 | 5.38 | 6.25 | 3.64 | 6.17 | 2.20 | 2.10 |
| **Tm** | 0.46 | 0.60 | 0.73 | 0.38 | 0.57 | 0.50 | 0.44 | 0.43 | 0.91 | 1.00 | 0.85 | 0.85 | 0.89 | 0.52 | 0.92 | 0.35 | 0.32 |
| **Yb** | 3.00 | 3.98 | 4.72 | 2.33 | 3.56 | 3.11 | 2.83 | 2.95 | 5.81 | 6.60 | 6.10 | 6.16 | 5.53 | 3.70 | 6.04 | 2.50 | 2.20 |
| **Lu** | 0.44 | 0.58 | 0.69 | 0.33 | 0.53 | 0.45 | 0.39 | 0.44 | 0.90 | 0.94 | 0.92 | 0.94 | 0.86 | 0.56 | 0.90 | 0.41 | 0.36 |

**Table 1.** Chemical analyses of magmatic rocks. ICP and ICP–MS methods at ACME–LABS in Canada.

| ORTHOGNEISS FACIES | code | composition | SiO2 wt. % | Na2O wt. % | K20 wt. % | A/CNK ratio | ƐNd | TDM (Ga) | $^{147}Sm/^{144}Nd$ | area |
|---|---|---|---|---|---|---|---|---|---|---|
| ***(1) Furongian-Mid Ordovician Suite*** | | | | | | | | | | |
| CIZ - Ollo de Sapo orthogneiss | OG | K-rich dacite to rhyolite | 75–60.3 | 3.9–0.1 | 5.9–3.4 | 3.1–1.0 | −5.1 to −1.8 | 1.8–1.1 | 0.15-0.09 | Sanabria (ca. 472 Ma ) and Guadarrama (ca. 488-473 Ma) |
| CIZ - Leucogneiss | LG | K-rich dacite to rhyolite | 75.9–73.6 | 3.1–2.7 | 5.3–4.2 | 1.3–1.1 | −5.1 to −4.9 | 4.1 | 0.22-0.18 | Guadarrama |
| CIZ - Metagranite | GRA | K-rich dacite to rhyolite | 77–64.6 | 4.8–0.5 | 6.3–2.5 | 1.8–1.0 | −5.2 to +2.6 | 3.6–0.9 | 0.19-.0.09 | NE Central System, Sanabria, Miranda do Douro (ca. 496-473 Ma), CIZ (496-471 Ma for Carrascal, Fermoselle, Ledesma, Portalegre and Vitigudino granites) |
| CIZ/GTMZ - Volcanic rocks | VOL | andesite to rhyolite | 79.3–64.6 | 3.2–0.1 | 6.3–2.2 | 2.7–1.1 | −5.5 to −1.6 | 1.7–1.3 | 0.15-0.13 | Saldanha Fm. in GTMZ, Ollo de Sapo Fm. in Sanabria, and Urra Fm. |
| CIZ - San Sebastián orthogneiss | OSS | rhyolite | 75.4–73.8 | 3.1–2.5 | 5.4–4.9 | 1.2–1.1 | −4.0 to 0 | 1.6–1.2 | 0.14-0.14 | Sanabria (ca. 470-465 Ma) |
| PYR - augengneiss | G2* | dacite to rhyolite | 73.6–68.3 | 3.9–3.2 | 4.4–2.5 | 1.2-1.1 | −4.4 to −3.0 | 1.4–1.2 | 0.14-0.13 | ca. 476-462 Ma |
| PYR - orthogneiss | G3* | K-rich dacite | 73.5–68.4 | 2.9–2.4 | 4.4 | 1.2 | −4.2 | 1.33 | 0.13 | ca. 463 Ma |
| PYR - volcanic rocks | V1 | Na-rich rhyolite | 73.5–68.4 | 7.8–2.4 | 3.2–1.3 | 2.0–1.1 | −5.1 to −2.6 | 1.7–1.6 | 0.19-0.13 | Pierrefite Fm. and Albera massif (ca. 472-465 Ma) |
| OCC - volcanic rocks | VOL-OD | K-rich dacite to rhyolite | 75.6–66.7 | 3.7–0.6 | 9.3–2.3 | 2.4–1.3 | | | | Saint-Sernin-sur-Rance and Saint-Salvi-de-Carcavès nappes |
| SAR - orthogneiss | OG-SMO | K-rich rhyolite | 74–67.2 | 3.8–2.6 | 5.8–2.3 | 1.3–1.1 | | | | ca. 469 Ma |
| SAR - volcanic rocks | VOL-SMO | K-rich dacite to rhyolite | 76.7–67.6 | 4.7–1.9 | 5.4–2.9 | 2.0–1.2 | | | 0.16 | ca. 464-462 Ma |
| ***(2) Upper Ordovician Suite*** | | | | | | | | | | |
| PYR - orthogneiss | G1* | K-rich dacite to rhyodacite | 76.4–73.4 | 3.1–2.6 | 5.3–4.7 | 1.2–1.1 | −5.3 to −3.1 | 2.7–1.5 | 0.17-0.12 | ca. 457 Ma |
| PYR - orthogneiss | CADí | K-rich dacite to rhyodacite | 69.4 | 3 | 4 | 1.2 | -4.1 | 1.5 | 0.13 | Cadí massif (ca. 456 Ma) |
| PYR - orthogneiss | CASEMí | K-rich dacite to rhyodacite | 76–71.9 | 4–1.8 | 6.3–3.2 | 1.2–0.9 | −3.6 to −1.3 | 2.6–1.3 | 0.17-0.13 | Casemí massif (ca. 451-446) |
| PYR - volcanic rocks | V2 | andesite to rhyodacite | 86.1–63 | 6–0 | 4.3–0.6 | 3.6–1 | −5.1 to −2.6 | 1.7–1.6 | 0.14-0.14 | Ribes de Freser, Andorra (ca. 457 Ma), Pallaresa (ca. 453 Ma), Els Metges (ca. 455.2 Ma) |
| OCC - orthogneiss | OG-OD | K-rich dacite to rhyolite | 73.9–67.4 | 3.3–2.8 | 4.7–4 | 1.3–1.2 | −4 to −3.5 | 1.8–1.4 | 0.15-0.13 | Gorges d'Héric (ca. 450 Ma; Caroux), S Mazamet (Nore), S Rouairoux (Agout), Le Vintrou |
| SAR - External Zone orthogneiss | OG-SUD | K-rich dacite to rhyolite | 76.6–72.1 | 3.3–1.6 | 7.8–4.8 | 1.3–1.1 | −3.3 to −1.6 | 4.2–1.2 | 0.19-0.12 | Capo Spartivento, Cuile Culurgioni, Tuerredda, Monte Filau, Monte Settiballas (ca. 458-457 Ma) |
| SAR - Nappe Zone volcanic rocks | VOL-SUD | K-rich dacite to rhyodacite | 76.7–70.7 | 3.3–1.6 | 7.8–4.8 | 1.3–1.1 | | | | Truzzulla Fm. at Monte Grighini |

**Table 2.** Summarized geochemical features of the Furongian and Ordovician felsic episodes described in the text; data from Lancelot et al. (1985), Calvet et al. (1988), Valverde-Vaquero and Dunning (2000), Roger et al. (2004), Vilà et al. (2005), Giacomini et al. (2006), Díez-Montes (2007), Montero et al. (2007, 2009), Solá (2007), Zeck et al. (2007), Castiñeiras et al. (2008b), Talavera (2009), Casas et al. (2010), Navidad et al. (2010, 2018), Liesa et al. (2011), Martínez et al. (2011, 2018), Navidad and Castiñeiras (2011), Gaggero et al. (2012), Talavera et al. (2013), Villaseca et al. (2016), Pouclet et al. (2017), Cruciani et al. (2018) and this work. Abbreviations: *CIZ* Central Iberian Zone, *GTOMZ* Galicia-Trás-os-Montes Zone, *OCC* Occitan Domain, *PYR* Pyrenees and *SAR* Sardinia; * *sensu* Guitard (1970); A/CNK ratio is always peraluminous.